RP TU Rheinland-Pfälzische Technische Universität Kaiserslautern Landau

Role of the chloroplast transporter ABCG7 in the acclimation of Arabidopsis to cold and freezing conditions

Rolle des chloroplastidären Transporters ABCG7 in der Akklimatisierung an Kälte- und Frostbedingungen

vom Fachbereich Biologie
der Rheinland-Pfälzischen Technischen Universität Kaiserslautern-Landau
zur Verleihung des akademischen Grades Dr. rer. nat. genehmigte

Dissertation

von

Katharina Waldemarowna Ebel, geboren in Kustanai (Kasachstan)

Mündliche Prüfung: 19.09.2025

Dekan:	Prof. Dr. Stefan Kins
Promotionskommissionsvorsitzende:	Prof. Dr. Nicole Frankenberg-Dinkel
Berichterstattende:	Prof. Dr. Ekkehard Neuhaus
	Prof. Dr. Matthias Hahn

D 386

For us.

Contents

1. Introduction 1
1.1. The chloroplast 1
1.2. Acclimation to chilling and freezing stress 3
1.2.1. Chloroplast membranes during low temperature stress 5
1.2.2. Cell wall remodelling during chilling and freezing temperatures 6
1.3. Dynamically responding chloroplast envelope proteins 7
1.4. ATP-binding cassette transporters 8
1.5. Significance of characterising the ABCG7 transporter 9
2. Material and methods 10
2.2. Plant cultivation 10
2.2.1. Arabidopsis lines and homozygosity testing 10
2.2.2. Plant cultivation on soil 10
2.2.3. Surface sterilisation of seeds and plate experiments 11
2.3. Physiological methods 12
2.3.1. Evaluation of freezing tolerance and recovery 12
2.3.2. Leaf disc experiments 12
2.3.3. Extraction of soluble metabolites 13
2.3.4. Starch extraction 14
2.3.5. Photometric sugar measurements 14
2.3.6. Quantification of sugars by IC-measurements 16
2.3.7. Analysis of amino acids by HPLC-measurements 16
2.3.8. Extraction of soluble sugars for GC-analysis 17
2.3.9. Extraction of amino and organic acids for LC-MS measurements 18
2.3.10. Extraction and quantification of cell wall sugars 19

2.3.11. Analysis of lipids by UPLC-measurements 20
2.3.12. Extraction and quantification of anthocyanins 21
2.4. Cultivation and transformation of bacteria 22
2.4.1. Bacterial strains 22
2.4.2. Plasmids 22
2.4.3. Bacterial cultivation 23
2.4.4. Production of competent *E. coli* cells and transformation 23
2.4.5. Production of competent *A. tumefaciens* cells and transformation 24
2.5. Molecular methods 25
2.5.1. Nucleic acid concentration 25
2.5.2. Polymerase chain reaction 25
2.5.3. Agarose gel electrophoresis 26
2.5.4. DNA agarose gel extraction 26
2.5.5. Gateway cloning 27
2.5.6. Plasmid DNA isolation 28
2.5.7. Genomic DNA extraction 29
2.5.8. RNA isolation 29
2.5.9. RNA sequencing 29
2.5.10. Reverse transcription of RNA into cDNA 30
2.5.11. Quantitative polymerase chain reaction 31
2.6. ABCG7 localisation studies 33
2.6.1. Microscopy 33
2.6.2. Cloning of constructs for confocal microscopy 33
2.6.3. Imaging of transfected tissue and protoplasts 34
2.6.4. Protein extraction and quantification from transfected tobacco leaves 35
2.6.5. SDS-PAGE and Western blotting of total protein extracts 35

2.6.6. Infiltration of tobacco leaves 36
2.6.7. Chloroplast isolation and protease treatment 37
3. Results 38
3.2. Localisation of the ABCG7 transporter 38
3.3. The *abcg7* loss-of-function lines exposed to cold conditions 41
3.3.1. Cold acclimation of the *abcg7* mutants 41
3.3.2. Metabolic profiling of cold-acclimating *abcg7* mutants 44
3.3.3. Expression of genes involved in amino acid biosynthesis 49
3.3.4. Transcription of cell wall genes in cold-acclimating *abcg7* mutants 51
3.4. Effects of galactose on wild type and *abcg7* loss-of-function lines 53
3.5. The *abcg7* loss-of-function lines under freezing stress 56
3.5.1. Freezing tolerance of the *abcg7* mutants 56
3.5.2. Variations in the cell wall metabolism of the *abcg7* mutants 58
3.5.3. Alterations in the lipid composition of the *abcg7* mutants 62
3.6. Analysis of ABCG7 and SFR2 interaction 64
4. Discussion 66
4.2. Outer envelope localisation of the chloroplast transporter ABCG7 66
4.3. Improved cold tolerance in *abcg7* loss-of-function lines 68
4.4. Effects of cold stress on the amino acid pools in *abcg7* mutants 71
4.5. Galactose induces anthocyanin production in *abcg7* mutants 74
4.6. The importance of the ABCG7 protein during frost 75
4.7. The chloroplast outer envelope proteins ABCG7 and SFR2 78
4.8. Conclusion 81
4.9. Outlook 82
5. Summaries in English and German 83
5.2. Summary 83

5.3. Zusammenfassung 84

6. References 85

7. Supplements V

7.1. Abbreviations V

7.2. Supplementary figures VIII

1. Introduction

1.1. The chloroplast

The chloroplast is the result of an evolutionary process that began with the endosymbiosis of an ancestral cyanobacterium and integration into the host metabolism of a eukaryotic cell. This process led to the emergence of a plant organelle, surrounded by 2 envelopes consistent of galactolipids and still harbouring an own genome (Finkemeier & Leister, 2010; McFadden, 1999, 2001). Until today, morphological, biochemical and molecular appearances of the plastids provide evidence of the prokaryotic origin, such as the components of the integral photosynthetic machinery, which are still encoded by the endogenous genome and allow the electron transport within the thylakoid membranes (McFadden, 1999, 2001). Other hallmarks, indicating towards the prokaryotic origin of plastids, can be found in the process of division, which relies on proteins that are very similar to those that facilitate bacterial division (Finkemeier & Leister, 2010; McFadden, 1999, 2001).

Plastids are responsible for a multitude of specialised functions that are essential for plant development and growth. These include photosynthesis, CO_2 fixation, starch synthesis and temporary storage, nitrite or sulphate reduction and assimilation, as well as biosynthesis of amino acids and fatty acids (Finkemeier & Leister, 2010).

The *de novo* synthesis of fatty acids is exclusively localised within the plastids. These fatty acids are used to synthesise either galactolipids in the plastid envelopes or to make phospholipids in the endoplasmic reticulum (Breuers *et al.,* 2011; Johnston *et al.,* 1997; Konishi *et al.,* 1996). Lipids fulfil diverse functions, including the formation of membranes, that serve as diffusion barriers and separate cells and organelles from each other. So far, more than 10 membrane lipid classes are known. The most common are phospholipids, galactolipids and sphingolipids, whereby variations in acyl chain composition increase the structural diversity to a number of several hundred possible lipid species (Li-Beisson *et al.,* 2013).

Thylakoid membranes harbour the photosynthetic machinery in chloroplasts and are exclusively composed of monogalactosyldiacylglycerol (MGDG), digalactosyldiacylglycerol (DGDG), phosphatidylglycerol (PG) and sulfoquinovosyldiacylglycerol (SQDG). Although the inner envelope of the chloroplast resembles to lipid composition found in thylakoids, the outer envelope has a higher proportion of phosphatidylcholine (PC; Andersson and Dörmann, 2008; Li-Beisson *et al.,* 2013).

Further, chloroplasts are also involved in the assimilation of ammonia into organic nitrogen in form of glutamine and glutamate, that serve as nitrogen donors for the biosynthesis of nitrogen-containing compounds, nucleic acids and amino acids (Coruzzi, 2003). Besides the role of the amino acids in protein biosynthesis, they also serve as substrates for a variety of primary and secondary plant metabolites. Especially the aromatic amino acids, have an outstanding importance in the plant metabolism, as over 30% of the photosynthetically fixed carbon is utilised by the shikimate pathway to produce chorismate, the final product and common precursor of the aromatic amino acids, whereby the majority of the carbon flux is directed towards phenylalanine biosynthesis (Herrmann & Entus, 2001; Lynch & Dudareva, 2020; Ramon *et al.,* 1998).

The metabolites derived from the aromatic amino acids tryptophan, tyrosine and phenylalanine have various important roles in maintaining plant growth, development, reproduction, defence responses as well as acclimation and adaptation to environmental stress. For example, tryptophan is a precursor for auxin, alkaloids, indole glucosinolates and phytoalexins, while tyrosine serves as a precursor to quinones, betalaines and isoquinoline alkaloids. Phenylalanine contributes to the production of over 8000 phenolic compounds, from which the most important are lignin, anthocyanins, flavonoid, isoflavonoids, tannins and volatiles (Rodney Croteau, Kutchan and Lewis, 2000; Herrmann and Entus, 2001; Bonawitz and Chapple, 2010; Maeda and Dudareva, 2012; Lynch and Dudareva, 2020).

Thus, to provide plastid-derived metabolites that are required for various specific functions and pathways in the surrounding plant cell, the plastid possesses highly specialised transport systems within its envelopes. The respective metabolic fluxes are adjusted in response to the developmental stage and environmental stimuli (Finkemeier & Leister, 2010). Thus, the chloroplast is a crucial component in plant growth and acclimation or adaptation, since this organelle is also able to sense environmental changes and actively participate in stress responses (Crosatti *et al.,* 2013; Kleine *et al.,* 2021; Kleine & Leister, 2013; Oliver Trentmann *et al.,* 2020).

1.2. Acclimation to chilling and freezing stress

The harmful effects of low temperatures on plant productivity and growth have been well documented (Boyer, 1982; Keller *et al.,* 2021; Mahajan & Tuteja, 2005). This phenomenon, at least partially, attributes to an imbalance between primary and secondary photosynthetic reactions within the chloroplasts, resulting in the production of reactive oxygen species (ROS). Although ROS can act as signalling molecules, cellular damage occurs when certain steady-state redox levels are exceeded (Choudhury *et al.,* 2017).

Further, ice crystals form at sub-zero temperatures, interrupting the CO_2 uptake, impairing the water oxidation system and dehydrating the cell (Boyer, 1982; Crosatti *et al.,* 2013). During the freeze-induced dehydration, plasma or tonoplast membranes and chloroplast envelopes become closely proximate. This proximity compromises the integrity of the bilayer membranes, potentially leading to the formation of inverted micellar intermediates (Figure 1A). In non-acclimated plants, these non-lamellar phases can form inverted, cylindrical micelles, known as the lamellar-to-hexagonal II phase transition (Figure 1B; Ruelland *et al.,* 2009; Moellering, Muthan and Benning, 2010; Moellering and Benning, 2011). In cold-acclimated plants, formation of micellar intermediates results in interlamellar attachments between the plasma and intracellular membranes (Figure 1C). Thus, closely appressed bilayer structures can rapture during the thawing process (Figure 1D; Gordon-Kamm and Steponkus, 1984; Ruelland *et al.,* 2009; Crosatti *et al.,* 2013).

To acclimate to low temperatures and enhance the freezing tolerance the CBF genetic systems is activated, which includes numerous C-repeat (CRT)/dehydration responsive element (DRE)-binding factors, such as CBF1, CBF2 or CBF3, also referred to as DREB1b, DREB1c and DREB1a, respectively (Cook *et al.,* 2004; Fowler & Thomashow, 2002; Gilmour *et al.,* 2000; Smallwood *et al.,* 2002; Thomashow, 1998, 1999). These transcriptional activators recognise cis-acting regulatory elements in the promoter regions of numerous cold-inducible genes, such as for example *COR15a* (Cook *et al.,* 2004; Gilmour *et al.,* 2000; Liu *et al.,* 2002; Medina *et al.,* 1999). The polypeptide COR15a has been shown to elevate the membrane phase transition temperature, protecting membranes from fusion and disruption (Steponkus *et al.,* 1998; Thalhammer *et al.,* 2010; Thomashow, 1998).

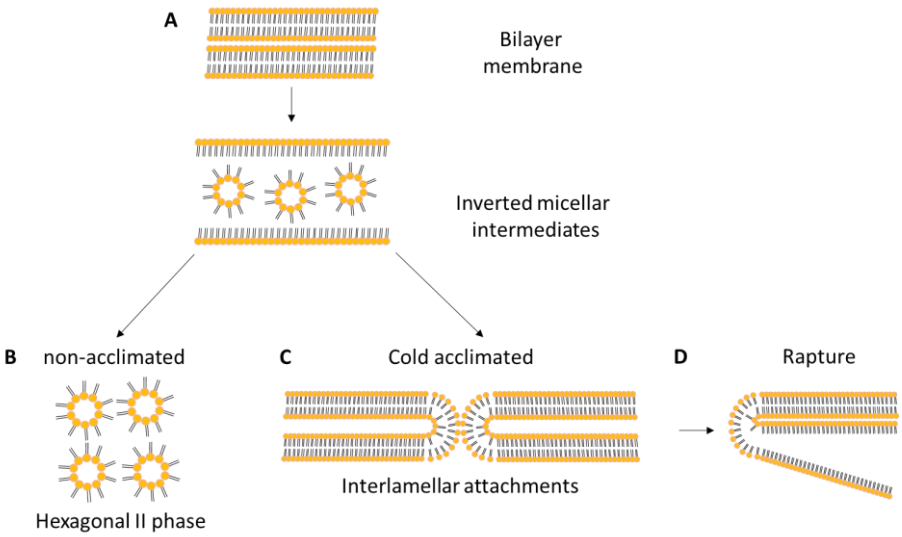

Figure 1: Destabilisation of bilayer membrane structure due to freezing-induced dehydration. The proximity of bilayer membranes results in the formation of inverted micellar intermediates (A). In non-acclimated plants a lamellar-to-hexagonal II phase transition occurs (B). In cold-acclimated plants, formation of micellar intermediates results in interlamellar attachments (C), which can rapture during the thawing process (D; Ruelland *et al.,* 2009).

In addition, extensive metabolic rearrangements appear during cold acclimation, such as an increase in soluble sugars e.g., glucose, fructose, inositol, galactinol, raffinose and sucrose, which act as cryoprotective osmolytes. Correspondingly, sugar accumulation may be accompanied by up-regulation of the citric acid cycle, which further leads to increased levels of α-ketoglutarate, fumarate, malate and citrate (Cook *et al.,* 2004; Gilmour *et al.,* 2000; McKown *et al.,* 1996; Reyes-Díaz *et al.,* 2006; Ruelland *et al.,* 2009; Taji *et al.,* 2002; Wanner & Junttila, 1999). The synthesis osmolytes, also includes various amino acids, such as proline, asparagine, aspartate, glutamine, glutamate, and alanine, which also have a cryoprotective function during freezing-induced dehydration and potential membrane damage (Cook *et al.,* 2004; Gilmour *et al.,* 2000; Hoermiller *et al.,* 2017; Klotke *et al.,* 2004; Steponkus, 1984; Steponkus *et al.,* 1988, 1998; Taji *et al.,* 2002; Uemura & Steponkus, 1997).

Another feature commonly observed in cold-acclimating plants is the accumulation of anthocyanins in leaves and stems. Anthocyanins are synthesised by the phenylpropanoid pathway, controlled by the key enzymes phenylalanine ammonia lyase (PAL) and chalcone synthase (CHS). The *PAL* and *CHS* transcripts accumulate in *Arabidopsis thaliana* during cold exposure in a light- or osmotic-dependent manner (Chalker-Scott, 1999; Leyva *et al.,* 1995; Ruelland *et al.,* 2009). The function of the anthocyanins is to protect the photosynthetic activity during photo-inhibitory conditions (Havaux & Kloppstech, 2001; Ruelland *et al.,* 2009). In addition to this, anthocyanins are also potent antioxidants, and due to their amphiphilic characteristics assumed to be involved in the protection of membranes (Korn *et al.,* 2008; Rice-Evans *et al.,* 1996; Ruelland *et al.,* 2009).

The accumulation of sugars, amino acids and anthocyanins has been shown to alter the osmotic potential (Guy, 1990; Ruelland *et al.,* 2009). A simple doubling of internal solute concentration can decrease the extent of cell dehydration by as much as 50% at sub-zero temperatures (Ruelland *et al.,* 2009; Steponkus, 1984). Furthermore, the presence of sugars has been shown to reduce ice nucleation in plants, as evidenced by studies demonstrating a correlation between sugar accumulation and ice nucleation at freezing temperatures (Reyes-Díaz *et al.,* 2006; Ruelland *et al.,* 2009). Thus, a new metabolic homeostasis is established in the cold, which is a highly energy-demanding process (Cook *et al.,* 2004).

1.2.1. Chloroplast membranes during low temperature stress

Chilling and freezing temperatures may damage chloroplast membranes, directly affecting light-dependent reactions of the photosynthetic activity. Therefore, the thylakoid membranes are stabilised by alterations in their lipid composition. For example, the degree of fatty acid desaturation increases during cold conditions to enhance membrane fluidity (Crosatti *et al.,* 2013; Uemura & Steponkus, 1997). Further, inner and outer envelopes of the chloroplast, also undergo membrane remodelling to reduce the amount of MGDG, as this lipids is likely to form hexagonal II phases when subjected to freezing stress (Moellering *et al.,* 2010; Moellering & Benning, 2011; Ruelland *et al.,* 2009; Song *et al.,* 2021; Yu *et al.,* 2021).

The reduction of MGDG contents under low temperatures is achieved by the galactolipid galactosyltransferase SENSITIVE TO FREEZING 2 (SFR2). The SFR2 protein resides in the outer envelope of the chloroplast and is activated in response to cytosolic acidification under freezing stress (Barnes *et al.,* 2016). SFR2 transfers galactosyl residues from the MGDG headgroup to other galactolipid acceptors, to increase the membrane proportion of DGDG and other oligo-galactolipids (Figure 2). Thereby the double layered membrane is stabilised and membrane leakage and shrinkage is prevented upon frost-induced dehydration (Barnes *et al.,* 2016). During the process of membrane remodelling, diacylglycerols (DAGs) are released. Since DAGs are non-bilayer forming lipids, DAG pools are rapidly transformed into triacylglycerols to prevent membrane destabilisation via the action of the diacylglycerol acyltransferase DGAT1 (Figure 2; Barnes, Benning and Roston, 2016; Arisz *et al.,* 2018).

Triacylglycerol accumulation and storage in oil lipid droplets operates as a reservoir for membrane lipids that have been altered, remodelled or removed from membranes (Lu et al., 2020). Functianlly, triacylglycerol pools serve as carbon and energy storage reserves, which undergo degradation under post-stress conditions (Baker *et al.,* 2006; Mueller *et al.,* 2017; Yu *et al.,* 2021).

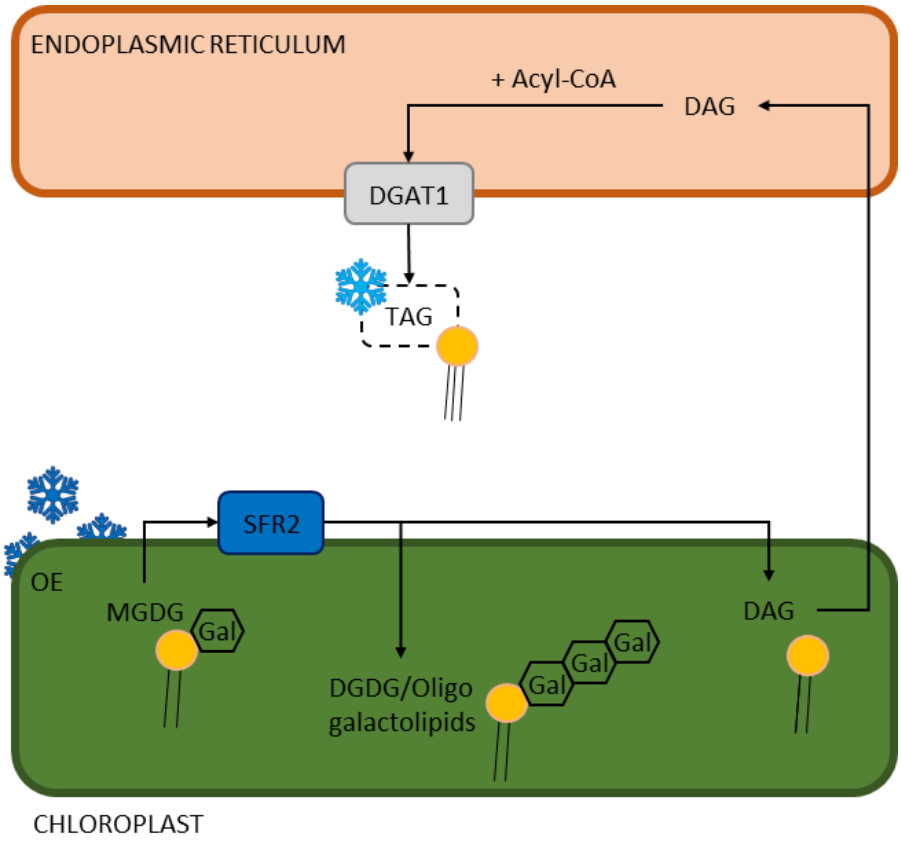

Figure 2: The function of SFR2 and DGAT1 in relation to chilling and freezing stress. SFR2 (SENSITIVE TO FREEZING 2) is a galactolipid galactosyltransferase located in the outer envelope of the chloroplast. During freezing stress, SFR2 facilitates the transfer of galactosyl residues from the monogalactosyldiacylglycerol (MGDG) headgroup to other galactolipid acceptors, increasing the membrane proportion of digalactosyldiacylglycerol (DGDG) and other oligo-galactolipids. Concurrently, diacylglycerols (DAGs) are released during the membrane remodelling. The DAGs are converted into triacylglycerols via the diacylglycerol acyltransferase 1 (DGAT1; Barnes, Benning and Roston, 2016; Arisz *et al.,* 2018).

1.2.2. Cell wall remodelling during chilling and freezing temperatures

The cell wall architecture, in addition to metabolic and membrane adjustments, is also modified in response to low, non-freezing temperatures (Ruelland *et al.,* 2009; Solecka *et al.,* 2008). Further, transcriptome and proteome studies indicate that cell wall remodelling is particularly important during sub-zero acclimation (Takahashi *et al.,* 2021). The cell wall plays a pivotal role in protecting cells from damage caused by ice nucleation, ensuring plant survival (Ruelland *et al.,* 2009).

For example, in oil-seed rape (*Brassica napus* ssp. *oleifera*), it has been observed that a temperature of 2°C leads to an increase in leaf tensile stiffness, which is associated with an increase in cell wall components such as pectin content, pectin methyl esterase activity and the abundance of low-methylated pectin (Ruelland *et al.,* 2009; Solecka *et al.,* 2008). Cold-dependent pectin modifications in cell wall structure protect the cells against freezing-induced damage and mechanical stress (Jarvis & McCann, 2000; Solecka *et al.,* 2008).

In Arabidopsis, cell wall alterations during at -3°C to 4°C affect cellulose, hemicellulose and pectin (Le *et al.,* 2008; Reiter *et al.,* 1997; Takahashi *et al.,* 2019, 2021, 2024). Cellulose microfibrils, composed of 1,4-β-D-glucan, associate with xyloglucan, creating a network embedded into a gel-like matrix formed by pectin. Xyloglucan consists of a 1,4-β-D-glucan backbone, decorated with mono-, di- or trisaccharide side chains of D-xylose, D-galactose or L-fucose (McNeil *et al.,* 1984; Reiter *et al.,* 1997). Pectin is predominantly comprised of homogalacturonan, rhamnogalacturonan I and II, which are rich in D-galactosyluronic acid, L-rhamnose, D-galactose, L-arabinose and L-fucose (Harholt *et al.,* 2010; McNeil *et al.,* 1984; Takahashi *et al.,* 2019, 2021).

Pectin can be demethylated by pectin methyl esterases (PMEs) during sub-zero acclimation. Demethylated homogalacturonan can cross-link with calcium cations (Ca^{2+}), which results in cell wall rigidification (Levesque-Tremblay *et al.,* 2015; Scheler *et al.,* 2015; Takahashi *et al.,* 2019, 2021). The total amount of methylated homogalacturonan affects the cell wall pore size and correlates with tensile strength and freezing tolerance (Murina *et al.,* 2019; Rajashekar & Lafta, 1996; Takahashi *et al.,* 2021).

Whereas xyloglucan endotransglucosylases/endohydrolases e.g., XTH19, XTH21 or XTH22, play a pivotal role in the remodelling of xyloglucan by cleaving and rearranging the xyloglucan backbone. The cell wall extensibility of the xyloglucan-cellulose network is thereby regulated in response to environmental stimuli (Eklöf & Brumer, 2010; Park & Cosgrove, 2012; J. K. C. Rose *et al.,* 2002; Takahashi *et al.,* 2021).

1.3. Dynamically responding chloroplast envelope proteins

Upon cold stress, proteins and transporters, particularly in the envelope system of the chloroplast, respond dynamically to low temperatures as part of the coordinated acclimation programme (Trentmann *et al.,* 2020). For instance, the nucleotide triphosphate transporter 2 (NTT2) increases in protein abundance to compensate for cold-induced energy limitations of photosynthetic activity, while the maltose exporter 1 (MEX1) was shown to decrease in protein abundance, retaining and elevating maltose levels in the chloroplast as protective mechanism (Kaplan *et al.,* 2004; Trentmann *et al.,* 2020). The fatty acid exporter FAX1, along with certain subunits of the trigalactosyldiacylglycerol (TGD) protein complex e.g., (TGD2/ABCI15 and TGD3/ABCI13), the latter of which serves to facilitate the ER-to-chloroplast lipid transfer, decrease in protein abundance upon cold stress to retain fatty acids in the chloroplast for galactolipid synthesis. In addition to the TGD subunits, various other ATP-binding cassette (ABC)-type proteins are also altered in abundance. For example, the ABCG7 protein declined after 4 days at 4°C (Trentmann *et al.,* 2020).

1.4. ATP-binding cassette transporters

The ATP-binding cassette transporter family is one of the most abundant transporter families, allowing the transport of diverse substrates among membranes by primary active transport (Higgins, 1992; Higgins and Linton, 2004; Roston *et al.,* 2014). Plants have eight subfamilies of ABC transporters (ABCA-G), of which some are already known to play a crucial role in various biological processes, such as xenobiotic detoxification, phytohormone or lipid transport (Higgins, 1992; Theodoulou, 2000; Higgins and Linton, 2004; Biemans-Oldehinkel, Doeven and Poolman, 2006).

Irrespective of the physiological function, ABC transporters are composed of 4 core domains. These include 2 transmembrane domains (TMDs), each consisting of multiple membrane-spanning α-helices that provide a pathway for the transported substrate across the lipid bilayer, and 2 nucleotide binding domains (NBDs) energising the transport process. Several characteristic motifs in the NBD of ABC proteins share an extensive amino acid sequence identity, such as the Walker A, Walker B and ABC signature motifs, which are required to facilitate ATP-binding and hydrolysis (Rea, 2007; Sánchez-Fernández *et al.,* 2001; Walker *et al.,* 1982).

Further, ABC type transporters are categorised into full-size and half-size transport proteins. Full-size transporters already consist of 2 TMDs and NBDs. Whereas half-size transporters, such as ABCG7, contain only one TMD and NBD domain (Rea, 2007; Sánchez-Fernández *et al.,* 2001). Half molecular transporters usually form homo- or heterodimers to become functional. Additionally, ABC transporters can be expressed in either forward or reverse orientation. In the forward orientation, the peptide sequence begins with a TMD, while in the reverse orientation, it starts with a NBD (Christopher F. Higgins & Linton, 2004; Rea, 2007; Sánchez-Fernández *et al.,* 2001).

Among the multiple subfamilies within the ABC transporter superfamily, the ABCG subfamily is the largest and most diverse. ABCG transporters, also known as white-brown-complex (WBC) transporters, respond to environmental stresses and play a role in plant development (Verrier *et al.,* 2008). In Arabidopsis, 29 half-size and 15 full-size ABCG subfamily transporters are known (Gräfe & Schmitt, 2021; Reinhold *et al.,* 2007; Sánchez-Fernández *et al.,* 2001).

1.5. Significance of characterising the ABCG7 transporter

Despite the identification of the decreasing ABCG7 abundance in proteome datasets of cold-acclimating Arabidopsis wild type plants, the physiological function of this ABC-type transporter remains elusive (Trentmann *et al.,* 2020). Further research is required to determine the exact subcellular localisation of this transporter and its role in acclimation to stress, particularly chilling and freezing conditions.

To investigate the localisation of the ABCG7 transporter, microscopic techniques and protease assays with isolated chloroplasts were conducted. The primary objective was to ascertain why the abundance of the ABCG7 transporter decreases during the process of cold acclimation, and to determine whether this might be an essential mechanism to ensure the successful acclimation of Arabidopsis to upcoming freezing stress.

To this end, *abcg7* loss-of-function lines were characterised during the acclimation processes to cold and frost stress. A RNA sequencing was conducted, with the aim to identify potential differences in the cold acclimation programme between wild types and *abcg7* mutants. Furthermore, a comprehensive metabolomic analysis was directed, encompassing sugars, organic acids, amino acids, and anthocyanins, to elucidate possible alterations in metabolic responses to cold and freezing stress in both, wild types and *abcg7* lines. The analysis was complemented by the measurement of cell wall sugars during subsequent freezing experiments and the assessment of major lipids classes, given the pivotal role of cell walls at low temperatures and sensitivity of membranes, especially during freezing conditions.

2. Material and methods

2.2. Plant cultivation

2.2.1. Arabidopsis lines and homozygosity testing

For experiments within this dissertation, the Columbia variety of the plant species *Arabidopsis thaliana* (L. Heynh.) was used. To identify the physiological function of the ABC-type transporter ABCG7/WBC7 experiments were carried out on wild types as well as the 2 T-DNA insertion lines, *abcg7-1* (SALK_110674) and *abcg7-2* (GABI_796G01). The T-DNA insertion lines were provided by the Nottingham Arabidopsis Stock Centre (http://arabidopsis.info/; Nottingham, UK). The homozygosity of the *abcg7* loss-of-function lines was verified using gene-specific *ABCG7* primers (*ABCG7*_fwd and *ABCG7*_rev), in combination with primers for the respective T-DNA insertion of *abcg7-1* or *abcg7-2* (LBb1.3 or o8474). An *EF1α* primer pair was utilised as control for successful amplification by polymerase chain reaction (PCR). The primer sequences are summarised in Table 1.

Table 1: Primers used for homozygosity screening of the *ABCG7* T-DNA insertion lines. The name of the primers and sequences 5`-3` (fwd) and 3`-5` (rev) are indicated.

Gene	Primer name	Sequence
ABCG7	*ABCG7*_fwd	ATGGCGCCTTTTGGC
	*ABCG7*_rev	TTACAAACCTTCGAGGACAAAG
T-DNA	LBb1.3	ATTTTGCCGATTTCGGAAC
	o8474	ATAATAACGCTGCGGACATCTACATTT
EF1α	*EF1α*_fwd	GAGACCACCAAGTACTACTGCAC
	*EF1α*_rev	GTTGGTCCCTTGTACCAGTCAAG

2.2.2. Plant cultivation on soil

The standardised soil ED-73 (300 mg/L N, 300 mg/L P_2O_5, 600 mg/L K_2O, 3 mg/L KCL, pH6 adjusted with $CaCl_2$) was used to cultivate Arabidopsis plants. Seeds were shown on soil and subsequently stratified for 2 days at 4°C in the dark (Weigel & Glazebrook, 2002). Stratified seeds were transferred to standard growth conditions for 7 to 10 days, whereafter seedlings were transplanted into individual pots (6 cm in diameter) and grown under standard conditions for further 4 weeks before starting cold, freezing or leaf disc experiments (see chapter 2.3). The standard growth conditions were 120 µE light for 10 hours at 22°C, followed by 14 hours of darkness at 18°C.

To investigate the cold acclimation of wild types and *abcg7* loss-of-function mutants, 4-week-old plants were transferred to a Fitotron growth chamber (Fitotron, Weiss Umwelttechnik GmbH, Reiskirchen-Lindenstruth, Germany). During the acclimation process to low temperatures, the plants were maintained at a temperature of 4°C for up to 10 days (10 hours of light and 14 hours of darkness). To characterise the phenotype of cold acclimated plants, the rosette morphology was photographed , and the rosette dry weight was determined. For the detailed description of the freezing experiments see chapter 2.3.1. A minimum of 4 to 5 plants per genotype were utilised for the study of cold and freezing tolerance.

2.2.3. Surface sterilisation of seeds and plate experiments

For plate experiments, seedlings were cultivated under sterile conditions. Therefore, seeds of wild types and *abcg7* loss-of-function lines were first surface sterilised. Seeds were incubated for 10 min in 1 mL of a solution of 70% (v/v) p.A. ethanol (EtOH) and 0.05% (v/v) TritonX, under constant invertation at 80 rpm. The seeds were sedimented at a speed of 11,000 rpm for 1 min, employing an Eppendorf Centrifuge 5417R (Hamburg, Germany). The supernatant was discarded, followed by an addition of 500 µL of 70% (v/v) EtOH for a second washing step of 10 min at 80 rpm. In the meantime, filter paper (Marchery-Nagel, Düren, Germany) was positioned within petri dishes. The closed petri dish, with the filter paper inside, was sterilised in the microwave at 600 W for 2 min. Surface sterilised seeds were transferred into the petri dishes to evaporate residual ethanol from the seed. The drying of the seeds was achieved under the clean bench (Kojair Tech Oy Kr-201 Safety, Finland) to dry ace.

To analyse the phenotypical appearance of wild types and *abcg7* mutants grown in the presence of galactose, first ½ MS plates were prepared. The ½ MS plates (0.5% (w/v) MS, 2 mM MES (w/v), pH 5.8 adjusted with KOH, 1% (w/v) plant agar) were prepared either without sugar or with 1 % (w/v) galactose. For this purpose, 50 mL of the respective medium was poured into sterile petri dishes. Both plate types contained 1 % (w/v) plant agar (Duchefa Biochemie, Netherlands). After the complete drying of the plates, about 20 seeds per line were plated and stratified for 2 days under 4°C in the dark. After stratification plates were transferred to standard growth conditions.

To characterise the phenotype of wild type and *abcg7* mutant seedlings, plates were photographed to document the rosette morphology, and the fresh weight of pooled samples was determined. Each biological replicate consisted of 20 seedlings, which were pooled together and a minimum of 4 to 5 replicates were harvested.

2.3. Physiological methods

2.3.1. Evaluation of freezing tolerance and recovery

Freezing tolerance and recovery of wild type and *abcg7* mutants were assessed in a Percival plant growth cabinet (type AR-36L/LT; www.plantclimatics.de) according to Trentmann *et al.,* 2020. The modifications of the experimental set-up are described as follows:

Approximately 4-week-old plants were cold acclimated for 4 days under short-day conditions (light 10h/4°C; dark 14h/4°C). The following day, the diurnal cycle was turned off and the temperature was lowered from 4°C to -10°C every hour (2°C to 4°C/h). The freezing temperature of -10°C was maintained overnight, after which the temperature was increased to 22°C. The temperature was increased by 2°C to 4°C/h. The plants were kept in the dark until the following day, when the diurnal cycle was restored (light 10h/22°C; dark 14h/18°C).

Frost-recovered plants were documented 2 to 3 weeks after freezing stress. Survival was determined by quantifying surviving versus dead plants. Furthermore, the expression of *ABCG7* during the experiment was investigated by quantitative PCR (qPCR), as well as the transcription pattern of cell wall and cell membrane related genes (see chapter 2.5.11). In addition to the analysis of transcription rates in wild type and *abcg7* mutants, the composition of cell wall sugars (see chapter 2.3.10) and cell membranes was also examined (see chapter 2.3.11).

2.3.2. Leaf disc experiments

For leaf disc experiments, wild type plants were grown under standard growth conditions for 4 weeks, after which leaf discs of 5 mm diameter were excised from individual leaves. Each biological replicate consisted of 5 pooled leaf discs from 3 to 5 different wild type plants. A minimum of 3 to 5 biological replicates were used for leaf disc experiments.

Leaf discs were incubated in 5 mL of 3 mM MES buffer (pH 5.6 adjusted with NaOH; Roth, Karlsruhe, Germany). For expression analysis of genes affected by the presence of galactose (AppliChem, Darmstadt, Germany), 50 mM of the respective sugar was added to 3 mM MES buffer. In addition, an osmotic control was used by preparing 3 mM MES buffer with 50 mM mannitol (Duchefa Biochemie, Haarlem, Netherlands).

For expression analysis of genes affected by the presence of chorismate (Merck; Darmstadt, Germany), phenylalanine or tryptophan (Thermo scientific, China), 50 to 200 µM chorismate, 200 µM phenylalanine or 200 µM tryptophan were added to the MES buffer. Due to the hydrophobicity of tryptophan, a stock solution of 500 mM tryptophan was previously prepared, whereby tryptophan was dissolved in 30% (v/v) dimethyl sulfoxide (DMSO, Thermo scientific, Belgium). The corresponding amount of 30% (v/v) DMSO was added to the MES buffer as a control for the tryptophan treatment. Leaf discs were incubated overnight in the dark with constant shaking at 100 rpm.

2.3.3. Extraction of soluble metabolites

Leaf material from 4-week-old plants, or 2-week-old seedlings grown on ½ MS agar plates, were harvested, snap-frozen and stored in liquid nitrogen until extractions of soluble metabolites, such as sugars and amino acids or starch were performed. For the extraction, samples were homogenised in liquid nitrogen using a mortar. About 50 mg of ground plant material was aliquoted into 1.5 mL reaction tubes with screw caps.

To each sample, 1 mL of 80% (v/v) EtOH was added and vigorously vortexed. The samples were subjected to an incubation step for 1 hour at 85°C with constant shaking (500 rpm; ThermoStat plus, Eppendorf for 1.5 mL reaction tubes, Hamburg, Germany) to extract sugars and amino acids. Subsequently, samples were subjected to centrifugation at 11,000 rpm. A volume of 800 µL of the supernatant was transferred to a fresh 2 mL reaction tube, while 1 mL of 80% (v/v) was added to the pellet, and the extraction and centrifugation steps were repeated.

After the second extraction step, 800 µL of the supernatant was transferred into the tube which already contained the ethanolic extract from the first extraction. The pooled extract was evaporated in the Speedvac concentrator plus (Eppendorf, Hamburg). After evaporation, the soluble metabolites were dissolved in 500 µL of ddH_2O. The pellet was utilised for starch extraction (see chapter 2.3.4).

Measurement of soluble sugars was achieved photometrically and is described in chapter 2.3.5.

Analysis of amino acids was achieved by high performance liquid chromatography (HPLC) described in chapter 2.3.6.

2.3.4. Starch extraction

After the extraction of soluble metabolites, a pellet from the ground plant material remained. This pellet is utilised to disintegrate the sedimented starch into glucose for quantification. The pellet was subjected to a washing procedure, comprising a single cycle of 500 µL of 80% (v/v) EtOH, followed by a further cycle with 1 mL of ddH_2O. During both washing cycles, the pellet was vortexed and subjected to a centrifugation step at 14,000 rpm for 5 min. Afterwards, 500 µL of ddH_2O was added to the pellet, followed by autoclaving at 120°C for 40 min.

After autoclaving, 200 µL of a 200 mM sodium acetate solution (pH 4.8), containing 5 units (U) of α-amlyase and 5 U of amlyglucosidase, was added to each sample to degrade the starch within the sample (SIGMA-ALDRICH, Switzerland). Samples were subjected to a digestive step at 37°C overnight, constantly shaking at 180 rpm. Enzyme activity was terminated by subjecting the samples to an incubation step at 95°C for a period of 10 min. This process of starch digestion resulted in a breakdown and release of the constituent glucose units into the supernatant. Following centrifugation at 14,000 rpm for a duration of 10 min, the glucose-containing supernatant was transferred to a new reaction tube and subsequently used to measure the glucose content (see chapter 2.3.5).

2.3.5. Photometric sugar measurements

To determine the contents of sucrose, glucose and fructose, a photometric enzyme assay was employed (Stitt *et al.,* 1989). The extinction of the enzyme-coupled NADH production was measured at 340 nm in a photometer (Tecan Infinite M Nano, Männedorf, Switzerland). For this purpose, 20 µL of a sample were mixed with 190 µL of a premix consisting of 100 mM HEPES pH 7.5, 10 mM $MgCl_2$, 2 mM ATP (GERBU, Heidelberg, Germany), 0.8 mM NAD (AppliChem, Darmstadt, Germany), and 5 U glucose-6-phosphate dehydrogenase (Roche, Mannheim, Germany).

The enzymes hexokinase (Roche, Mannheim, Germany) and phospho-gluco-isomerase (Roche, Mannheim, Germany), which are required to determine glucose and fructose contents, are diluted 1:10 in 333 mM HEPES pH 7.5 prior to usage. The enzyme invertase (Sigma-Aldrich, St. Louis, USA), which is required for the measurement of sucrose contents, is added to a 1.5 mL reaction tube until the 500 µL mark and reconstituted in 300 µL volume of 333 mM HEPES solution, pH 7.5.

Initially, 15 measurement cycles are conducted, which serve as a blank measurement. Subsequently, 1.5 µL of hexokinase is added, followed by and 40 measurement cycles. Hexokinase converts glucose into glucose-6-phosphate, accompanied by adenosine triphosphate (ATP) consumption and release of

adenosine diphosphate (ADP). Subsequently, the enzyme glucose-6-phosphate dehydrogenase converts glucose-6-phosphate into 6-phosphogluconolactone. The nicotinamide adenine dinucleotide hydrogen (NADH) yield in this reaction step is directly proportional to the respective enzymatic reaction (Figure 3, step 1). This is followed by the addition of 1.5 µL PGI to the samples, after which 30 cycles of measurement are performed. The fructose present in the sample is phosphorylated by the hexokinase. The resulting fructose-6-phosphate is converted into glucose-6-phosphate by the phospho-gluco-isomerase and thus subsequently undergoes quantification by the production of NADH (Figure 3, step 2). Finally, 1.5 µL of invertase is added to the sugar samples for photometric measurements. The measurement is completed within 40 cycles. The invertase catalyses the hydrolysis of sucrose into glucose and fructose. The previously added hexokinase and phosphor-gluco-isomerase enzymes phosphorylate and convert both monosaccharides to allow the formation of NADP during the production of 6-phosphogluconolactone. It is imperative to acknowledge that the cleavage of sucrose results in a signal from the measurement of glucose and fructose (Figure 3, step 3).

Each measurement cycle is one minute in duration, during which the absorption of NADH at 340 nm is measured. This process enables the calculation of the contents of glucose, fructose and sucrose, by the Lambert-Beer law.

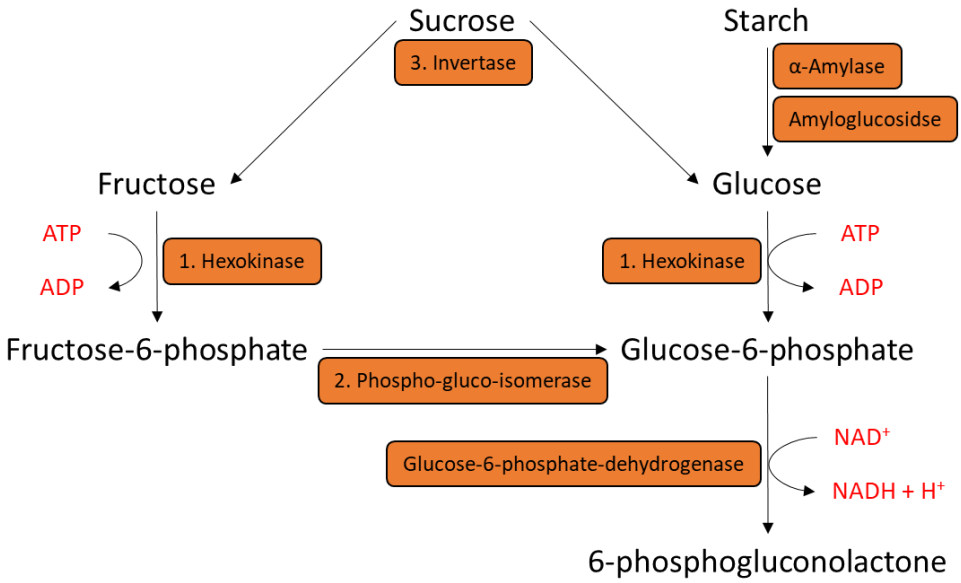

Figure 3: Enzymatic reactions during photometric sugar measurements. Starch digestion was achieved by the enzymes α-amlyase and amlyglucosidase to obtain glucose, which allows determination of the respective glucose units to estimate the starch content indirectly. The numerical values assigned to each enzyme denote the sequence in which hexokinase (1), phosphor-gluco-isomerase (2) and invertase (3) were added. The enzyme glucose-6-phosphate dehydrogenase, which was added into the pre-mix for the photometric measurement converts glucose-6-phosphate into 6-phosphogluconolactone, which yields NADH. The absorption of NADH is measured at 340 nm to calculate calculation the contents of glucose, fructose and sucrose, by the Lambert-Beer law. The following abbreviations are employed: ADP, adenosine diphosphate; ATP, adenosine triphosphate; NAD^+, nicotinamide adenine dinucleotide; NADH, nicotinamide adenine dinucleotide hydrogen.

2.3.6. Quantification of sugars by IC-measurements

The sugars sucrose, fructose, glucose and galactose within the extract of the soluble metabolites (see chapter 2.3.3) were measured in a 930 Compact IC Flex (Metrohm, Switzerland). For amperometric quantification with Au-, Pd- and Fe-electrodes, a Metrosep Carb 2-250/4.0 column was used during ion chromatography. The column temperature was set to 32°C and the detector to 35°C. As mobile phase 100 mM NaOH with 10 mM sodium acetate (NaOAc) was used with a velocity of 0.5 mL/min. The resulting peaks were analysed using the MagICNet 4.0 software (Version: 4.0 Build: 137; Metrohm, Switzerland).

2.3.7. Analysis of amino acids by HPLC-measurements

The obtained samples of soluble metabolites (see chapter 2.3.3) were centrifuged for 10 min at maximum speed, whereafter a sample volume of 20 µL was mixed with 60 µL of borate buffer (0.2 M borate, pH 8.8 adjusted with NaOH). Subsequently, 20 µL of 6-aminoquinolyl-N-hydroxysuccinimidyl carbamate (3 mg AQC/1.5 mL acetonitrile) was added to the sample and vigorously vortexed for 10 sec, followed by an incubation step at 55°C for 10 min for metabolite derivatisation. Next, a volume of 100 µL was transferred into glass vials for HPLC measurements.

The amino acid contents within the extracts were measured by HPLC in a Dionex system (Dionex Softron, Germering, Germany). The HPLC system consists of a Dionex ASI-100 automatic sample injector, a Dionex P680 HPLC pump and a Dionex RF2000 fluorescence detector. Further, a 250/4 Nucleodur 100/5 c18ec column (Macherey Nagel, Germany) with an 8/4 nucleodur 100-5 c18ec pre-column (Macherey Nagel, Düren, Germany) was employed. The measurement was performed at a column temperature of 32°C, with a velocity of 6 mL/min for the separation of amino acids. The utilised buffers were as follows: buffer A consisted of 100 mM sodium acetate with 7 mM triethanolamine (pH 5.2, adjusted with acetic acid) and buffer B was composed of 90% (v/v) acetonitrile. The gradient flow started with 2 min of 0% buffer B, followed by 26 min of 3% buffer B. At timepoint 28.5 min 11% of buffer B were followed by 12% buffer B at 31 min, 17% buffer B at 35 min, 24% buffer B at 42 min, 30% buffer B at 47 min, 100% buffer B at 52 min and 0% buffer B at 61 min. Peaks were subsequently analysed using Chromeleon software (version 6.70, DIONEX, Sunnyvale, USA).

2.3.8. Extraction of soluble sugars for GC-analysis

For the extraction of soluble sugars from cold-acclimated wild types and abcg7 mutants, plants were grown under standard growth conditions for 4 weeks and then transferred to 4°C for 4 days. For each biological replicate, 3 rosettes were pooled and immediately snap frozen in liquid nitrogen. The frozen samples were lyophilised (Alpha 2-4 LD plus, Christ, Harz, Germany) and subsequently homogenised using an MM 301 ball mill (Retsch, Retsch GmbH, www.retsch.de).

The extraction process was started by adding 400 µL of 80% (v/v) EtOH and incubating at 80°C for 1 hour, with ribitol as the internal standard in the first extraction step (20 µg of ribitol was added). After this, the extracts were dried in a Speedvac concentrator and dissolved in 100 µL ddH_2O (Nägele *et al.,* 2012). Prior to the GC measurement, soluble sugars were first derivatized with 65 µL of 20 mg methyloxamine/mL pyridine. Sugar extracts were subjected to derivatisation by incubation at 30°C for a period of 90 min on a shaker at 100 rpm. Followed by a brief centrifugation, extracts were further incubated for 90 min at 65°C. This was followed by a second brief centrifugation. Derivatised extracts were transferred into GC glass vials for analysis of soluble sugars. Sugar measurements were completed in collaboration with Prof. Dr. Andreas Richter at the University of Rostock.

The GC analysis was performed on an Agilent technologies 6890N GC system equipped with a TG-5MS column (ThermoScientific). Samples were injected with an inlet temperature of 250°C and a nitrogen gas flow of 40 mL/min at a split ratio of 20:1. A flow of 1.8 mL/min nitrogen gas (mobile phase) and an average velocity of 45 cm/sec at 172 kPa were used for chromatography. The oven temperature was initially set at 160°C for 2 min, followed by a stepwise increase to 190°C (10°C/min) for 5 min. The temperature was increased in a stepwise gradient (1°C/min) to 200°C within 15 min, followed by a gradual increase to 280°C (15°C/min) for 5 min. The flame ionisation detector (FID) was set at 250°C, 40 mL/min hydrogen and 400 mL/min compressed air and a make-up gas flow (nitrogen) of 8.2 mL/min. Authentic standards (GC grade) were used for qualitative and quantitative analysis. The processing of chromatograms, peak detection, and integration were performed using the software: ChemStation (Agilent).

2.3.9. Extraction of amino and organic acids for LC-MS measurements

For the extraction of amino acids and organic acids, wild type and *abcg7* mutant plants were grown for 4 weeks under standard growth conditions at 22°C and afterwards transferred to 4°C for 10 days. Amino acids and the organic acids malate, fumarate and succinate were extracted from cold acclimated samples after 4 and 10 days. Like the extraction of sugars for GC measurements, ach biological replicate consisted of 3 pooled rosettes. A minimum of 3 to 5 biological replicates was used.

Frozen samples were lyophilised (Alpha 2-4 LD plus, Christ Freeze Dryers, Osterode am Harz, Germany) and homogenised using an MM 301 ball mill (Retsch, Retsch GmbH, www.retsch.de). About 10 mg of the dried and homogenised plant material was aliquoted into fresh 1.5 mL reaction tubes. Extraction of the homogenised material was performed on ice and started by the addition of the extraction solution consisting of 150 µL chloroform/350 µL methanol/1 µL MES (1 mg/mL morpholinoethanesulfonic acid, internal standard) per sample.

After all samples were processed, a volume of ice-cold 400 µL LC-MS grade water was added to the samples, which were vortexed and incubated at -20°C for 2 hours. Samples were centrifuged at maximum speed for 10 min and the supernatant was transferred to a fresh reaction tube. Further, a volume of 400 µL of ice-cold LC-MS grade water was added to the pellet of ground plant material, vortexed and centrifuged again as described to extract residual metabolites. The extracts were combined and lyophilised in a Speedvac. To reconstitute the metabolites, 400 µL of LC-MS grade water was added for subsequent LC-MS measurements. The metabolite measurements were performed by Dr. Stefan Timm at the University of Rostock, as described in Araguirang *et al.,* 2024.

For the measurements of the abovementioned metabolites, a liquid chromatography coupled to tandem mass spectrometry (LC-MS/MS), using the LCMS-8050 system (Shimadzu, Japan), was conducted. Metabolites were quantified by multiple reaction monitoring (MRM) according to the LC-MS/MS method and LabSolutions software package (Shimadzu, Japan). Authentic standards for amino acids (Merck, Germany) were used. Calibration and peak areas were normalised to the signals of the internal standard (MES). Data were evaluated using the Lab solution software package (Shimadzu, Japan).

2.3.10. Extraction and quantification of cell wall sugars

Cell wall sugars were extracted from wild type and *abcg7* mutant plants after 4 weeks of growth under standard conditions at 22°C and during the recovery phase post-freezing stress, when the temperature reached -2°C. Samples were harvested and snap-frozen in liquid nitrogen. After grinding, the homogenised material was subjected to an incubation period with 70% (v/v) EtOH to remove soluble sugars twice. For the measurements, samples were shipped to Prof. Dr. Tenhaken Raimund, to the University of Salzburg.

Subsequent extraction of cell wall sugars was carried out with 70% (v/v) EtOH, followed by 100% (v/v) acetone, whereafter the samples were dried. The resulting dry cell wall pellet was hydrolysed with 0.5 mL of 2 M TFA (tri-fluor acetic acid) at 121°C for 60 min. The hydrolysed sample was dried in a vacuum concentrator, and the resulting pellet dissolved in 1 mL of ddH_2O. This solution was diluted 1:5 with ddH_2O, and the separation of the sample was conducted on an HPLC system. The separation process was operated on a Dionex ICS 3000 HPLC system, equipped with electrochemical detection. Samples were chromatographed on a CarboPac PA20 column (3x150 mm with 3x50 mm precolumn). The flow rate was set at 450 µL/min.

The buffers employed were as follows: buffer A contained 200 mM NaOH, buffer B was 15 mM NaOH, buffer C was 50 mM NaOH with 0.5 M NaOAc, and buffer D consisted of 2.5 mM NaOH. The gradient flow was conducted as follows: the first gradient started with 0% buffer B at timepoint -20 min until -8 min, at -7 min 100% of buffer B followed until 12 min. At timepoint 12,1 min until 20 min 75% of buffer B was flowing through the column, until at timepoint 20,1 until 25 min, 100% buffer of B followed.

The samples were measured again in a second run with the following gradient, which separates xylose from mannose: At timepoint -20 min to -14 min 0% of buffer B are followed by 10% buffer B and 90% buffer D until timepoint 25 min. The peak areas were quantified with Chromelion 7.2 together with authentic standards. The measured cell wall sugars were then normalised to the authentic standards to ensure that each sugar of the standard elicited a consistent response. The measured cell wall sugars were then converted to %mol to ensure that the sum of all cell wall sugar values of a sample equals 100%.

2.3.11. Analysis of lipids by UPLC-measurements

Lipids were extracted from wild type and *abcg7* mutant plants subjected to freezing stress (see chapter 2.3.1). Samples were harvested after 4 weeks of growth under standard conditions at 22°C, to serve as control points, and during the recovery phase, when temperature reached -2°C. The harvested samples were snap-frozen in liquid nitrogen and ground in the presence of liquid nitrogen. About 50 mg of the homogenised material was aliquoted into 2 mL reaction tubes and subjected to an lipid extraction according to the methyl tert-botyl ether:methanol:water system described by Salem *et al.,* 2017. Lipid measurements and analysis was performed by Dr. Saleh Alseekh at the Max-Planck-Institut in Potsdam.

The extraction of samples was conducted in accordance with the methodologies outlined by Giavalisco *et al.,* 2011 and Salem *et al.,* 2020, with minor adjustments. In summary, 1 mL of pre-cooled extraction buffer (1:3 (v/v) methanol: methyl-tert-butyl-ether) was utilised to extract lipids. Following a 10-minute incubation at 4°C and a 10-minute sonication in a sonic bath, a volume of 500 µL of 1:1 (v/v) water:methanol mixture was added. Subsequently, the samples were subjected to a centrifugation process (5 min at 14,000 rpm). The lipophilic phase was collected and dried under vacuum conditions. The dry extracts were resuspended in 500 µL of a 7:3 (v/v) acetonitrile:isopropanol mixture and analysed using ultra-performance liquid chromatography coupled with Fourier transform mass spectrometry (UPLC-FT–MS) on a C8 reverse phase column (100 x 2.1 mm x 1.7 µm particle size, Waters) at 60 °C.

The mobile phase comprised 1% (v/v) 1 M NH_4OAc and 0.1% (v/v) acetic acid in water (Buffer A) and 7:3 (v/v) acetonitrile:isopropanol (UPLC grade, BioSolve), with the addition of 1 M NH_4OAc and 0.1% (v/v) acetic acid (Buffer B). The applied gradient profile was as follows: 1 min with 45% buffer A, 3 min linear gradient from 45% buffer A to 35% buffer A, 8 min linear gradient from 25% to 11% buffer A, 3 min linear gradient from 11% to 1% buffer A. After washing the column for 3 min with 1% buffer A, the buffer was set back to 45% buffer A, and the column was re-equilibrating for 4 min, leading to a total run time of 22 min. The flow rate of the mobile phase was 400 µL/min.

Mass spectra were acquired using an Exactive mass spectrometer (Thermo Fisher, http://www.thermofisher.com) equipped with an ESI interface. All spectra were recorded using both, altering full scan and all-ion fragmentation scan modes, covering a mass range from 100–1500 Cm/z at a capillary voltage of 3.0 kV with a sheath gas flow value of 60 and an auxiliary gas flow of 35. The resolution was set to 10,000 with 10 scans per second, and the Orbitrap loading time was restricted

to a maximum of 100 Cms with a target value of 1E6 ions. The capillary temperature was set to 150 °C, while the drying gas in the heated electrospray source was set to 350 °C. The skimmer voltage was maintained at 25 kV, while the tube lens was set to a value of 130 V. The spectra were recorded from minute 1 to minute 20 of the UPLC gradient. The processing of chromatograms, peak detection, and integration were performed using REFINER MS 14.0 (GeneData, www.genedata.com). The workflow encompassed the following steps: peak detection, retention time alignment, chemical noise and isotopic peak removal from the MS data. The resulting mass features were characterised by specific peak identification, retention time, and m/z values. An in-house lipid database was used for annotation based on the retention time and exact mass. The identification of lipids was confirmed by manual verification of the chromatograms using Xcalibur (Version 3.0, Thermo-Fisher, Bremen, Germany).

2.3.12. Extraction and quantification of anthocyanins

Anthocyanins were extracted from wild type and *abcg7* mutant plants after 4 weeks of growth under standard conditions at 22°C and after subsequent transfer to 4°C for up to 10 days. Further, anthocyanins were also extracted from seedlings grown on ½ MS agar plates either without, or with 1% (w/v) galactose. For both experiments, plant material was harvested in the middle of the light phase, after 4 hours of illumination, and immediately shock-frozen in liquid nitrogen. Plant material was homogenised within 2 to 3 days post-harvest with a mortar in liquid nitrogen. The homogenised material was aliquoted to 50 mg, and the extraction of anthocyanins was initiated according to the method of Mancinelli, 1984, except isopropanol was used instead of methanol.

A volume of 1 mL of extraction buffer (1:18:81 (v/v/v) HCl:isopropanol:ddH_2O) was added to 50 mg of the homogenised sample. Following an overnight incubation of the samples in the dark, a centrifugation step for 10 min at 14,000 rpm was performed. The resultant supernatant was used to determine the anthocyanin content photometrically. The absorption was measured at 535 nm, the maximum absorption of anthocyanins, and 650 nm, the maximum absorption of chlorophyll. The formula for calculating the anthocyanin content is as follows:

$$Anthocyanins = Abs_{535\,nm} - 2.2 * Abs_{650\,nm}$$

2.4. Cultivation and transformation of bacteria

2.4.1. Bacterial strains

Escherichia coli (*E. coli*) was utilised for the amplification of plasmids, while *Agrobacterium tumefaciens* (*A. tumefaciens*) was used to transfect *Nicotiana benthamiana* (*N. benthamiana*). The bacterial strains utilised are shown in Table 2.

Table 2: Bacterial strains. The name and description of the bacterial strains are indicated.

Strain	Genotype	Application	Literature
E. coli **XL1 Blue**	*rec*A1 *end*A1 *gyr*A96 *thi*-1 *hsd*R17 *sup*E44 *rel*A1 *lac* F´ *pro*AB *lac*IqZΔM15 Tn10 Tet^R	Cloning and plasmid amplification	Bullock, 1987
E. coli **DH5α**	F^- ϕ80*lac*ZΔM15 Δ(*lac*ZYA-*arg*F)U169 *rec*A1 *end*A1 *hsd*R17(r_K^-, m_K^+) *pho*A *sup*E44 λ^- thi-1 *gyr*A96 *rel*A1	Cloning and plasmid amplification	Taylor, Walker and Mclnnes, 1993
A. tumefaciens **GV3101**	Derivative of pTIC58, Rif^R, Kan^R	Transfection of *N. benthamiana*	Koncz and Schell, 1986

2.4.2. Plasmids

Plasmids used for the purpose of cloning in *E. coli* or for the transfection of *N. benthamiana* by *A. tumefaciens* are summarized in Table 3.

Table 3: Plasmids. The name and description of the plasmids are indicated.

Plasmid	Characteristics	Application
pBSK	β-gal$^+$, Amp^R	Cloning
pDONRzeo	Zeo^R	Entry vector GATEWAY cloning
pUBC-GFP-DEST	Bar^R $Spec^R$ *pUBQ10* *ccdB* Green fluorescent protein (GFP) *T35S*	Destination vector GATEWAY cloning
pUBC-nYFP-DEST	Hyg^R $Spec^R$ *pUBQ10* *ccdB* N-terminus of yellow fluorescent protein (nYFP) *T35S*	BIFC vector GATEWAY cloning
pUBC-cYFP-DEST	Hyg^R $Spec^R$ *pUBQ10* *ccdB* C-terminus of yellow fluorescent protein (cYFP) *T35S*	BIFC vector GATEWAY cloning

2.4.3. Bacterial cultivation

To produce competent *E. coli* cells, or after heat shock and transformation, the cultivation was conducted in ΨB medium (0.5% (w/v) yeast extract; 2% (w/v) peptone; 0.4% (w/v) $MgSO_4$, 10 mM KCl; pH 7.6 adjusted with KOH). Bacteria containing the pBSK plasmid were cultivated in YT medium (0.5% (w/v) yeast extract; 0.8% (w/v) peptone; 0.25% (w/v) NaCl; pH 7.0 adjusted with NaOH; Sambrook and Russell, 2001). After transformation with the GATEWAY constructs bacteria were cultivated in low-salt LB medium (0.5% (w/v) yeast extract; 1% (w/v) peptone; 0.5% (w/v) NaCl; pH 7.0 adjusted with NaOH; Bertani, 1951)

E. coli cultivation in liquid media was conducted at a temperature of 37°C under constant shaking at 180 rpm. The cultivation of *A. tumefaciens* was carried out under constant shaking at 180 rpm at 30°C in liquid YEB medium (0.1% (w/v) yeast extract; 0.5% (w/v) peptone; .0.5% (w/v) beef extract; 2 mM $MgSO_4$; 0.5% (w/v) sucrose; 1.5% (w/v) agar). *A. tumefaciens* cultivation in liquid media was conducted at a temperature of 30°C under constant shaking at 180 rpm.

The liquid media and media containing agar for the preparation of plates were subjected to autoclaving at 140°C for a duration of 20 min. After this, antibiotics were added to the medium under sterile conditions for the purpose of selection (200 µg/mL ampicillin for pBSK, 25 µg/mL zeocin for pDONRzeo or 100 µg/mL spectinomycin for *E. coli* or 50 µg/mL spectinomycin for *A. tumefaciens* for GATEWAY destination vectors). For the preparation of plates, 1.5% (w/v) agar was added to the respective media prior autoclaving.

2.4.4. Production of competent *E. coli* cells and transformation

In molecular biology, the term 'competence' refers to the ability of bacteria to take up free DNA from the environment of the bacterial cells without coming into direct contact with another cell or a virus (Cypionka 2010). The chemical rubidium chloride method was utilised to produce competent *E. coli* cells of the XL1blue and DH5α strains (Mandel & Higa, 1970).

For this purpose, an overnight culture was inoculated in 100 mL of ΨB medium (see chapter 2.4.3) at a ratio of 1:100 and cultivated under constant shaking at 180 rpm at 37 °C. At an OD_{600} of 0.5 (measured using an Eppendorf Bio-Photometer in Hamburg), the cells were incubated on ice for 10 min, after which they were subjected to a centrifugation step (7,000 rpm, 4 °C, 10 min). Pelleted cells were taken up in 40 mL of sterile-filtered, ice-cold TFB1 buffer (100 mM RbCl; 50 mM $MnCl_2$; 30 mM KCH_3CO_2; 10 mM $CaCl_2$; 15% (v/v) glycerol; pH 5.8 adjusted with acetic acid), incubated on ice

for a further 10 min, and subjected to a second centrifugation step (7,000 rpm, 4 °C, 10 min). The resulting pellet was resuspended in 4 mL of sterile-filtered, ice-cold TFB2 buffer (75 mM $CaCl_2$; 10 mM MOPS; 10 mM RbCl, 15% (v/v) glycerol; pH 7.0 adjusted with NaOH). About 200 µL of the in TFB2 resuspended cells were aliquoted into a 1.5 mL reaction tube, frozen in liquid nitrogen and stored at -80°C until use.

A so-called heat shock transformation was performed with the chemically competent *E. coli* cells. To this end, an aliquot of competent cells was thawn on ice for 10 min and following the addition of DNA incubated on ice for 30 min. This was followed by subjecting the cells to a heat shock at 42°C for 5 sec to facilitate the uptake of the DNA into the cell. The cells were subjected to a 5-minute incubation on ice, followed by an addition of 800 µL of ΨB medium and incubation at 37°C for a duration of 1 hour under constant shaking at 180 rpm. Subsequently, 50 µL, 100 µL and 200 µL of the culture were streaked on YT or LB agar plates with the corresponding selection antibiotics and incubated overnight at 37°C (see chapter 2.4.3).

2.4.5. Production of competent *A. tumefaciens* cells and transformation

The production and transformation of competent *A. tumefaciens* cells was conducted in accordance with the methods outlined by Höfgen and Willmitzer, 1988. To produce competent cells, an overnight culture of *A. tumefaciens* was diluted in 200 mL YEB medium at 30°C (see chapter 2.4.3). After 3 to 4 hours cells were subjected to centrifugation at 3,000 rpm for 20 min at 4°C. The resulting pellet was washed in 10 mL of chilled TE buffer (10 mM Tris-HCl, pH 7.5; 1 mM EDTA) and resuspended in 20 mL of fresh YEB medium. The *A. tumefaciens* cells were aliquoted as a volume 500 µL into individual 1.5 mL reaction tubes, frozen in liquid nitrogen and stored at -80°C.

For the process of transformation, an aliquot of competent *A. tumefaciens* cells was thawn on ice, after which 0.5 to 2 µg of plasmid DNA was added. This was followed by incubation on ice for 5 min, shock freezing in liquid nitrogen for a further 5 min and thawing again at 37°C for 5 min. Following this, 1 mL of YEB medium was added, and the bacteria were incubating them for a period of 4 to 6 hours at 30°C under constant shaking at 180 rpm. Subsequently, 50 µL, 100 µL and 200 µL of the culture were streaked on YEB agar plates with the corresponding selection antibiotics and incubated for 2 to 3 days at 30°C (see chapter 2.4.3).

2.5. Molecular methods

2.5.1. Nucleic acid concentration

For cloning or qPCR, it is imperative to know the precise nucleic acid concentration. This determination was conducted photometrically using the NanoPhotometer N50 (Implen GmbH, Munich) in accordance with the manufacturer's instructions. The maximum absorption of nucleic acids occurs at a wavelength of 260 nm, whereas proteins exhibit a maximum absorption at 280 nm, while carbohydrates demonstrate maximum absorption at 230 nm. The purity of a DNA or RNA sample is determined by the ratio of absorption at 260 nm/280 nm and at 260 nm/230 nm. The A260nm/A280nm ratio of 1.8 is indicative of DNA purity, while RNA is considered pure at a ratio of 2.0 (Desjardins & Conklin, 2010).

2.5.2. Polymerase chain reaction

The PCR is a method for the *in vitro* amplification of specific DNA sequences (Saiki *et al.,* 1988). DNA segments to be amplified are determined by short oligonucleotide primers that are complementary to opposite DNA strands. Each PCR reaction contains 50 pmol of the sense and antisense oligonucleotide primers. The DNA template is added to the PCR reaction (about 10 to 100 ng) or bacterial cells can be used for colony PCR. Further, 200 µM deoxyribonucleoside triphosphates (dNTPs), containing the 4 deoxynucleosides dATP, dGTP, dCTP and dTTP are added, as well as 2 U of DNA polymerase and its corresponding buffer.

Taq and Pfu polymerase were utilised in accordance with the manufacturer's recommendations. Taq polymerase originates from the heat-stable bacterium *Thermus aquaticus*. Optimal activity is observed at 74°C. However, Taq polymerase retains stable even at 94°C, being resistant to DNA denaturation by heating (Saiki *et al.,* 1988). For cloning purposes, the heat-stable Pfu polymerase was employed, which originates from *Pyrococcus furiosus* and possesses a 3' → 5' exonuclease activity and a proofreading function (Mülhardt, 2009). The PCR reactions were performed in a T Professional Basic Gradient, or in a T Personal thermocycler (Biometra, Göttingen).

PCR starts with denaturation of the DNA double helix at 95°C for 5 min. In total, 30 to 35 cycles are conducted, each starting with denaturation at 95°C for 30 sec, followed by primer annealing at 40°C to 65°C for 30 sec, depending on primer composition. The cycle continues with elongation at 72°C for 30 sec to 5 min, depending on DNA length and polymerase. A final elongation step is performed at 72°C for 5 min.

2.5.3. Agarose gel electrophoresis

Gel electrophoresis was utilised to separate DNA fragments according to their length. The gel matrix is composed of agarose, a polysaccharide containing galactose, which, when boiled and dissolved in the buffer, forms a three-dimensional network when cooled. The agarose is boiled in 1x TAE buffer (1:50 diluted 50x TAE stock: 242 g Tris, 57.1 mL acetic acid, 146.12 g EDTA, pH adjusted to 5.8 with HCl) and allowed to cool down until lukewarm under constat stirring. Afterwards ethidium bromide (3,8-diamino-5-ethyl-6-phenylphenanthridinium bromide) was added to achieve a final concentration of 0.5 µg/mL. The intercalation of ethidium bromide in the helical structure of the nucleic acids results in fluorescence, that can be detected at 260 nm wavelength.

The DNA samples were mixed with 10x TAE loading buffer (30% (v/v) glycerol, 0.25% (w/v) bromophenol blue) in a 1:10 ratio to facilitate the loading of the DNA sample. As DNA size marker the GeneRuler Plus DNA Ladder Mix (Thermo Scientific, Germany) was selected. After loading of samples and marker the agarose gel electrophoresis was performed in a horizontal gel electrophoresis chamber filled with 1x TAE buffer medium at a voltage of approximately 125 mV for 15 to 30 min.

2.5.4. DNA agarose gel extraction

DNA fragments were extracted from agarose gels after gel electrophoresis by a NucleoSpin Extract kit (Macherey Nagel, Düren) in accordance with the manufacturer's instructions. The method of this kit is dependent upon the adsorption of DNA on a silica membrane in the presence of high salt concentrations. Salts, proteins and fragments of agarose are removed from the DNA that has bound to the membrane. The DNA is subsequently eluted from the silica membrane using ddH_2O. Subsequent sequencing of the PCR product was conducted by Eurofins Genomics GmbH (Ebersberg, Germany).

2.5.5. Gateway cloning

For cloning with the GATEWAY system (Invitrogen, Gaithersburg, USA) DNA sequences were first generated with attB attachment sites by PCR (Figure 4, step 1). Entry clones are created by recombining the attB sites of the previously generated DNA fragment with the attP sites of the pDONRzeo plasmid (Figure 4, step 2 and 3). This reaction is catalysed by the Gateway BP clonase enzyme mix during the so-called BP reaction. For this purpose, 150 ng of the amplified PCR product are mixed with 150 ng of the pDONRzeo vector. Additionally, 1 µL of the BP clonase enzyme mix is added and the whole reaction volume is adjusted to 10 µL with TE buffer (10 mM Tris-HCl pH 8.0; 0.1 mM EDTA). Subsequently the reaction was incubated at 30°C for 1 hour, followed by the addition of proteinase K and incubation of the reaction at 37°C for 10 min. In addition to the zeomycin resistance, the donor vector (pDONRzeo) contains the *ccdB* gene. The *ccdB* product inhibits the bacterial gyrase, resulting in bacterial death. During the BP reaction, the *ccdB* gene is replaced by the PCR product, consequently being absent from the resulting entry clone, which contains attL sites.

For the subsequent LR reaction, a recombination of the entry clone with the target vector was mediated by the LR clonase enzyme mix, which leads to the formation of the expression clone (Figure 4, step 4 and 5). For this purpose, 150 ng of the entry clone DNA was mixed with 150 ng of the destination vector pUB-DEST, pUBC-GFP-DEST or the Bimolecular Fluorescence Complementation (BiFC) vectors pUBC-DEST-nYFP and pUBC-DEST-cYFP. The recombination takes place between the attR sites of the target and the attL sites of the entry clone, mediated by 1 µL of LR clonase enzyme mix in an end volume of 10 µL, adjusted with TE buffer (Karimi *et al.,* 2002). Subsequent incubation was performed at 30°C for 1 hour, followed by the addition of proteinase K to stop the LR recombination reaction at 37°C for 10 min.

The BP and LR reaction were transformed into DH5α *Escherichia coli* cells after respective recombination streps (see chapter 2.4.4). Afterwards entry clones were selected on zeocin containing agar plates, whereas target vectors were selected on spectinomycin containing agar plates (see chapter 2.4.3).

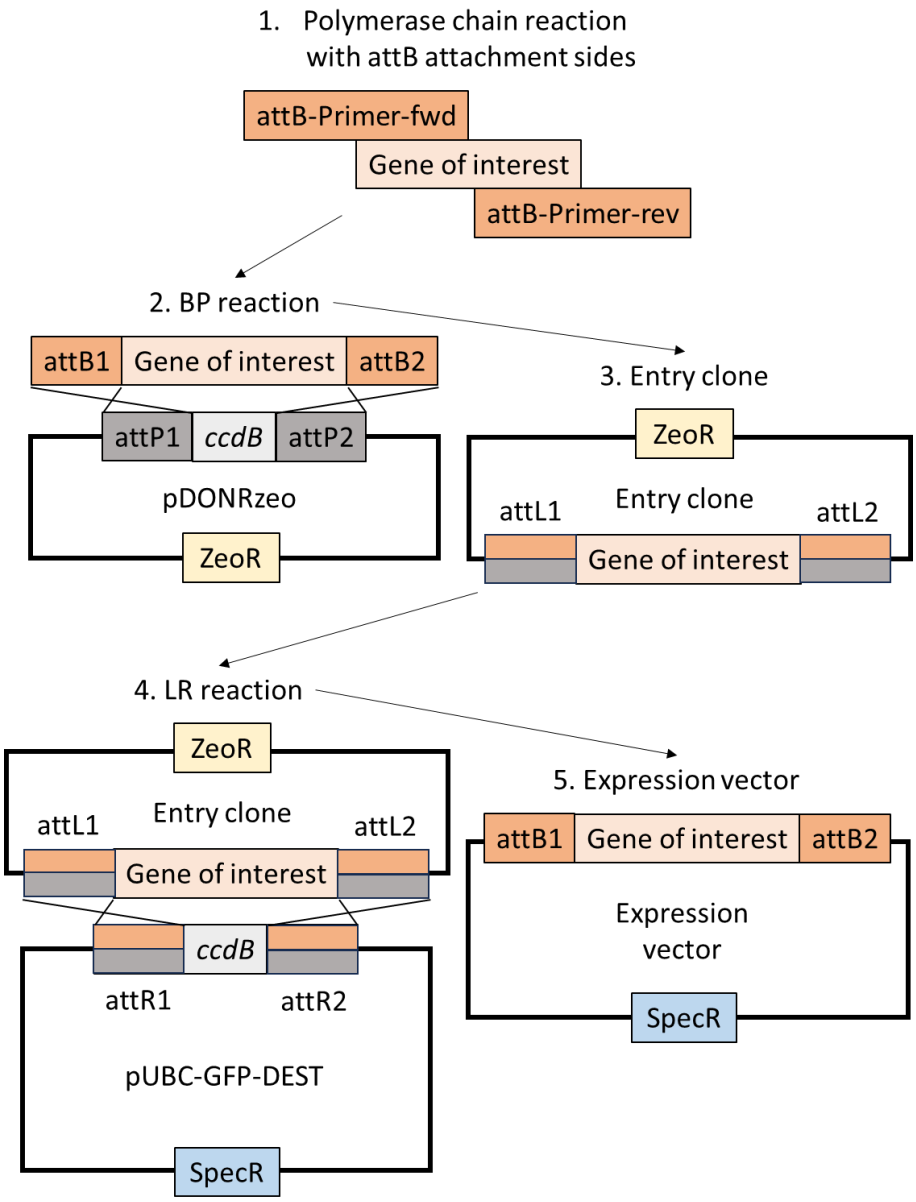

Figure 4: Gateway cloning workflow. For cloning with the GATEWAY system DNA sequences were amplified with attB attachment sides by PCR (1). BP recombination (2) results in the generation of the entry clone (3). In the LR reaction the entry clone recombines with a destination vector (4), resulting in the generation of an expression vector (5). att, attachment sites; *ZeoR*, zeocin resistance gene; *SpecR*, spectinomycin resistance gene; *ccdB* selection marker; pDONRzeo, donor vector; pUB-DEST or pUBC-GFP-DEST are examples of destination vector to produce overexpression or C-terminal GFP fusion constructs.

2.5.6. Plasmid DNA isolation

The isolation of plasmids can be achieved through alkaline lysis process, which employs the divergent precipitation properties exhibited by plasmid DNA, chromosomal host DNA, proteins, and RNA (Birnboim & Doly, 1979; Sambrook & Russell, 2006). The isolation of the plasmid was conducted using the NucleoSpin Plasmid Kit (Macherey-Nagel GmbH, Düren, Germany). The kit was used according to the manufacturer's instructions.

2.5.7. Genomic DNA extraction

Genomic DNA was extracted from Arabidopsis leaf material. Leaves of a 4-week-old plants were harvested into 1.5 mL reaction tubes and snap frozen in liquid nitrogen. Afterwards 500 µL of Shorty buffer (400 mM LiCl, 200 mM Tris-HCl pH 9.0, 25 mM EDTA, 1% (w/v) sodium dodecyl sulphate (SDS)) was added to the leaf sample, whereafter the leaf was homogenised by grinding. Subsequently, samples were subjected to a centrifugation process at 14,000 rpm for a duration of 10 min. Thereafter, 350 µL of the resulting upper layer was transferred to a fresh 1.5 mL reaction tube. DNA precipitation was initiated by the addition of 350 µL ice cold isopropanol. The samples were subjected to repeated inversion and centrifugation at 14,000 rpm for a duration of 10 min. The resulting pellet was washed with ice cold 80% (v/v) EtOH, followed by centrifugation at 14,000 rpm for a duration of 10 min. The supernatant was discarded, and the obtained pellet was dried in the Speedvac concentrator overnight. The next morning the dried gDNA was resuspended in 20 to 50 µL of ddH_2O.

2.5.8. RNA isolation

In order to carry out the expression analyses by quantitative real time PCR (see chapter 2.5.10), complementary DNA is required, which is synthesised by reverse transcription from total RNA. Total RNA was isolated using the NucleoSpin RNA plant kit (Macherey-Nagel, Düren, Germany) in accordance with the manufacturer's instructions. The quantification of the RNA was carried out using the NanoPhotometer N50 (see chapter 2.5.1)

2.5.9. RNA sequencing

For the RNA sequencing of cold-acclimating wild types and *abcg7* loss-of-function lines, plants were grown for 4 weeks under standard growth conditions. The plants were divided into 2 batches. From one batch, three rosettes of the 4-week-old plants grown under standard growth conditions were pooled and snap frozen in liquid nitrogen. The remaining plants were transferred to 4°C for subsequent cold acclimation. Similarly, three rosettes were pooled after a period of 4 days at 4°C and snap frozen in liquid nitrogen. Three biological replicates of wild types*, abcg7-1* and *abcg7-2* were prepared for RNA sequencing.

To this end, the frozen samples were ground in the presence of liquid nitrogen. About 50 mg of homogenized material was aliquoted into individual 1.5 mL reaction tubes. Total RNA was isolated using the NucleoSpin RNA plant kit (Macherey-Nagel, Düren, Germany) following the manufacturer's instructions. Prior the shipment of RNA to the sequencing company, the RNA was quantified using a

nanophotometer (see chapter 2.5.1). As RNA sequencing requires high quality, non-degraded RNA, the integrity of the isolated RNA was validated according to Aranda, LaJoie and Jorcyk, 2012. The addition of 1% (v/v) sodium hypochlorite to TAE-buffer prior agarose gel preparation and electrophoresis, inhibits RNAses and allows denaturation of the secondary RNA structure for analysis.

The RNA sequencing was carried out by Novogene (Munich, Germany). For library preparation a polyA-tailed mRNA enrichment with magnetic beads of oligos d(T) was performed. The mRNA was randomly fragmented, and cDNA synthesis was carried out using random hexamers and the enzyme reverse transcriptase. Fragments of the appropriate size are enriched by PCR using indexed P5 and P7 primers, and the final products are purified. Novogene NGS RNA Library Prep Set (PT042) was used for library preparation (based on NEB Next Library Prep Kit). The library was verified using Qubit 2.0 and real-time PCR for quantification and Agilent 2100 Bioanalyzer for size distribution detection. Quantified libraries were pooled and sequenced on the Illumina Novaseq 6000 platform according to the effective library concentration and data amount (6 Gb/9 Gb).

The qualified libraries were sequenced by next-generation sequencing (NGS) based on Illumina's Sequencing by Synthesis (SBS) - detection by fluorescence of the nucleotide added during the synthesis of the complementary chain. The libraries are sequenced on the Novaseq6000 sequencing system, using the paired end 150bp (PE150) strategy. The bioinformatic analysis of sequencing results was performed by Novogene. The results were provided as publication-ready, with calculated mean log2FC data of the provided biological replicates and statistical analysis.

2.5.10. Reverse transcription of RNA into cDNA

The qScript cDNA Synthesis Kit (Quantabio, Boston, USA) was utilised for the synthesis of cDNA from previously isolated RNA (see chapter 2.5.8). In order to synthesise cDNA, 4 µL of 5x iScript reaction mix and 1 µL of iScript reverse transcriptase were added to 0.5 to 1 µg of the previously isolated total RNA. The volume was adjusted to 20 µL with RNAse-free water. The reaction mix used contains all the necessary components for cDNA synthesis, with the exception of the RNA and the reverse transcriptase. The components of the reverse transcriptase buffer are magnesium, oligo (dT) primer (complementary to the poly-A tail of the eukaryotic mRNA), random hexamer oligonucleotides and dNTPs. Following the careful mixing of the reaction mixtures, the samples were heated in a thermocycler (T Personal from Biometra, Göttingen, Germany) for 5 min at 22 °C, incubated for 30 min at 42°C and finally the reaction was stopped after incubation at 82°C for 5 min.

2.5.11. Quantitative polymerase chain reaction

The quantitative polymerase chain reaction is employed to quantify the expression of specific genes, from total RNA extracts which were previously transcribed into cDNA (see chapter 2.5.8 and 2.5.10). Expression analysis by qPCR was employed for 4-week-old plants grown under standard growth conditions and subsequent transfer to 4°C for up to 10 days to investigate expression patterns of *ABCG7* and the cold marker *COR15a* during cold acclimation. Further, the expression of *ABCG7* cell wall and membrane related genes was analysed during a the freezing experiment performed according to Trentmann *et al.,* 2020 (see chapter 2.3.1). Additionally, the qPCR was also used to analyse expression patterns in leaf discs incubated either with galactose or aromatic amino acids (see chapter 2.3.2).

During the qPCR, the amplified DNA content is determined during each cycle by fluorescent measurement at 524 nm of the DNA-intercalating fluorescent dye SybrGreen (IQTM SYBR Green Supermix; Bio-Rad, Munich, Germany; Zipper *et al.,* 2004). The relative fluorescence of a sample is determined after exceeding a defined cycle threshold value (ct value), which is automatically set by the employed MyIQ real-time PCR cycler from BIO-RAD (Munich, Germany). The relative fluorescence of a specific primer pair, designed for the gene of interest, and the constitutively expressed housekeeping gene *SAND*, was used to calculate the relative transcript content by the $2^{-\Delta\Delta ct}$ method (Livak & Schmittgen, 2001). The Primer sequences used for qPCR analysis can be found in Table 4.

Table 4: qPCR primer. Tested genes and the corresponding qPCR primer sequences 5`-3` (fwd) and 3`-5` (rev) are indicated.

Gene	Primer name	Sequence
ABCG7	*ABCG7*_qPCR_fwd	ACACCCCAATCATCTTCCGT
	*ABCG7*_qPCR_rev	GAGCTGCTATCGTCTCCCTT
COR15A	*COR15A*_qPCR_fwd	GAAAAAAACAGTGAAACCGCAGAT
	*COR15A*_qPCR_rev	GAAAAAAACAGTGAAACCGCAGAT
DGAT1	*DGAT1*_qPCR_fwd	CACTTAGCTCCGACGCAATC
	*DGAT1*_qPCR_rev	ACACATGAAAAGCGGCCAAT
MUR3	*MUR3*_qPCR_fwd	GAGTTGGTCGATTGGCTCAT
	*MUR3*_qPCR_rev	AAAGCCACTTCCTTTCCAGG
PME41	*PME41*_qPCR_fwd	TCGCTCGCATTATTCACCAA
	*PME41*_qPCR_rev	TGAAATTCCCCGTTCCGTTT
SAND	*SAND*_qPCR_fwd	CAAGGCAGGAAATCACCAGGTTG
	*SAND*_qPCR_rev	CTGTACAGCTGATGCAGACCAG
SFR2	*SFR2*_qPCR_fwd	ATGGAATTATTCGCATTGTT
	*SFR2*_qPCR_rev	CTAGTCAAAGGGTGAGG
XTH19	*XTH19*_qPCR_fwd	CTGGTAACTCTGCTGGAACC
	*XTH19*_qPCR_rev	CACGTGACTCGGCATTCATA
XTH21	*XTH21*_qPCR_fwd	CCGCGTTCCACAACTACTCT
	*XTH21*_qPCR_rev	AGAGGCTACGAATGGTCCCT
XTH22	*XTH22*_qPCR_fwd	TTCACTGCTTCTTACCGTGG
	*XTH22*_qPCR_rev	GCACCCATCTCATCCTTTGT
XXT1	*XXT1*_qPCR_fwd	TGTCACAGGTTCAGCTCCTA
	*XXT1*_qPCR_rev	CCGTGAACATGGCATCACTA

As the primers utilised for qPCR were required to meet specific criteria, they were designed employing the Primer3 online input tool (https://primer3.ut.ee/) and subsequently subjected to a primer efficiency test. For this purpose, the cDNA samples to be tested were pooled and a dilution series was prepared. The evaluation of an exemplary primer efficiency test is shown in Figure 5.

The ct values of the various dilutions were plotted against the decadic logarithm of the estimated number of cDNA copies. The coefficient of determination was used as a metric of the quality of the experimental procedure and should not fall below a value of 0.9. The amplification efficiency was analysed using the linear equation with the aid of the online tool Primer Efficiency Calculator from Thermofischer (https://www.thermofisher.com/de/de/home/brands/thermo-scientific/molecular-biology/molecular-biology-learning-center/molecular-biology-resource-library/thermo-scientific-web-tools/qpcr-efficiency-calculator.html). Primers with an efficiency of 80 to 120% were used for expression studies.

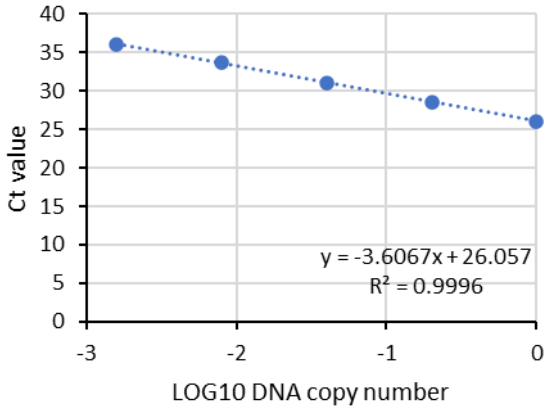

Figure 5: Primer efficiency test of the primer pair for the house keeping gene *SAND*. The pooled cDNA was diluted by a factor of 5, after which a qPCR was performed. The decadic logarithm of the estimated number of cDNA copies was plotted against the Ct value. The linear equation and the coefficient of determination (R^2) are shown. The primer efficiency of the SAND primer pair was calculated with the slope (-3.6067) with the help of the Primer Efficiency Calculator from Thermofischer. The primer efficiency is 89.35%, which is equivalent to an amplification factor of 1.89.

2.6. ABCG7 localisation studies

2.6.1. Microscopy

Microscopic images captured during this dissertation were recorded on a Leica TCS SP5II Microscope at the Rheinland-Pfälzische Technische University of Kaiserslautern or a Leica Stellaris 5 Confocal Scanning Microscope at the Ludwig-Maximilians-University in Munich (Leica Biosystems, Wetzlar, Germany). The microscopic samples were prepared between 2 coverslips or in a Petri dish with water.

2.6.2. Cloning of constructs for confocal microscopy

To verify the plastid localisation of ABCG7, a corresponding GFP-tagged fusion construct was cloned. The *ABCG7* coding sequence was amplified from wild type complementary DNA with *ABCG7*_fwd and *ABCG7*_rev primers (Table 1). The amplified sequence was cloned without the stop codon and subsequently introduced into the plasmid pDONR/Zeo. The entry clone obtained was used to recombine with the fluorophore-encoding vector pUBC-GFP-Dest.

For BiFC analysis N- or the C-terminus of the split YFP fluorophore was cloned to full-length *ABCG7*, *SFR2* or *LACS9* (Kerppola, 2008; Kodama & Hu, 2012). Coding sequences were obtained from wild type complementary DNA with *SFR2*_gw_fwd and *SFR2*_gw_rev primers or *LACS9*_gw_fwd and *LACS9*_gw_rev primers (Table 1, Table 5). The amplified sequences were transferred into the plasmid

pDONR/Zeo, and the subsequently obtained entry clone was used to recombine with the fluorophore-encoding vectors pUBC-nYFP-Dest or pUBC-cYFP-Dest, respectively (Grefen *et al.,* 2010).

The Gateway Clonase II Enzyme Mix for BP or LR recombination reactions was utilised in accordance with the manufacturer's instructions (Invitrogen, Heidelberg, Germany). Constructs were transformed into *Agrobacterium tumefaciens* strain GV3101 for transient expression of corresponding fusion proteins in 2 to 4-week-old *Nicotiana benthamiana* plants (see chapter 2.4.5 and 2.6.6).

Table 5: Primers used for PCR to clone fluorescent fusion protein. The name of the primers and sequences 5`-3` (fwd) and 3`-5` (rev) are indicated.

Gene	Primer name	Sequence
SFR2	*SFR2*_gw_fwd	GGGGACAAGTTTGTACAAAAAAGCAGGCTTAATGGAATTATTCGCATT
	*SFR2*_gw_rev	GGGGACCACTTTGTACAAGAAAGCTGGGTAGTCAAAGGGTGAGGC
LACS9	*LACS9*_gw_fwd	GGGGACAAGTTTGTACAAAAAAGCAGGCTTAATGATTCCTTATGCTGC
	*LACS9*_gw_rev	GGGGACCACTTTGTACAAGAAAGCTGGGTAGGCATATAACTTGGTGAG

2.6.3. Imaging of transfected tissue and protoplasts

About 4-week-old *Nicotiana benthamiana* leaves were subjected to transfection to express the pUBC-*ABCG7-GFP* plasmid or to co-express BIFC constructs. After a period of 3 to 5 days, transfection sites were excised and examined for fluorescence (Leica TCS SP5II microscope, Leica Biosystems, Wetzlar, Germany) at 514 nm excitation and 524 to 582 nm emission detection, through an HCX PL APO 63 × 1.2 W water immersion objective with a Vis Argon Laser. Chlorophyll autofluorescence was detected at an excitation wavelength of 514 nm and 627 to 704 nm.

Inoculated leaves exhibiting strong GFP signals were cut into thin strips and placed in enzyme buffer (0.45 M sorbitol, 10 mM $CaCl_2$, 20 mM MES-KOH, 1% (w/v) cellulase (cellulase onozuka R-10, Duchefa Biochemie, Haarlem, Netherlands), 0.25% (w/v) macero-enzyme (macro enzyme R-19, Yakult pharmaceutical IND., Tokyo, Japan)). The incubation was performed overnight to facilitate the release of intact protoplasts. The protoplasts were filtered through a 125 µm steel mesh (Retsch Laborgeräte, Haan, Germany) and sedimented for 2 min at 100 rpm. The sedimented protoplasts were gently resuspended in W5 buffer (145 mM NaCl, 125 mM $CaCl_2$, 5 mM KCl, 5 mM Glucose, 20 mM MES, pH 5.6) and examined under the LC-microscope.

2.6.4. Protein extraction and quantification from transfected tobacco leaves

To investigate whether ABCG7 is localised in the inner or outer envelope membrane, an immunological analysis approach was chosen. To this end, the pUBC-*ABCG7-GFP* plasmid, containing the ABCG7 open reading frame and a GFP fused to the C-terminus, was used to transfect tobacco leaves. To verify the functionality of the approach the total protein of the transfected leaf area was extracted. Therefore, the transfected leaf area was excised, transferred into 1.5 mL reaction tube and snap-frozen in liquid nitrogen.

Prior to the protein extraction, a 2x stock of extraction buffer was prepared: 100 mM Tris-HCl pH 7.5, 300 mM NaCl, 5 mM EDTA, 20% (v/v) glycerol, 1% (v/v) NAP-40. A volume of 400 µL of the 2x extraction buffer was mixed with 320 µL ddH_2O, 80 µL of 2 M DTT, and 1:100 diluted protease inhibitor (Complete, EDTA-free, Roche, Mannheim, Germany). The buffer was added in a ratio of 2:1 to the plant material., to first grind and sonifiy the sample for 10x 1 sec, at an output strength set to 20% (Branson Sonifier 250, USA). Subsequently, 10% (v/v) SDS was added to the sample to achieve a final concentration of 1% (v/v) SDS. Samples were incubated for 30 min under constant invertation.

After the incubation process, a centrifugation step at full speed for 10 min at 4°C was performed. The supernatant was transferred and into a fresh reaction tube to measure the protein concentration with 1x Bradford at 595 in a photometer (BioPhotomere, Eppendorf, Hamburg, Germany) according to Bradford, 1976.

2.6.5. SDS-PAGE and Western blotting of total protein extracts

An amount of 15 µg protein of total protein lysate was separated by sodium dodecyl sulphate-polyacrylamide gel electrophoresis (SDS-PAGE; Broglie *et al.,* 1980). The SDS-PAGE was performed using Mini-Protean TGX Gels (BIO-RAD, USA). Protein lysates were loaded using 5x SDS loading dye (200 mM Tris-HCl pH 6.8, 30% (v/v) Glycerol, 4 % (w/v) SDS, 1.3 mM DTT; 0.05 % (w/v) bromphenol blue). The electrophoresis was performed at 180 V for 40 min in 1x Tris-glycine-SDS running buffer (25 mM Tris, 192 mM glycine, 0.1% (w/v) SDS, pH 8.3; BIO-RAD, USA). The proteins were stained by Coomassie Brilliant Blue G-250 (0.25 % (w/v) in 45 % (v/v) Methanol and 9 % (v/v) Acetic acid) for 30 min and destained by incubation in a destaining solution (5 % (v/v) methanol and 7.5 % (v/v) acetic acid) or were blotted to a nitrocellulose membrane for immunological detection.

Proteins from the SDS-PAGE were blotted to a nitrocellulose membrane for immunological detection and analysis. The Mini-Protean TGX Gel was placed on a nitrocellulose membrane pre-wetted in 1x Trans-Blot Turbo Transfer buffer (BIO-RAD, USA). The membrane on top of the nitrocellulose membrane was placed between 2 Trans-Blot Turbo Mini-size Transfer Stacks (BIO-RAD, USA) that were soaked in the transfer buffer. The stack-membrane-gel-stack-sandwich was placed into the blotting Trans-Blot Turbo transfer system apparatus (BIO-RAD, USA). The transfer was performed at 25 V for 30 min.

Subsequently, the nitrocellulose membrane was incubated for 30 min in blocking solution (3% (w/v) milk powder in 1× PBS (137 mM NaCl, 2.7 mM KCl, 10 mM Na_2HPO_4, 1.8 mM KH_2PO_4, pH 7.4) with 0.1% (v/v) Tween-20) to avoid unspecific antibody binding. The blot was washed three times with PBS-Tween before incubation with a GFP-specific primary rabbit antibody and a secondary anti-rabbit IgG-HRP conjugate (Abcam, Cambridge, UK), both diluted 1:3,000 and 1:10,000 in blocking solution. The membrane was incubated for 1 h in antibody solution and washed again. For immunological detection, ECL Prime Western Blotting Detection Reagents (GE Healthcare, Amersham Biosciences, UK) were used. Afterwards, the blot was stained with Ponceau S (5 mg in 5% (v/v) acetic acid) for 5–10 min, then rinsed with ddH_2O before imaging. Functionality and specificity of the GFP-antibody was confirmed by immunological analysis of total protein extract from corresponding leaves (Supplementary Figure 3). The pUBC-*ABCG7-GFP* plasmid, was provided to Dr. Bettina Bölter at the Ludwig-Maximilians-University in Munich to determine the exact envelope localisation of the ABCG7 transporter (see chapter 2.6.6 to 2.6.7).

2.6.6. Infiltration of tobacco leaves

The pUBC-*ABCG7-GFP* plasmid was transformed into the competent Agrobacteria strain GV3101. Positive colonies were selected on YEB plates containing Rifampicin and Spectinomycin and transferred into liquid cultures grown at 28 °C under constant shaking until an OD of 0.6 was reached. Bacteria were sedimented (15 min, 4,000 g), resuspended to an OD of 1 in buffer (10 mM MES pH 6.0, 10 mM $MgCl_2$, 150 µM acetosyringone), and incubated in the dark for 1.5 h at room temperature. In parallel, Agrobacteria containing the p19 helper plasmid (Voinnet *et al.,* 1998) were treated the same way. Both suspensions were mixed at a 1:2 ratio and injected into *Nicotiana benthamiana* leaves. The plants were kept in the dark overnight.

2.6.7. Chloroplast isolation and protease treatment

Following a 4-day growth period of transfected *N. benthamiana* leaves, chloroplasts were isolated. Leaf samples were homogenised in isolation buffer (0.3 M sorbitol, 5 mM $MgCl_2$, 5 mM EDTA, 20 mM HEPES-KOH, 10 mM $NaHCO_3$, pH 8.0) and filtered through gauze. The suspension was centrifuged at 1,500 rpm for 3 min at 4 °C. The pellet was resuspended and layered onto a Percoll gradient (30%/82% in 0.3 M sorbitol buffer) and centrifuged for 5 min at 3,000 rpm. Intact chloroplasts were collected, washed, and resuspended in wash buffer (50 mM HEPES-KOH, 0.3 M sorbitol, 3 mM $MgCl_2$, pH 8.0). Chlorophyll content was determined according to Arnon, 1949.

For protease assays, chloroplasts were adjusted to 1 mg/mL chlorophyll in buffer suitable for trypsin (with 0.5 mM $CaCl_2$) or thermolysin (with 5 mM $MgCl_2$ and 0.5 mM $CaCl_2$). Trypsin treatment (0.5 or 1.0 mg/mg chlorophyll) was performed for 45 min at 23 °C, and thermolysin treatment (100 µg/mg chlorophyll) for 20 min at 0 °C. Both reactions were stopped using protease inhibitors for trypsin or EDTA for thermolysin, washed, and prepared in high-urea Laemmli buffer. About 15 µg chlorophyll was loaded per lane onto a 10% SDS gel.

Following SDS PAGE, proteins were transferred onto PVDF membranes by Western transfer in Towbin buffer medium (25 mM Tris-HCl pH 8.3, 192 mM glycine, 1% (w/v) SDS, 20% (v/v) methanol) in a wet blot apparatus at 400 mA, for 1 hour at room temperature. Following blocking with 5% (w/v) skimmed milk in TBS-T, the membranes were incubated with the respective antibodies in TBS-T at a 1:1,000 dilution overnight at 4 °C. The membranes were washed three times in TBS-T and exposed to secondary antibodies coupled to horseradish peroxidase (HRP). Detection was accomplished through chemiluminescence in an LAS4000 (GE Healthcare, Heidelberg, Germany). The following antibodies were used: Anti-PsToc75 (Seedorf and Soll, 1995), Anti-PsTic40 (Stahl *et al.,* 1999), Anti-AtKEA (Bölter *et al.,* 2020) and Anti-GFP (Chromotek, Munich, Germany).

3. Results

3.2. Localisation of the ABCG7 transporter

Acclimation, centrally coordinated by chloroplasts, relies on dynamically responsive proteins to mediate the acquisition of stress tolerance (Trentmann *et al.,* 2020; Kleine *et al.,* 2021). Nevertheless, the number of transport proteins that are grouped into different membrane transport families is surprisingly limited. Whereby, the ATP-binding cassette superfamily is one of the largest and most diverse (Higgins, 1992). ATP-binding cassette transporters play a crucial role during plant development and in response to environmental stress (Ashraf *et al.,* 2021; Buda *et al.,* 2013; Leslie *et al.,* 2005; Matsuda *et al.,* 2012). To accomplish their function, ABC transporters require transmembrane and nucleotide-binding domains. To identify the respective domains in the ABCG7 protein sequence of *Arabidopsis thaliana*, a protein alignment was performed with the corresponding homolog of *Pisum sativum*. This was due to the fact that the respective homolog in pea had previously been found and identified as chloroplast protein (Gutierrez-Carbonell *et al.,* 2014; Supplementary Figure 1).

Alignment of the ABCG7 protein sequences from Arabidopsis and pea revealed a high similarity, except for the first 90 and last 60 amino acids (Supplementary Figure 1). In accordance with the hydrophobic caloric analysis in Jalview, it was determined that the initial 60 amino acids of the N-terminus in *At*ABCG7 are highly hydrophobic. Transmembrane domains were identified using domain predictions from ARAMEMNON (https://aramemnon.botanik.uni-koeln.de/; Supplementary Figure 1). Additionally, several conserved motifs within the NBD, such as Walker A, Walker B, and the ABC signature motif, were identified (Sánchez-Fernández et al., 2001) The Walker motifs facilitate ATP-binding and are usually separated by approximately 120 amino acids, with the ABC motif located between them (Martinoia *et al.,* 2002; Rea, 2007; Sánchez-Fernández *et al.,* 2001).

Despite the absence of a signal peptide in the ABCG7 protein, which is typically required for nuclear-encoded proteins that are targeted to the chloroplast (Von Heijne, 1990), this transporter has been reported in plastid proteomes of Arabidopsis and pea (Schleiff *et al.,* 2003; Gutierrez-Carbonell *et al.,* 2014; Trentmann *et al.,* 2020). However, the identified hydrophobic N-terminus of ABCG7 may act as an important signal, guiding this protein towards the chloroplast envelopes, as a highly hydrophobic N-terminus is a typical feature of proteins that are targeted to the chloroplast outer membrane by the secretory pathway (Armenteros *et al.,* 2019; H. M. Li & Chen, 1996).

Thus, to confirm the chloroplast localisation a construct, encoding an ABCG7-GFP fusion protein was cloned. The construct was transiently expressed in *Nicotiana benthamiana* leaves (Supplementary Figure 2). A strong green, fluorescent signal, derived from the ABCG7-GFP protein was detected in transfected leaf tissue (Supplementary Figure 2). Leaves showing successful expression and a strong GFP signal were used to isolate protoplasts (Figure 6). Isolated and intact protoplasts also showed a clear green, fluorescent signal surrounding the red chlorophyll autofluorescence of the chloroplasts, confirming the chloroplast localisation of the ABCG7 protein (Figure 6).

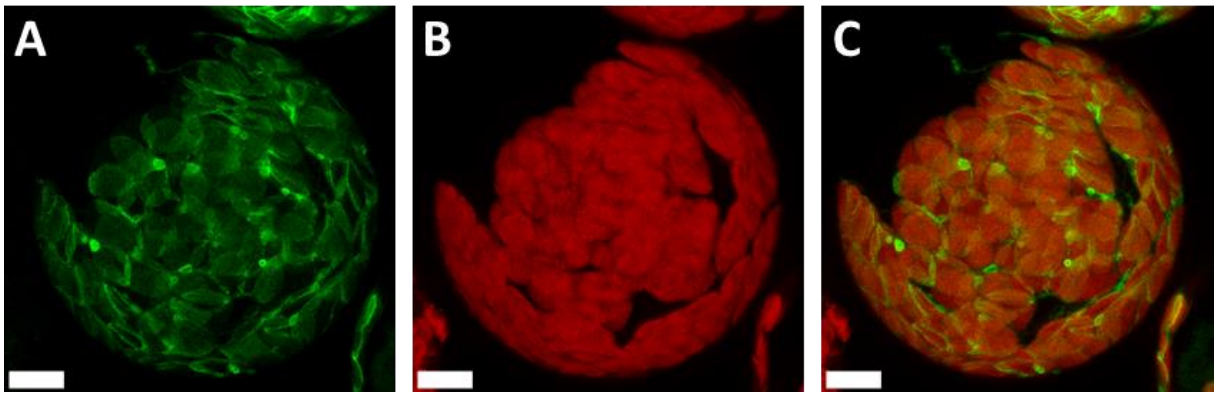

Figure 6: ABCG7-GFP localises to the chloroplast envelope. *N. benthamiana* protoplasts transiently expressing ABCG7-C-GFP. The *in planta* expression was driven by a *UBQ10* promoter. The following microscope images were taken: GFP signal (A), chlorophyll autofluorescence (B), and merge (C). The white bar indicates the 10 µm scale. Images were taken 3 to 4 days after infiltration using a Leica Stellaris 5 Confocal Scanning Microscope at the Ludwig-Maximilians-University in Munich.

The chloroplast is separated from the cytosol by 2 closely spaced membranes, the inner and outer envelope (Finkemeier & Leister, 2010; McFadden, 1999). To verify whether ABCG7 is localised to the inner or outer envelope membrane, an immunological analysis on chloroplasts enriched from transiently transfected tobacco plants expressing the ABCG7-GFP construct was performed. Prior to this, the specificity of the GFP-antibody was confirmed by immunological analysis of total protein extract from the corresponding leaves (Supplementary Figure 3). Subsequently, intact chloroplasts were isolated from ABCG7-GFP-expressing tobacco leaves and treated with thermolysin and trypsin (Figure 7).

Thermolysin is a protease that, when used at low concentrations, digests proteins and protein fragments only when they are accessible, whereas high concentrations of trypsin can penetrate the outer, but not the inner, envelope of the chloroplast (Bölter *et al.,* 2020; Jackson *et al.,* 1998; Stahl *et al.,* 1999). Following thermolysin and trypsin treatments, plastids were subjected to gel separation and were transferred to nitrocellulose membranes to conduct immunoblotting (Figure 7).

Antibodies against the plastidial outer envelope protein TOC75 (Eckart *et al.,* 2002) and the stroma-facing inner envelope protein TIC40 (Chou *et al.,* 2003), both components of the translocase machinery in chloroplasts, were used as controls. TOC75 serves as a control for the intactness of the outer envelope, whereas an immunological signal for TIC40 is only detectable in chloroplasts with an intact inner envelope due to its mainly stomal-facing protein domains (Bölter *et al.,* 2020; Jackson *et al.,* 1998; Stahl *et al.,* 1999). The use of antibodies against the potassium cation efflux antiporter KEA facilitated the determination of the protease degradation pattern of inner envelope proteins (Bölter *et al.,* 2020). ABCG7 was detected using an antibody that specifically recognised GFP fused to the transporter, allowing the determination of the membrane localisation in intact chloroplasts (Figure 7).

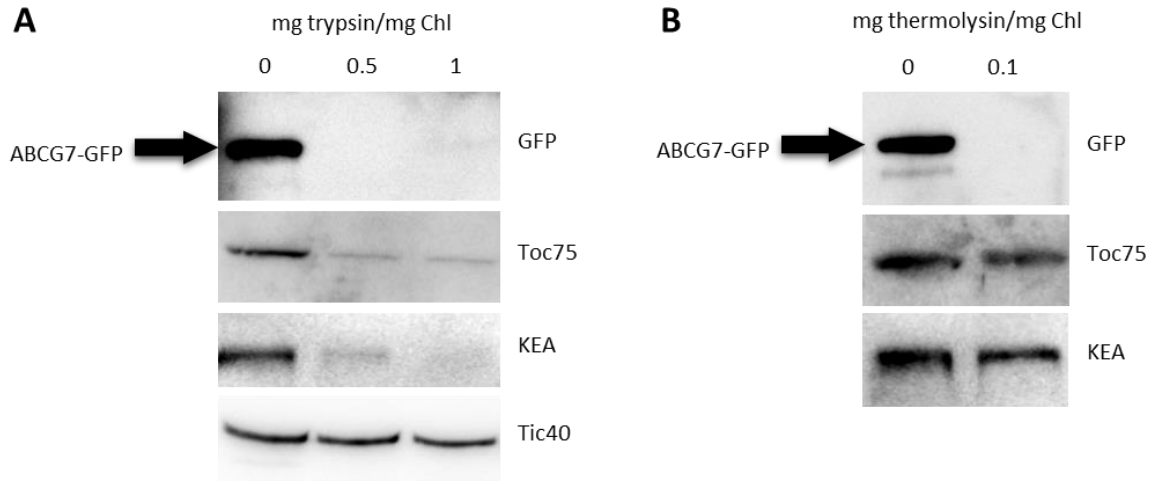

Figure 7: ABCG7 is an outer envelope protein. About 100 µg of chloroplasts were isolated from ABCG7-C-GFP-expressing *N. benthamiana* leaves and were incubated with either 0, 0.5 or 1 mg trypsin/mg chlorophyll (A) and 0 or 0.1 mg thermolysin/mg chlorophyll (B). After separation by SDS-PAGE and western blotting, corresponding proteins were detected with antibodies against the outer envelope protein TOC75, the inner envelope potassium carrier KEA, the stroma-facing protein TIC40 or the fluorophore GFP. The Western Blot was performed in collaboration with Dr. Bettina Bölter at the Ludwig-Maximilians-University in Munich.

Trypsin treatment resulted in almost complete degradation of TOC75 and KEA, whereas the inner envelope protein TIC40, which is mainly exposed on the stromal side, remained intact (Figure 7A). The deeply embedded outer envelope channel TOC75 remained largely intact upon thermolysin treatment as well as the inner envelope potassium transporter KEA (Figure 7B). This demonstrated the protease accessibility of the outer and inner envelope proteins TOC75 and KEA, while the corresponding chloroplast membranes were still intact, as shown by the strong TIC40 signal (Figure 7A). The ABCG7-GFP fusion protein was highly susceptible to both proteases (Figure 7). Intactness of both chloroplast membranes and the fact that thermolysin can only degrade proteins that are facing outward the chloroplast outer envelope, revealed the outer envelope localisation of ABCG7 within the chloroplast (Figure 7).

3.3. The *abcg7* loss-of-function lines exposed to cold conditions

Chloroplasts play a central role in coordinating the acclimation process, and several chloroplast proteins change in their abundance or localisation during cold stress, such as the protein ABCG7, which decreases in abundance (Garcia-Molina *et al.,* 2020; Trentmann *et al.,* 2020; Kleine *et al.,* 2021). Thus, to better understand the role of the ABCG7 protein in acclimation and adaptation to low temperatures, the T-DNA insertion lines, *abcg7-1* (SALK_110674) and *abcg7-2* (GABI_796G01), were employed in experiments (Supplementary Figure 4). The T-DNA insertions were identified by sequencing and are located between exons 5 and 6 in the *abcg7-1* line and within exon 9 in the *abcg7-2* line (Supplementary Figure 4A). The homozygosity of the T-DNA insertion lines was confirmed by PCR (Supplementary Figure 4B). Further, *ABCG7* transcript levels were assessed via qPCR, confirming *abcg7-2* as knock out line, while *abcg7-1* showed residual *ABCG7* expression and therefore is considered as knock down line (Supplementary Figure 4C).

3.3.1. Cold acclimation of the *abcg7* mutants

Since it is unclear what molecular mechanisms cause the rapid decrease in ABCG7 protein abundance after exposure to low temperature (Trentmann *et al.,* 2020), an analysis of the *ABCG7* transcription, was initiated by exposing wild types to 4°C for up to 10 days. Further, to examine how the absence of the ABCG7 protein affects the cold tolerance of Arabidopsis, wild types and *abcg7* loss-of-function lines were phenotypically characterised during cold exposure (Figure 8).

The *ABCG7* transcription in wild types revealed that respective mRNA levels decreased to approximately 70% already after 1 day at 4°C and remained low for the following days (Figure 8A). When the effects of cold temperatures on wild types and *abcg7* lines were investigated, mutants exhibited an increase in size relative to the wild types (Figure 8B). The increased rosettes size of the *abcg7* mutants was accompanied by a 35 to 40% increase in biomass compared to wild types at 10 days of cold treatment (Figure 8C).

The expression pattern of the cold-induced marker gene *COR15A* (Cook *et al.,* 2004; Steponkus *et al.,* 1998; Thalhammer *et al.,* 2010) was analysed by qPCR in wild types and *abcg7* mutants during exposure to cold temperatures (Figure 8D). In wild types, *COR15A* transcript levels increased 92-fold after 1 day at 4°C, whereas in *abcg7* lines, *COR15A* expression increased by 57 to 73-fold and remained consistently lower than in the corresponding wild type plants (Figure 8E).

Further a RNA sequencing analysis on wild type and *abcg7* mutants was conducted after 4 days at 4°C to elucidate further relevant changes in the cold acclimation programme between wild types and *abcg7* loss-of-function lines (Figure 9).

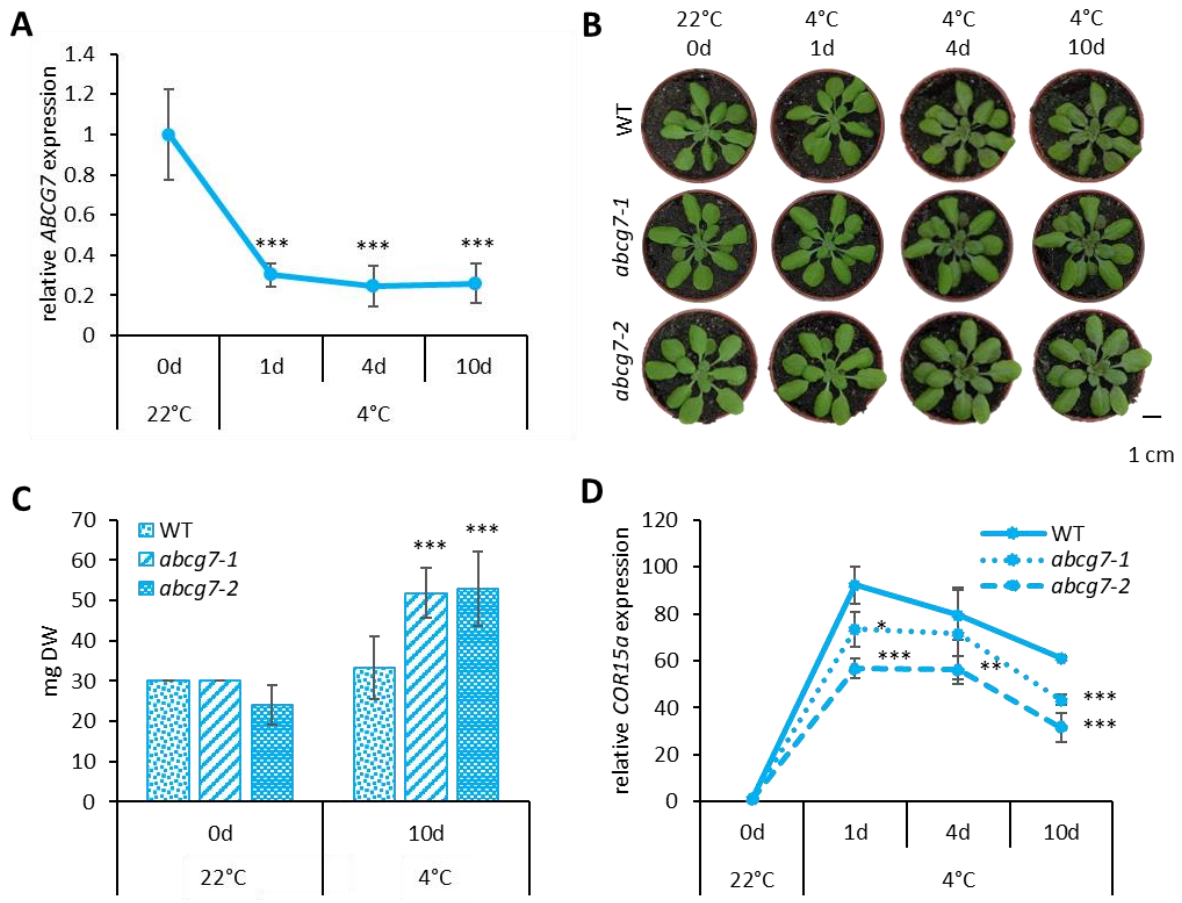

Figure 8: Growth of the *abcg7* mutants under cold conditions. The expression of *ABCG7* during the exposure of wild types to 4°C for up to 10 days was analysed via qPCR (A). Phenotypes of wild types and *abcg7* lines were photographed during the cold treatment (B) and the dry weight (C) was determined after ten days at 4°C (B). The expression of the cold-marker gene *COR15A* was evaluated via qPCR (D). Transcriptional analysis of *ABCG7* and *COR15a* was performed relative to the housekeeping gene *SAND*. The relative expression pattern was normalised to control conditions (0d at 22°C). Asterisks indicate significant differences relative to control conditions, 0d at 22°C. The significant differences were analysed by Student´s T-test (n≥4; *P<0.05; **P<0.01; ***P<0.005).

RNA sequencing confirmed the previously observed lower levels of *COR15A* transcript in the *abcg7* mutants. With a few exceptions, other genes relevant to the cold acclimation programme mutants (Doherty *et al.,* 2009; Garcia-Molina *et al.,* 2020), showed a decreased transcription pattern in cold-acclimating *abcg7* mutants compared to wild types (e.g., *COR15B*, several CBF/*DREB* genes, and the ROS markers *ZAT10* and *ZAT12;* Figure 9).

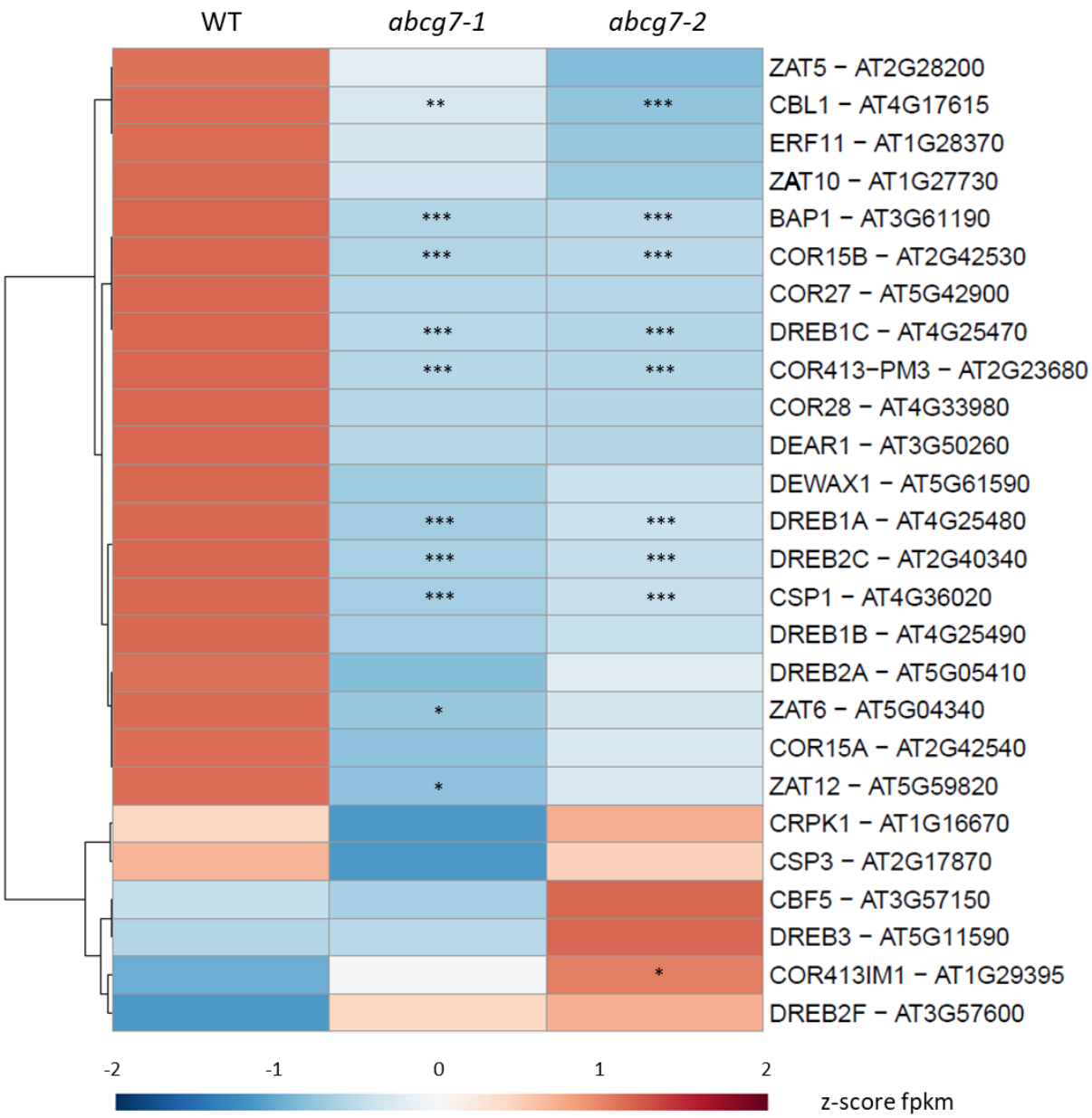

Figure 9: Altered cold-induced acclimation programme in the *abcg7* mutants. For RNA sequencing 4-week-old wild types and *abcg7* lines, grown on soil under standard conditions, were transferred for cold acclimation from 22°C to 4°C for 4 days (n=3, 3 rosettes per n). The z-score for the mean fpkm values (fpkm>1) was visualised as a heat map using R studio version 2023.12.1 build 402. Asterisks indicate significant differences relative to the wild type (*padj<0.05; **padj<0.01; ***padj<0.005). Bioinformatic analysis and statistical analysis of the RNA sequencing results was performed by Novogene.

3.3.2. Metabolic profiling of cold-acclimating *abcg7* mutants

Cold-induced metabolic reprogramming has been shown to result in the accumulation of sugars, including glucose, fructose and sucrose, as well as variations in metabolites of the tricarboxylic acid cycle or amino acids, such as proline (Cook *et al.,* 2004; Doherty *et al.,* 2009). Consequently, sugar contents, organic acids and amino acids, were monitored during the cold acclimation of wild types and *abcg7* mutants, revealing major alterations on the 4th day of cold treatment for sugars (Figure 10, Supplementary Figure 5). Whereas, the main significant changes in organic acids (Figure 11) and amino acids (Figure 12, Supplementary Figure 6) were observed at the 10th day of cold acclimation.

The transfer from 22°C to 4°C resulted in lower glucose levels in the *abcg7* mutants compared to wild types (Figure 10A). Initially, glucose levels in all plant lines were around 2.0 to 2.5 µmol glucose/g DW. However, after 4 days at 4°C, glucose levels increased to 23.5 µmol glucose/g DW in wild types, while only a content of 13.5 to 16.2 µmol glucose/g DW was reached in the *abcg7* lines (Figure 10A).

The fructose and sucrose contents did not differ significantly between the three lines during cold acclimation (Figure 10B-C). Fructose contents in all plant lines were around 0.7 to 1 µmol fructose/g DW under control conditions, whereas after cold acclimation 5.8 µmol fructose/g DW in wild types and *abcg7-1* was reached, while in *abcg7-2* a content of 3.6 µmol fructose/g DW was measured (Figure 10B). The sucrose content at 22°C in the *abcg7* lines of 5.0 to 5.7 µmol sucrose/g DW was significantly lower in comparison to sucrose contents of 7.4 µmol sucrose/g DW in wild types. However, following a cold acclimation phase of 4 days at 4°C, the sucrose levels increased in the three lines to contents ranging from 16.4 to 19.2 µmol sucrose/g DW (Figure 10C).

Further, both *abcg7* lines showed higher galactose levels when exposed to 4°C for 4 days, accumulating a maximum of 10 µmol galactose/g DW, while the wild types contained only 1 µmol galactose/g DW (Figure 10D).

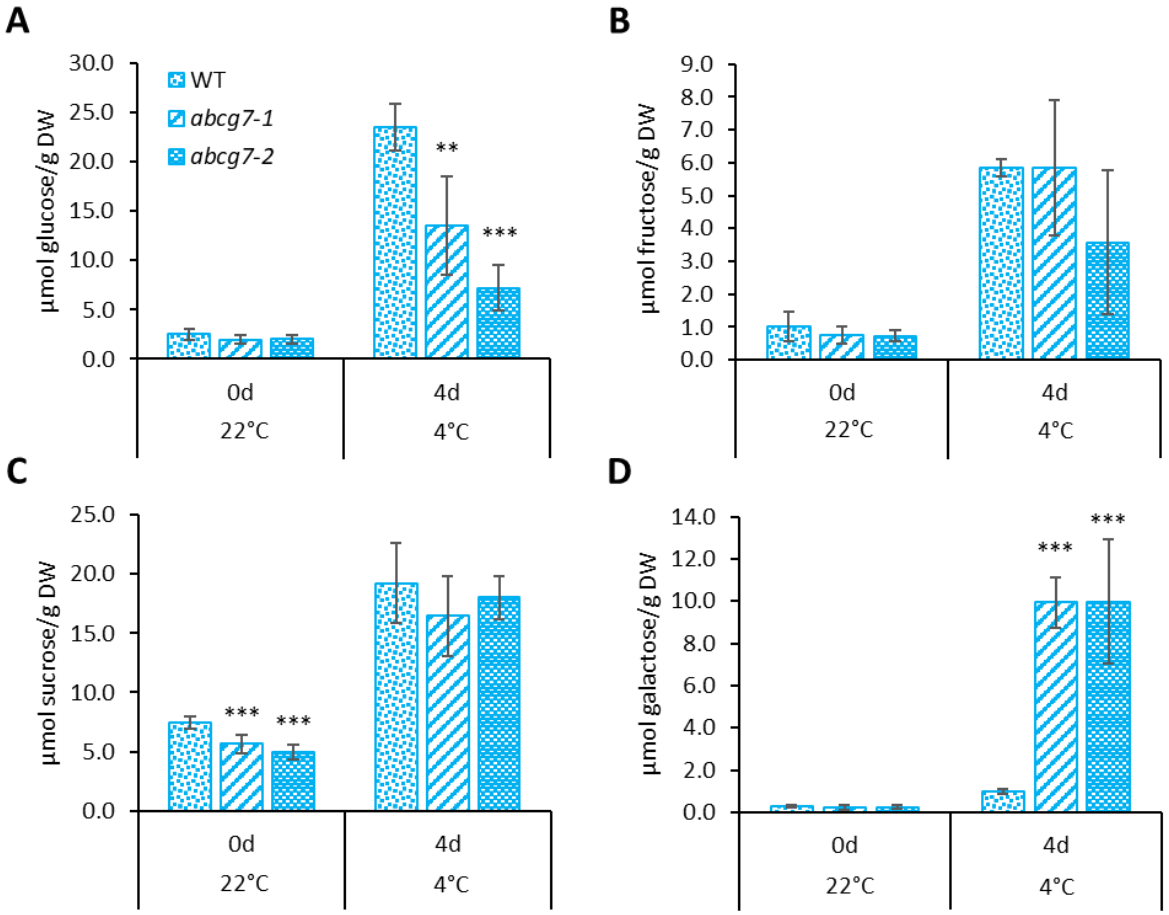

Figure 10: Sugar contents of cold-acclimating *abcg7* lines. The 4-week-old Arabidopsis wild type and *abcg7* lines, grown on soil under standard conditions, were transferred for cold acclimation from 22°C to 4°C for 4 days. The contents of glucose (A), fructose (B), sucrose (C) and galactose (D) were measured. Asterisks indicate significant differences relative to wild types (n≥3; *P<0.05; **P<0.01; ***P<0.005). The Student's T-test was calculated using Microsoft Excel. The measurements were conducted in collaboration with Prof. Dr. Andreas Richter at the University of Rostock.

The levels of these organic acids were significantly lower in the *abcg7* mutants under control conditions at 22°C in comparison to wild types (Figure 11). In wild types, the level of malate was found to be 362.5 µg malate/mg DW, whereas in the *abcg7* mutants, contents of 237.4 and 268.4 µg malate/mg DW were measured, respectively (Figure 11A). A similar trend was observed for fumarate levels in *abcg7-1* and *abcg7-2* (12.04 µg/mg DW and 10.7 µg/mg DW, respectively) compared to wild types (16.41 µg fumarate/mg DW; Figure 11B). For succinate, 884.3 ng/mg DW was detected in wild types, versus 616 ng succinate/mg DW in *abcg7-1* and 699 ng succinate/mg DW in *abcg7-2* (Figure 11C).

However, after 4 days at 4°C, the contents of malate and fumarate increased to wild type levels, ranging between 315.8 to 333 µg malate/mg DW (Figure 11A), and 9 to 9.3 µg fumarate/mg DW in in the mutants (Figure 11B). A strong tendency of increased succinate levels in *abcg7-1* (468.4 ng succinate/mg DW) and significantly higher contents with 515.3 ng succinate/mg DW in *abcg7-2* were measured in comparison to wild types (381.71 ng succinate/mg DW; Figure 11C).

After 10 days at 4°C, the contents of the organic acids were significantly higher in *abcg7* mutants compared to wild types. The content of malate was found to be 388.4 µg/mg DW in wild types, in comparison to 477 to 500 µg malate/mg DW measured in the *abcg7* mutants (Figure 11A). Furthermore, a fumarate content of 8.6 to 10.3 µg fumarate/mg DW in the *abcg7* lines was measured, whereas the content in wild types was 7.6 µg fumarate/mg DW (Figure 11B). Succinate content in wild types was measured at 456 ng/mg DW, whereas in *abcg7-1* and *abcg7-2*, contents of 600 and 652.2 ng succinate/mg DW were detected, respectively (Figure 11C).

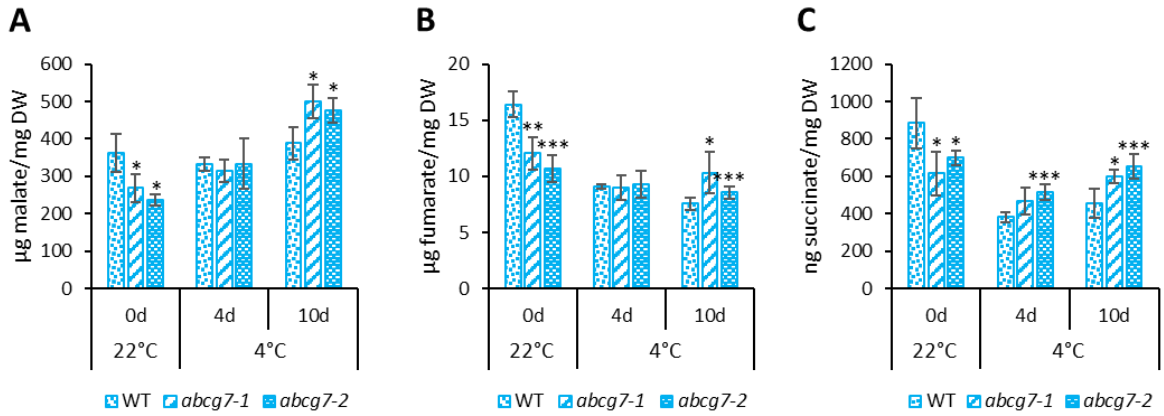

Figure 11: Organic acids analysed in *abcg7* mutants after cold acclimation. The 4-week-old wild types and *abcg7* lines, grow on soil under standard conditions, were transferred for cold acclimation from 22°C to 4°C. Changes in malate (A), fumarate (B), and succinate (C) were measured in wild types and *abcg7* lines after 4 and 10 days of cold. Asterisks indicate significant differences relative to wild types (n≥3; *P<0.05; **P<0.01; ***P<0.005). The Student's T Test was calculated using Microsoft Excel. The measurements were conducted in collaboration with Dr. Stefan Timm at the University of Rostock.

Under control conditions at 22°C, with some exceptions, a variety of amino acids were observed to be significantly lower in the *abcg7* mutants in comparison to wild types. These included the charged amino acids lysine and arginine, the nonpolar amino acids alanine and valine, the polar amino acid asparagine and the aromatic amino acids tryptophane and phenylalanine (Supplementary Figure 6).

After 1 day at 4°C, the levels of the above-mentioned amino acids increased to levels comparable to those observed in wild types. However, after 4 days of at 4°C, only the aromatic amino acids tyrosine and tryptophan showed a significant increase in the *abcg7* mutants relative to wild types. By contrast, after 10 days at 4°C, serine, proline and histidine were the only amino acids that were elevated in the *abcg7* mutants (Supplementary Figure 6).

As the aromatic amino acids tyrosine and tryptophan were specifically elevated after 4 days at 4°C, these aromatic acids and phenylalanine were shown in Figure 12.

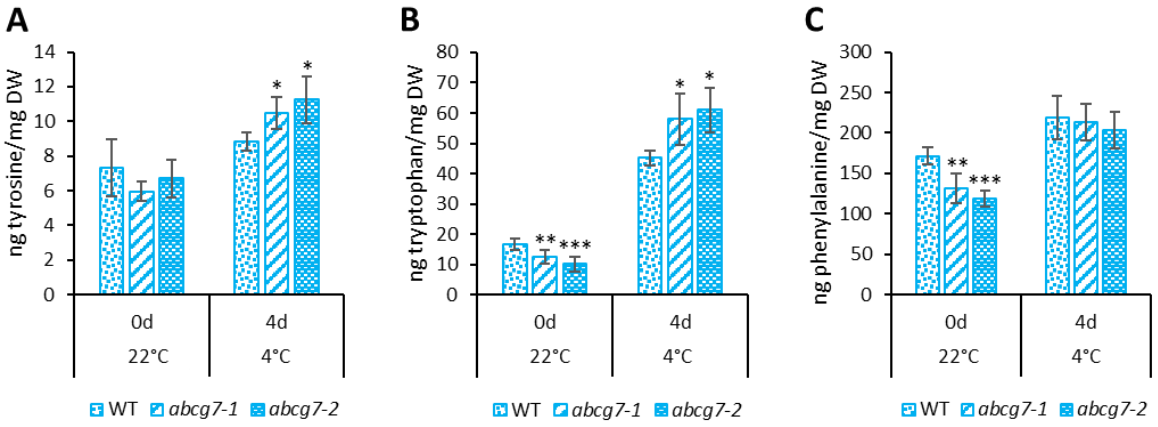

Figure 12: Alterations in aromatic amino acids in *abcg7* mutants during cold acclimation. The 4-week-old wild types and *abcg7* lines, grown on soil under standard conditions, were transferred for cold acclimation from 22°C to 4°C. Changes in tyrosine (A), tryptophan (B) and phenylalanine (C) were measured in wild types and *abcg7* lines after 4 days of cold treatment. Asterisks indicate significant differences relative to wild types (n≥3; *P<0.05; **P<0.01; ***P<0.005). The Student's T Test was calculated using Microsoft Excel. The measurements were conducted in collaboration with Dr. Stefan Timm at the University of Rostock.

Under control conditions at 22°C, tyrosine levels ranged from 6 to 6.7 ng tyrosine/mg DW in *abcg7* mutants, thus were marginally lower compared to wild types with contents of 7.3 ng tyrosine/mg DW (Figure 12A). However, significantly lower tryptophan and phenylalanine levels were observed in the *abcg7* mutants under control conditions at 22°C. The measured contents ranged from 10.2 to 12.6 ng tryptophan/mg DW and 118.1 to 131 ng phenylalanine/mg DW in *abcg7* mutants, whereas wild types exhibited levels of 16.6 ng tryptophan/mg DW and 171.6 ng phenylalanine/mg DW at 22°C (Figure 12B-C).

Interestingly, after 4 days at 4°C, tyrosine and tryptophan contents were significantly elevated in *abcg7* mutants (10.5 to 11.3 ng tyrosine/mg DW and 58 to 61 ng tryptophan/mg DW) compared to corresponding wild types (8.8 ng tyrosine/mg DW and 45.2 ng tryptophan/mg DW; Figure 12A-B). However, in *abcg7* mutants, phenylalanine levels remained comparable to those observed in wild types, ranging between 203.6 and 219 ng phenylalanine/mg DW (Figure 12C). As phenylalanine is the primary substrate for the phenylpropanoid metabolic pathway, leading to the production of various secondary metabolites, including anthocyanins (Li *et al.,* 2017), the total anthocyanin content was measured in both, wild types and *abcg7* mutants (Figure 13).

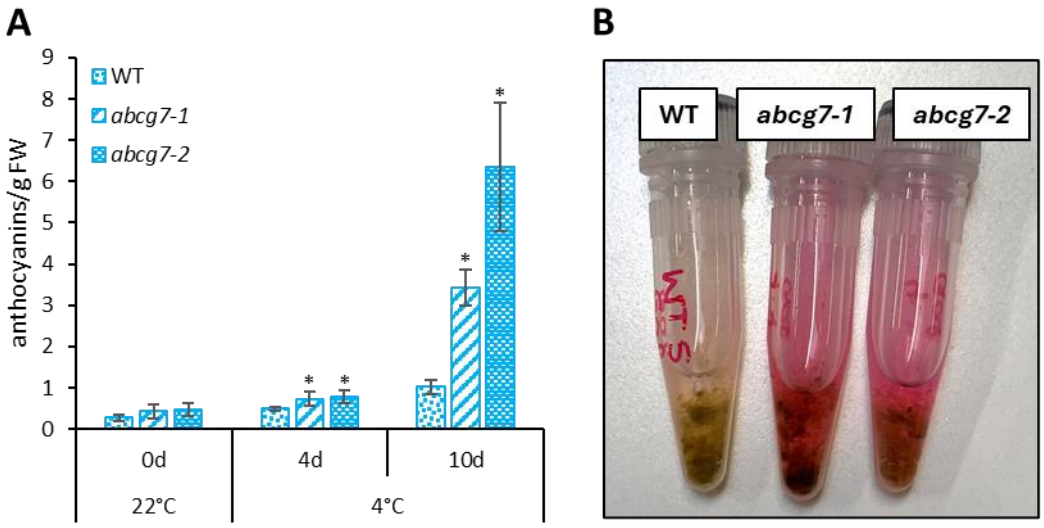

Figure 13: Anthocyanin production under cold conditions in *abcg7* mutants. During the cold experiment 4-week-old wild types and *abcg7* lines, grown on soil under standard conditions, were transferred from 22°C to 4°C. Anthocyanin production was measured in wild types and *abcg7* lines after 4 and 10 days of cold stress (A). During the extraction process after 10 days at 4°C, the difference in anthocyanin accumulation between wild types and *abcg7* lines was clearly visible by eye (B). Asterisks indicate significant differences relative to wild types (n≥3; *P<0.05; **P<0.01; ***P<0.005). The Student's T Test was calculated using Microsoft Excel.

Following the extraction and measurement of total anthocyanin contents from cold-acclimating wild types and *abcg7* mutants, significantly elevated pigment levels were detected after 4 days at 4°C (Figure 13A). The highest anthocyanin levels were detected after 10 days under cold conditions (Figure 13A), and were clearly visible and observable during the extraction process due to their remarkable purple colouration (Figure 13B). The anthocyanin levels measured at the 10th day at 4°C were found to be approximately 3-times higher in *abcg7-1* and approximately 6-times higher in *abcg7-2* in comparison to wild types (Figure 13A).

3.3.3. Expression of genes involved in amino acid biosynthesis

The most notable changes in the amino acid metabolism during cold acclimation were affecting tyrosine, tryptophan and phenylalanine (Figure 12; Supplementary Figure 6). Therefore, RNA sequencing data obtained from wild types and *abcg7* mutant plants after 4 days at 4°C, was re-evaluated. The analysis focused on genes involved in the amino acid biosynthesis (Reyes-Prieto and Moustafa, 2012). Since transcript variations were found in genes affecting the synthesis of phenylalanine, *PAL* genes were also included into the analysis (Figure 14). *PAL* genes encode for phenylalanine ammonia-lyases, which consume phenylalanine as a substrate for the phenylpropanoid pathway to produce secondary metabolites, such as anthocyanins (Dixon & Paiva, 1995).

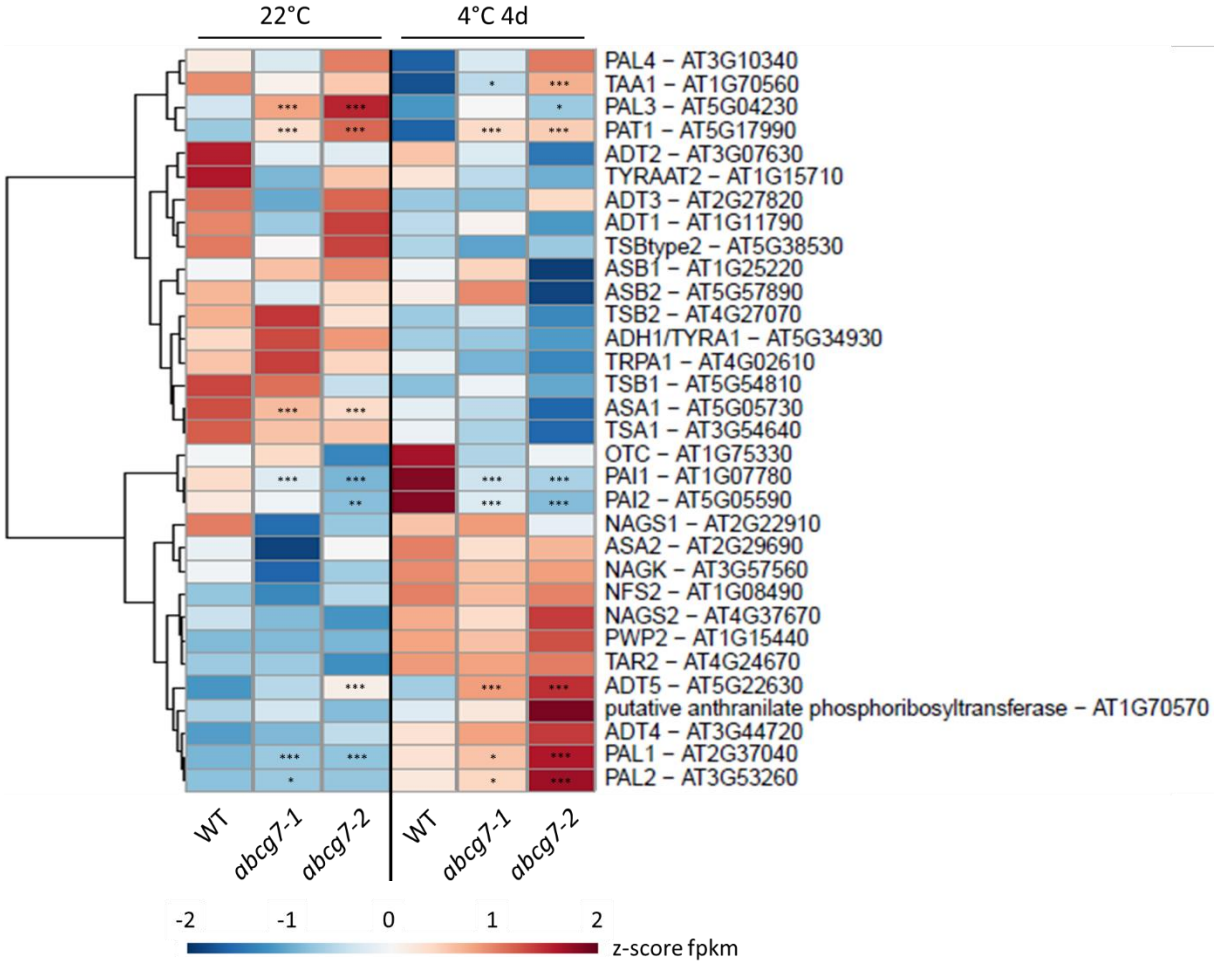

Figure 14: Altered expression of genes involved in aromatic amino acid synthesis and the *PAL* genes in the *abcg7* mutants. For RNA sequencing 4-week-old wild types and *abcg7* lines, grown on soil under standard conditions, were transferred for cold acclimation from 22°C to 4°C for 4 days (n=3, 3 rosettes per n). The z-score for the mean fpkm values (fpkm>1) was visualised as a heat map using R studio version 2023.12.1 build 402. Asterisks indicate significant differences relative to wild types at the respective day (*padj<0.05; **padj<0.01; ***padj<0.005). Bioinformatic analysis and statistical analysis of the RNA sequencing results was performed by Novogene.

Although some transcriptomic changes were found to affect the tryptophan biosynthesis, the expression differences between wild types and *abcg7* mutants persisted at 22°C and after 4 days at 4°C. For example, variations were identified in genes encoding for the enzymes phosphoribosyl anthranilate transferase 1 (*PAT1*), the α-subunit of the anthranilate synthase complex (*ASA1*) or some phosphoribosyl anthranilate isomerases (*PAI1* and *PAI2;* Li *et al.,* 1995; Rose and Last, 1997). The *PAT1* and *ASA1* transcription was significantly higher in the *abcg7* mutants at 22°C, while lower transcription was observed for *PAI1* and *PAI2* in comparison to wild types. After 4 days at 4°C, the observed transcriptional patterns of *PAT1* and *PAI1* or *PAI2* were still detectable and showed a stronger expression difference between wild types and the *abcg7* mutants (Figure 14).

The *ADT* genes encode enzymes known as arogenate dehydratases, which catalyse the rate-limiting step of phenylalanine biosynthesis (El-Azaz *et al.,* 2022). Except for *ADT2*, an increased tendency towards transcription was observed for *ADT1* in *abcg7-1* and *ADT3* in *abcg7-2* during cold acclimation in the mutants. Moreover, the analysis of both mutants revealed a tendency of higher expression levels for *ADT4* and significantly increased transcript levels for the gene *ADT5* after 4 days at 4°C compared to wild types (Figure 14).

In addition, significantly lower transcript levels for *PAL1* in both mutants, as well as significantly lower expression of *PAL2* in *abcg7-1*, were observed under control conditions at 22°C compared to wild types. However, mRNA levels of *PAL3* were higher in the *abcg7* mutants relative to wild types, whereas the expression of *PAL4* was in tendency lower in *abcg7-1*, but higher levels were observed in *abcg7-2* in comparison to wild types at 22°C (Figure 14).

PAL expression changed completely during cold acclimation in *abcg7* mutants versus wild types. After 4 days at 4°C a significant increase in the transcription of *PAL1* and *PAL2* was observed in *abcg7-1* and *abcg7-2* compared to wild types. A tendency towards increased expression in the mutants was also noted for *PAL4*. In contrast, *PAL3* expression exhibited a tendency to decrease in *abcg7-1* and a significant decline in mRNA levels was observed in *abcg7-2* relative to wild types at 4°C (Figure 14). Thus, the changes in *ADT* and *PAL* expression, could indicate a channelling of the aromatic amino acid phenylalanine towards the anthocyanin accumulation in the *abcg7* loss-of-function lines.

3.3.4. Transcription of cell wall genes in cold-acclimating *abcg7* mutants

In addition to the metabolic and expressional variations in the amino acid metabolism in the cold acclimated *abcg7* lines (Figure 12; Supplementary Figure 6), the observed accumulation of galactose, (Figure 10D), necessitates further investigation. Therefore, a detailed re-examination of the RNA sequencing data obtained from wild types and *abcg7* mutants after 4 d at 4°C was performed. To this end, a Gene Ontology (GO) term analysis was carried out to determine whether other pathways besides those involved in the cold acclimation programme or amino acid metabolism might be altered in the *abcg7* mutants. The most prominent expression changes were identified exclusively in the knock out line *abcg7-2*, revealing several significantly down regulated GO terms (Supplementary Figure 7).

The affected GO terms were associated with a response to chitin, jasmonic acid, or the cell wall (Supplementary Figure 7). Subsequent analysis of the genes within the GO terms related to chitin or jasmonic acid revealed that most of their functions were either uncharacterised or related to signalling. Since, jasmonic acid is positively regulating the CBF transcriptional pathways, leading to the up-regulation of cold-responsive genes and interacts with other hormonal signalling pathways, such as ethylene or auxin (Hu *et al.,* 2017), the most intriguing GO terms were those pertaining to cell wall-related processes (Supplementary Figure 7). The significant transcriptomic changes within the cell wall-related GO terms were visualised in Figure 15.

The analysis of the transcriptome showed that the *abcg7* mutants, especially *abcg7-2*, had lower transcript levels of genes involved in the metabolism of pectin and xyloglucan in comparison to wild types (Figure 15). For example, the genes encoding pectin methyl esterases (*PME*) that are involved in pectin modification, such as *PME2* and *PME41* genes, showed lower expression levels in comparison to wild types after 4 days at 4°C (Figure 15). Similarly, the *abcg7* mutants showed a lower transcript pattern in several genes encoding for enzymes that are involved in xyloglucan synthesis such as xyloglucan α-1,6-xylosyltransferase 1 (*XXT1*) or α-1,4-fucosyltransferase (*FUT13*) and xyloglucan remodelling as evidenced by changes in the expression of various xyloglucan endotransglucosylase/hydrolases (*XTH*), such as for example *XTH18*, *XTH19* and *XTH22* (Figure 15). Respective changes in transcription patterns of cell wall-related genes might be a sign towards an altered cell wall organisation or modification in the *abcg7* loss-of-function lines under cold conditions.

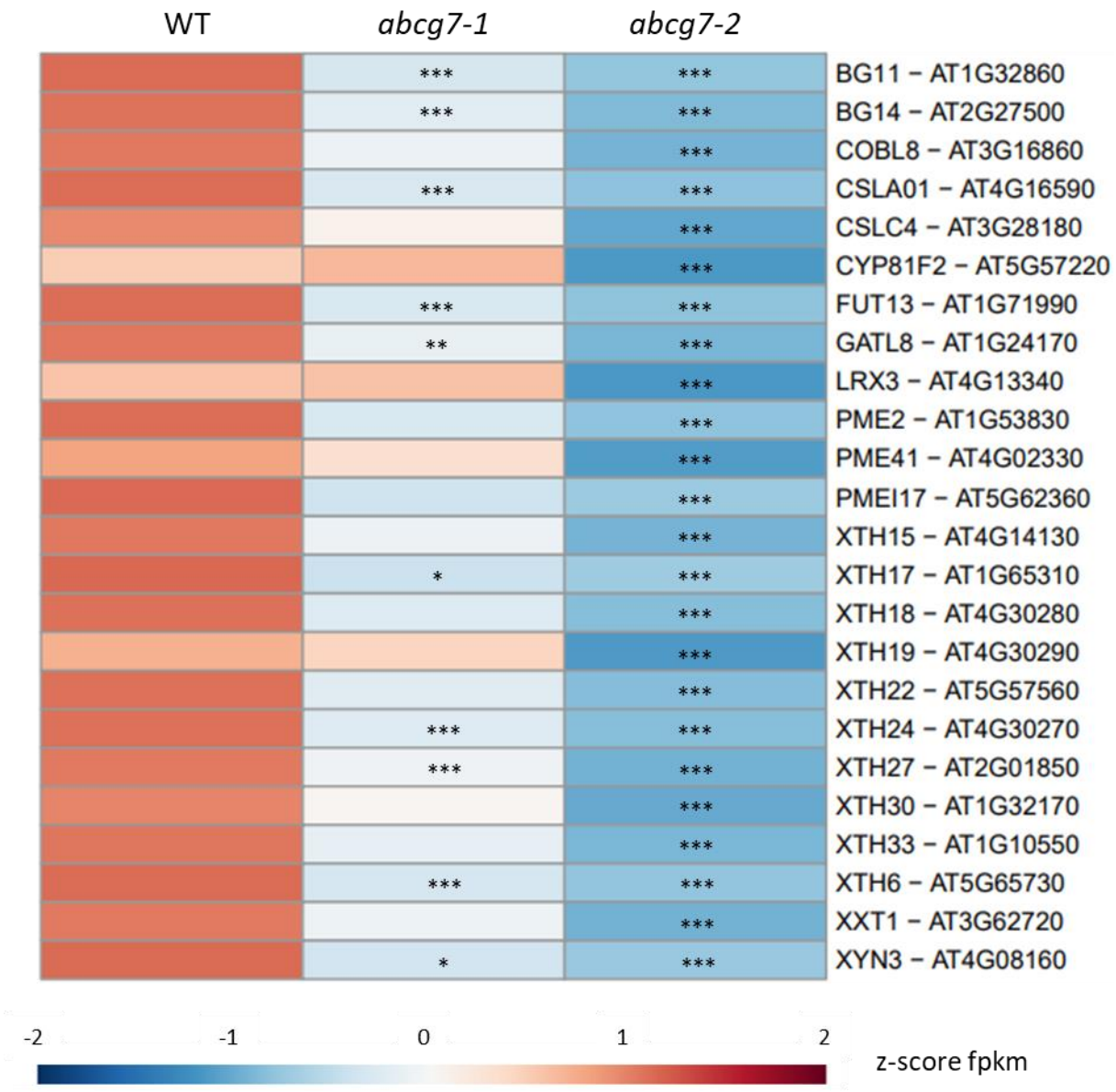

Figure 15: Cold temperatures affect the expression of cell wall genes in *abcg7* mutants. Plants were grown at 22°C for 4 weeks under standard conditions before being transferred to 4°C for 4 days. RNA sequencing samples were harvested on the 4th day at 4°C (n=3, 3 rosettes per n). The z-score for the mean fpkm values (fpkm>1) was visualised as a heat map using R studio version 2023.12.1 build 402. Asterisks indicate significant differences relative to the wild type at the respective day (*padj<0.05; **padj<0.01; ***padj<0.005). Bioinformatic analysis and statistical analysis of the RNA sequencing results was performed by Novogene.

3.4. Effects of galactose on wild type and *abcg7* loss-of-function lines

During the phenotypical characterisation of wild types and *abcg7* mutants under cold conditions, *abcg7* loss-of-function lines exhibited an accumulation of galactose (Figure 10D). Since sugars, such as sucrose, glucose or fructose, have been identified as key molecular signals required to regulate environmental stress responses, for example by inducing anthocyanin synthesis (Pereyra *et al.,* 2023; Seguela-Arnaud *et al.,* 2015), it is unclear whether galactose can modify metabolic responses during acclimation to cold temperatures.

To investigate whether galactose accumulation could induce anthocyanin production, wild types and *abcg7* mutants were grown on ½ MS plates, without or with the addition of 1% (w/v) galactose. After 2-weeks of cultivation under control conditions at 22°C, the physiological appearance of the seedlings was documented, and the fresh weight was determined. Further, total anthocyanins were extracted, and specifically the content of the amino acid phenylalanine was measured (Figure 16).

The *abcg7* loss-of-function lines demonstrated a smaller size and fresh weight in comparison to wild types when cultivated on ½ MS plates without galactose (Figure 16A-B). No galactose was detected in wild type or mutant seedlings, when grown on ½ MS plates without galactose (Supplementary Figure 8A). Further, measurement of carbohydrates revealed that the *abcg7* mutants exhibited significantly lower sucrose (Supplementary Figure 8B) and starch contents in comparison to the corresponding wild types (Supplementary Figure 9).

Wild types and *abcg7* seedlings grown on ½ MS plates supplemented with galactose, showed an intrinsic galactose accumulation, however no significant differences in the carbohydrate levels of sucrose, glucose, fructose (Supplementary Figure 8) or starch were detected (Supplementary Figure 9). An impaired growth of wild type and *abcg7* seedlings grown on galactose-containing plates was observed in comparison to the ½ MS plates without sugar (Figure 16A-B). Despite the obvious growth inhibitory effect of galactose on the three lines, *abcg7* seedlings displayed a larger size in comparison to wild types (Figure 16A). These visual observations were supported by the determined fresh weight (Figure 16B).

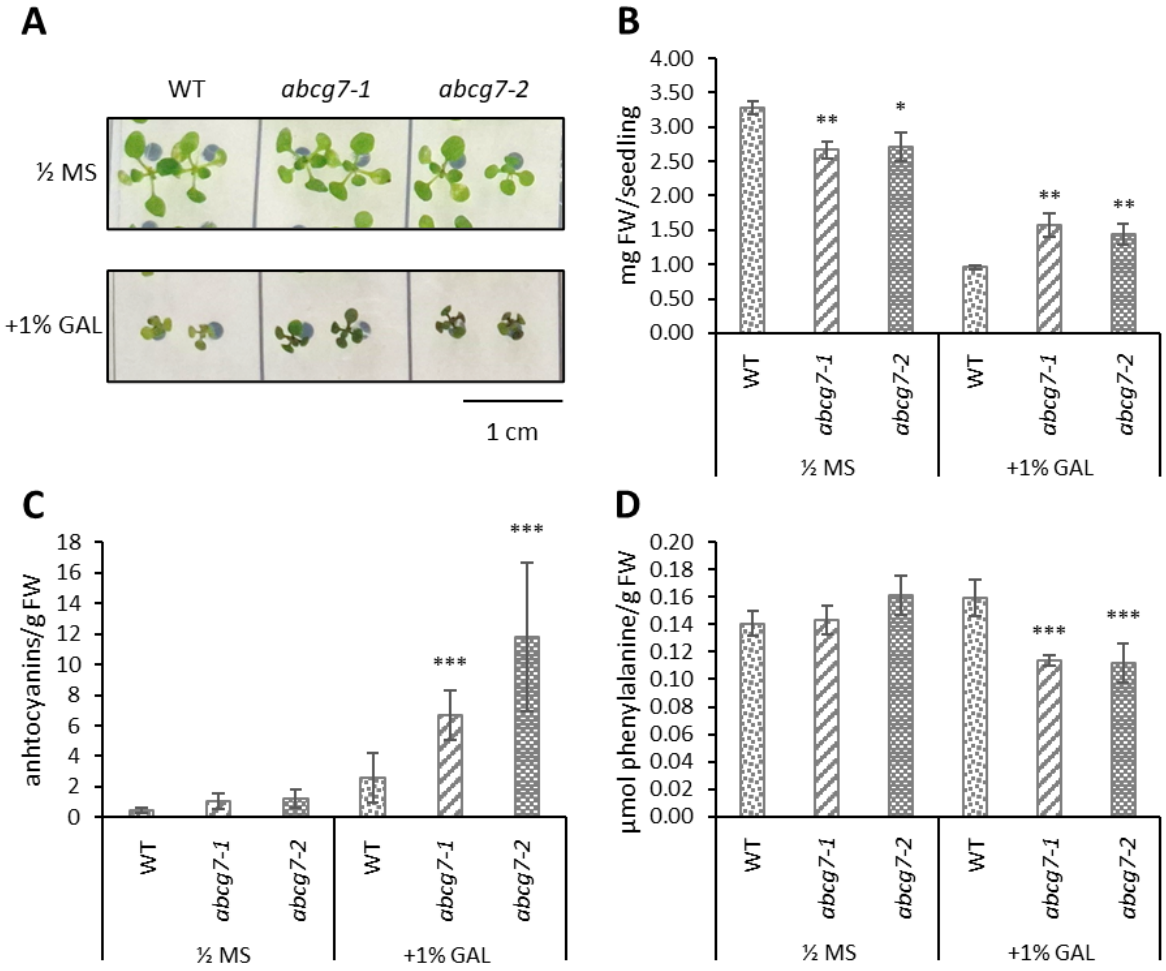

Figure 16: Seedlings of wild types and *abcg7* mutants after growth on ½ MS plates with galactose. Photographs were taken after 14 days of growth on ½ MS plates, either without or with 1% (w/v) galactose under standard conditions (A). The fresh weight (B), anthocyanin (C) and phenylalanine contents were determined (D). Asterisks indicate significant differences relative to wild types (n≥3; 20 seedlings per n; *P<0.05; **P<0.01; ***P<0.005). The Student's T-test was calculated using Microsoft Excel.

As the *abcg7* loss-of-function lines displayed a dark purple colouration on ½ MS plates with galactose (Figure 16A), total anthocyanin contents were extracted (Figure 16C). The extraction revealed significantly elevated levels of respective pigments in the presence of galactose in wild type and *abcg7* seedlings. The anthocyanin content was 3-fold higher in *abcg7-1* and 6-fold higher in *abcg7-2* in comparison to corresponding wild types (Figure 16C). This observation is in alignment with the measured phenylalanine contents in *abcg7* mutants cultivated on galactose containing plates. Phenylalanine levels were significantly lower in the *abcg7* mutants compared to wild types (Figure 16D). This suggests that the presence of high levels of galactose can induce anthocyanin accumulation, which is even more pronounced in the *abcg7* loss-of-function lines, presumably due to the elevated consumption of phenylalanine by anthocyanin synthesis.

To provide a comprehensive understanding of the underlying reasons why the mutants demonstrated a higher tolerance level to galactose, an examination of the *ABCG7* expression in wild type leaf discs in the presence of 50 mM mannitol or 50 mM galactose was conducted. *ABCG7* expression showed a 53% decrease with mannitol and a 43% decrease with galactose (Figure 17). Apparently, the reduction in *ABCG7* transcription is generated due to an osmotic response, rather than a galactose specific effect. Apparently, *abcg7* loss-of-function mutants have an advantage in the presence of galactose in comparison to wild types.

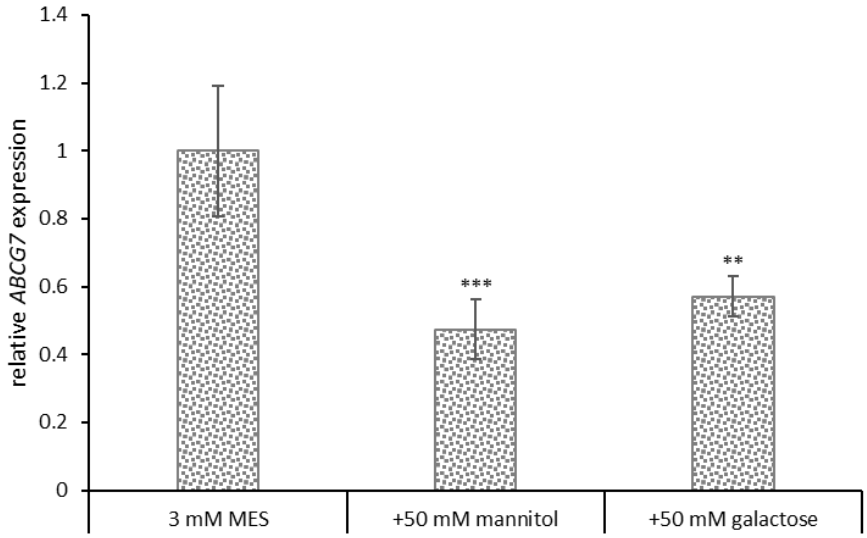

Figure 17: *ABCG7* gene expression in leaf discs of wild types in presence of mannitol or galactose. Approximately 4-week-old wild type plants cultivated under standard conditions were utilised for the extraction of leaf discs (5 mm in diameter each). About 5 leaf discs per n were incubated in 5 mL of 3 mM MES (pH 5.6) and in respective MES buffer with 50 mM mannitol or 50 mM galactose. The expression levels of *ABCG7* were evaluated via qPCR, with *SAND* serving as the reference gene. Asterisks indicate significant differences relative to the MES buffer (n≥3; *P<0.05; **P<0.01; ***P<0.005). The Student's T Test was calculated in Microsoft Excel.

3.5. The *abcg7* loss-of-function lines under freezing stress

Plants enhance their freezing tolerance when exposed to low, non-damaging and non-freezing temperatures, a process referred to as cold acclimation (Jaglo-Ottosen *et al.,* 1998; Wanner & Junttila, 1999). During the exposure of the *abcg7* loss-of-function mutants to 4°C, an increase in rosette size and biomass was observed (Figure 8B-C). The improved growth and performance suggest that the *abcg7* mutants have an enhanced cold tolerance in comparison to wild types (Figure 8B-C). In addition, several transcriptional changes related to cell wall organisation were identified during exposure to 4°C in the *abcg7* mutants (Figure 15).

Since it has been shown that modifying the response to cold temperatures can lead to an increase in freezing tolerance (Jaglo-Ottosen *et al.,* 1998; Wanner & Junttila, 1999) and that changes in cell wall constituents, especially the modification of mechanical properties, are crucial for the establishment of freezing tolerance (Takahashi *et al.,* 2019, 2021, 2024), the characterisation of the *abcg7* lines was extended to investigate their behaviour during and post-freezing exposure.

3.5.1. Freezing tolerance of the *abcg7* mutants

Freezing injuries are a significant environmental stress that has the capacity to limit plant productivity and geographical distribution. However, *Arabidopsis thaliana* has been shown to possess the capacity to withstand temperatures as low as -6°C, provided it has been acclimated to 4°C for a minimum period of 3 days (Jaglo-Ottosen *et al.,* 1998; Li *et al.,* 2004; Wanner & Junttila, 1999; Zheng *et al.,* 2016). Thus, to investigate the freezing tolerance and survival rate of wild types and *abcg7* loss-of-function lines a method with a sublethal freezing temperature of -10°C was adapted from Trentmann *et al.,* 2020.

To this end, 4-week-old plants grown under standard conditions were transferred to 4°C for 4 days, after which the temperature was gradually decreased by 2°C/h until it reached -10°C. During this gradual temperature decrease from 4°C to -10°C, the light was switched off. The plants were maintained at -10°C temperature for 15 hours in the dark, after which a gradual thawing process was initiated at a rate of 2°C/h in the dark, as previously described by Trentmann *et al.,* 2020. Once the temperature had reached 22°C, the plants were returned to control conditions for a recovery period of 2 weeks. Afterward the recovery period the survival rate was quantified and the *ABCG7* expression was analysed in wild types during the freezing experiment (Figure 18).

After the recovery period, wild types and *abcg7* loss-of-function lines were phenotypically examined, displaying differences in appearance and size. The mutants demonstrated a reduction in rosette size when compared to the wild types. Furthermore, a number of the smaller *abcg7* plants exhibited dark purplish leaves, indicative of anthocyanin accumulation, and signs of wilting. In contradistinction, wild types exhibited only wilted leaves (Figure 18A). The quantification of the survival rate showed a decreased freezing tolerance for *abcg7-1* and *abcg7-2* relative to wild types. The survival rate of *abcg7-1* and *abcg7-2* was diminished by approximately 30 to 50% in comparison to wild types, which showed a freezing survival rate of 90% (Figure 18B).

The analysis of the *ABCG7* transcript in wild types revealed a significant transient downregulation of mRNA during periods of cold and initial freezing temperatures in comparison to the control temperature of 22°C (Figure 18C). As demonstrated in Figure 18C, a 44% decrease in *ABCG7* transcript levels during the phases of cold acclimation and freezing stress was observed. The transcription rate remained low, until a temperature of -2°C was reached during the thawing phase. At -2°C, a significant increase in *ABCG7* transcript of approximately 28% was observed in comparison to the control temperature of 22°C. However, during further elevation of temperature, *ABCG7* expression appeared to adjust back to the transcript level observed under the control temperature prior the stress treatment (Figure 18C).

Besides physiological, biochemical and molecular changes which are known to take place during cold acclimation at low, non-freezing temperatures, there are a number of further modifications which can take place specifically at sub-zero temperatures. These changes can significantly contribute to the build-up of freezing tolerance, thus ensuring the survival of plants during phases of recovery subsequent to freezing stresses (Takahashi *et al.,* 2019, 2021, 2024).

Thus, the specific increase in *ABCG7* expression at -2°C during the thawing phase may indicate a necessary event for the survival of freezing temperatures in Arabidopsis. Consequently, the thawing process was identified as a critical phase of the experiment where the temperature of -2°C was found to be the most important (Figure 18C).

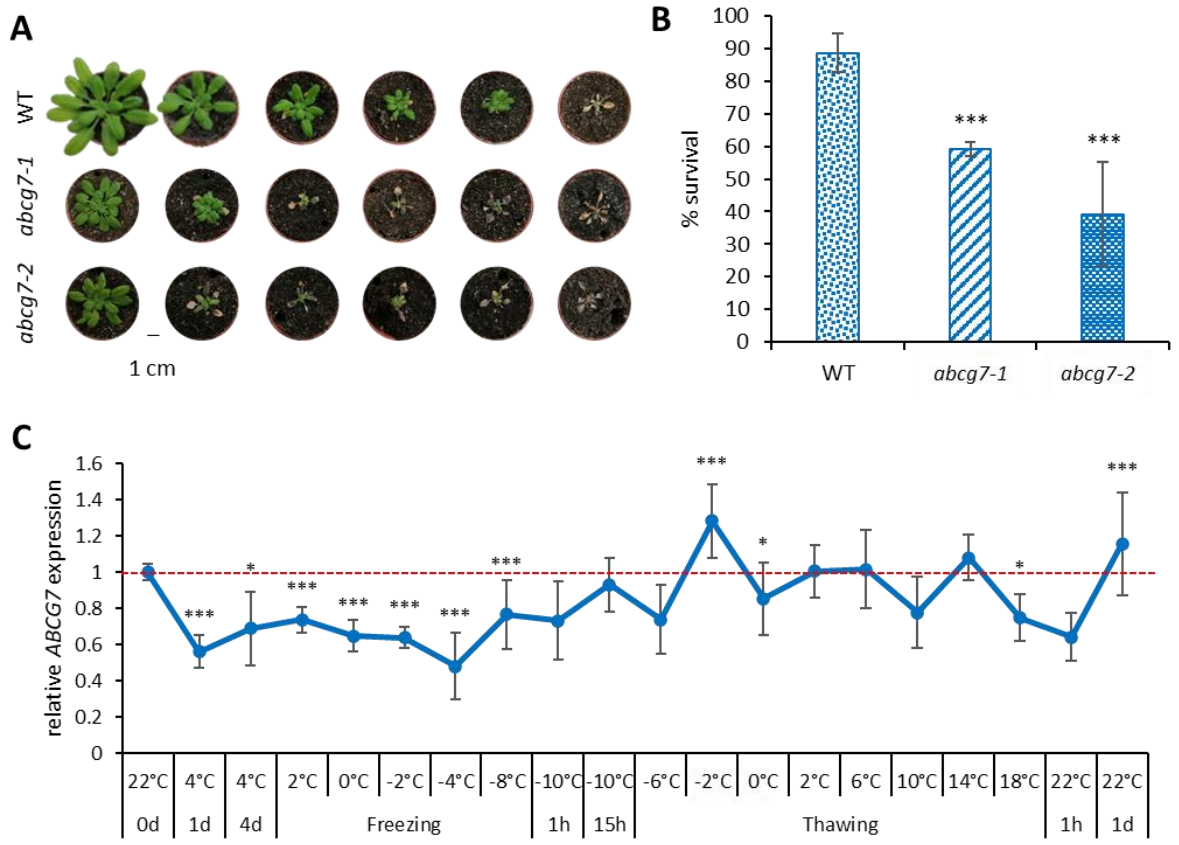

Figure 18: Freezing tolerance of the *abcg7* mutants. The 4-week-old wild type, *abcg7-1* and *abcg7-2* plants grown on soil under short day conditions (120 µE 10h light at 22°C/14h dark at 18°C) were transferred to 4°C for 4 days, followed by freezing at -10°C for 15h before returning to 22°C. After 2 weeks of recovery, surviving plants were sorted in a gradient from best to worst survivors (A) and the survival rate was quantified (B). The relative expression of *ABCG7* in wild types was analysed during cold acclimation, freezing, thawing and initial recovery by qPCR relative to the housekeeping gene *SAND*. The relative expression pattern was normalised to the transcription level to the control temperature of 22°C (0d; C). Asterisks indicate significant difference relative to 22°C (0d; n≥3; *P<0.05; **P<0.01; ***P<0.005). The Student's t-test was calculated in Microsoft Excel.

3.5.2. Variations in the cell wall metabolism of the *abcg7* mutants

During the expression analysis of RNA sequencing data obtained from cold-acclimating wild types and *abcg7* lines, several cell wall metabolizing enzymes were altered in their expression in the mutants (Figure 15). Respective genes, such as *PMEs* or *XTHs,* are known to be involved in the cell wall metabolism and are of critical importance for the survival of freezing temperatures. For example, *PME41* contributes greatly to the total PME activity in wild types during chilling stress (Qu *et al.,* 2011; Takahashi *et al.,* 2019; Ishida and Yokoyama, 2022). Further, *XTH17* to *XTH20* knock out mutants were shown to be important in the architectural and organisational remodelling of cell walls during cold and sub-zero acclimation, thus playing an important role in the build-up of freezing tolerance (Takahashi *et al.,* 2019, 2021, 2024).

To this end, a transcript analysis of the xyloglucan synthesis-related genes *XXT1* and *MUR3* (Cavalier *et al.,* 2008; Peña *et al.,* 2004), as well as the cell wall remodelling genes *XTH19*, *XTH21*, *XTH22* (Ishida & Yokoyama, 2022; Takahashi *et al.,* 2019), and *PME41* (Qu *et al.,* 2011) was performed to investigate the contribution of the cell wall to the freezing tolerance in the *abcg7* mutants. Since the RNA sequencing data revealed the most significant changes within the *abcg7-2* knock out mutant (Figure 15), the expression pattern of the aforementioned cell wall-related genes were assessed only in this line during the thawing process (Figure 19).

For the genes *XXT1* and *MUR3*, which encode for the xylosyltransferase 1 and galactosyltransferase MURUS3 (Peña *et al.,* 2004; Cavalier *et al.,* 2008), a 3.3 and 3.5-fold increase in transcript levels was observed during the thawing process in wild types, while the respective genes exhibited significantly lower mRNA levels in *abcg7-2* plants. The transcriptional increase in the mutant was only about 1.3-fold in comparison to the control temperature of 22°C (Figure 19A-B).

In wild types the expression of the *XTH22* gene was approximately 13.3-fold higher during the thawing phase at -2°C, while *XTH21* and *XTH19* expression remained unchanged in comparison to the control temperature of 22°C (Figure 19C-E). The thawing induced response of *XTH22* was found to be lower in *abcg7-2* compared to wild types, with mRNA levels increasing only 5.8-fold (Figure 19C). Furthermore, during the thawing phase, in tendency elevated transcript levels were observed for the genes *XTH19* and *XTH21* in *abcg7-2* relative to wild types. The *XTH19* expression levels increased by 1.2-fold (Figure 19D), while *XTH21* expression levels increased by 1.3-fold in *abcg7-2* plants at -2°C in comparison to the control temperature of 22°C (Figure 19E).

In addition, the *PME41* gene was found to be responsive to thawing conditions in wild types, with a 3.3-fold increase in mRNA levels observed. However, this increase was observed to be less substantial (approximately 2.1-fold increase) in *abcg7-2* (Figure 19F). To support these findings, cell wall sugars were measured in collaboration with Professor Dr. Raimund Tenhaken at the Paris Lodron University in Salzburg (Figure 20).

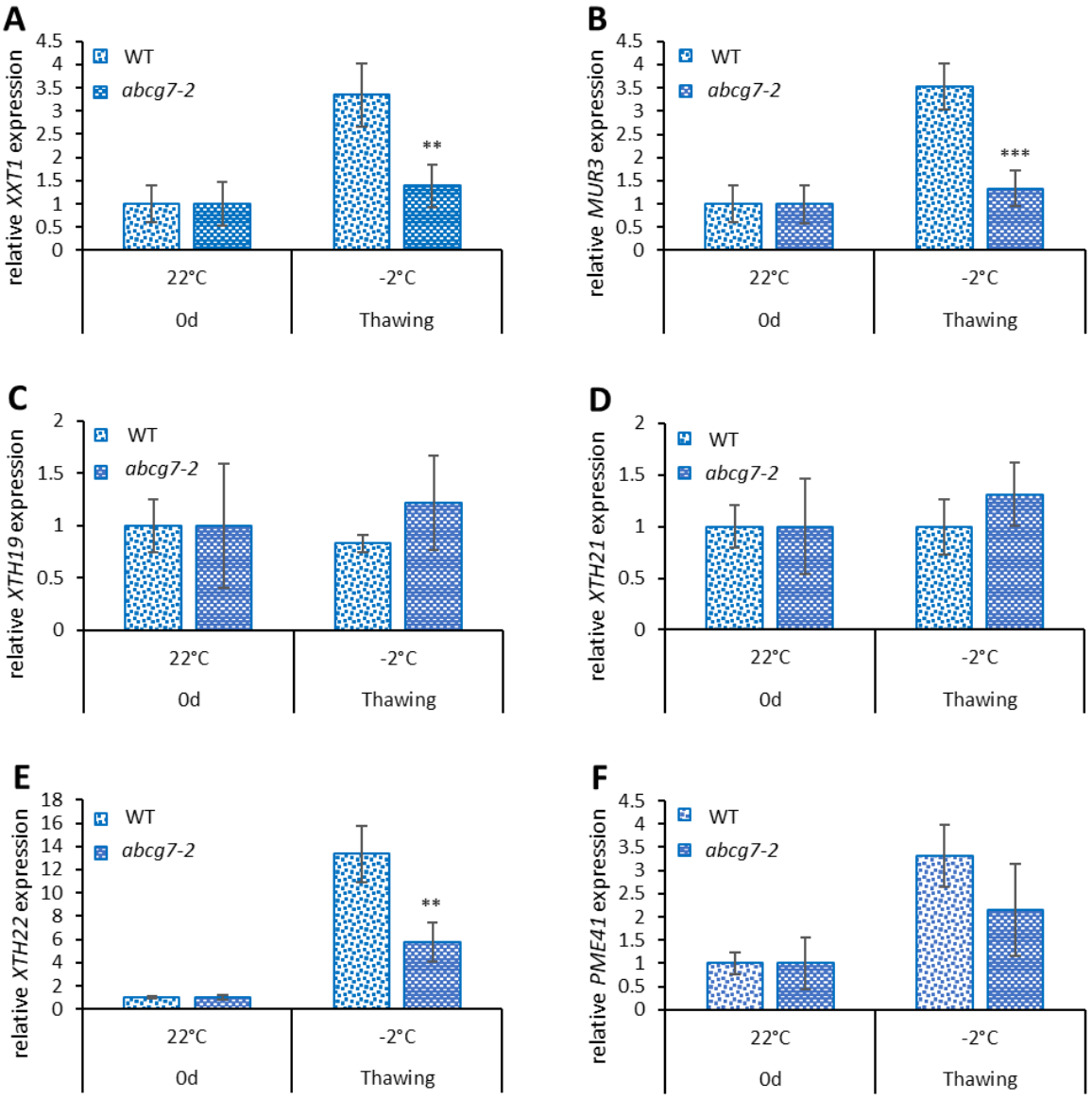

Figure 19: Gene expression of cell wall-related genes during the thawing phase in the *abcg7-2* lines. The 4-week-old wild type and *abcg7-2* and plants were transferred from 22°C to 4°C for 4 days, followed by freezing at -10°C for 15h before returning to 22°C. The gene expression was analysed during the thawing phase, when temperature was recovered to -2°C for the genes *XXT1* (A), *MUR3* (B), *XTH19* (C), *XTH21* (D), *XTH22* (E) and *PME41* (F) by qPCR relative to the housekeeping gene *SAND*. The relative expression pattern was normalised to transcription levels of the control temperature (0d at 22°C). Asterisks indicate significant difference relative to wild types (n≥3; *P<0.05; **P<0.01; ***P<0.005). The Student's t-test was calculated in Microsoft Excel.

To facilitate a comprehensive understanding of potential alterations in the cell wall of the *abcg7* loss-of-function lines, a detailed investigation of the cell wall composition was conducted in wild types and *abcg7* mutants under control temperatures of 22°C and thawing conditions at -2°C.

The analysis of the *abcg7* loss-of-function lines revealed an alteration in the composition of cell wall sugars already under control conditions. The galactose contents were significantly increased in *abcg7-1* (27.6 %mol) and *abcg7-2* mutants (28.4 %mol) in comparison to the wild types (26.5 %mol). Further, minor changes that affected at least one of the *abcg7* lines were observed, such as for example higher fucose and glucuronic acid (GlcA) contents in *abcg7-2* or lower arabinose contents in *abcg7-1* compared to wild types (Figure 20).

However, during thawing, galactose levels increased equally in wild types and *abcg7* mutants, but lower levels of fucose and arabinose were detected in the mutants. The fucose content was approximately 3.2 %mol in wild types, and 2.5 to 2.6 %mol fucose was measured in the *abcg7* lines. The level of arabinose measured in wild types was 21.7 %mol, whereas only 19.1 to 20.1 %mol arabinose was detected the mutants (Figure 20). The galacturonic acid (GalA) content of the wild type was found to be 17.8 %mol, whereas the *abcg7* lines exhibited a content of 19.7 %mol GalA. The GlcA level measured in *abcg7-1* was with 0.7 %mol lower, while the GlcA content of 1.8%mol in *abcg7-2* was higher in comparison to measured 0.8 %mol GlcA in wild types (Figure 20). This finding suggests that the *abcg7* lines do not increase the fucose or arabinose cell wall content during the thawing phase, while a thawing-specific increase in GalA was observed in the mutants, indicating alterations in the cell wall sugar composition.

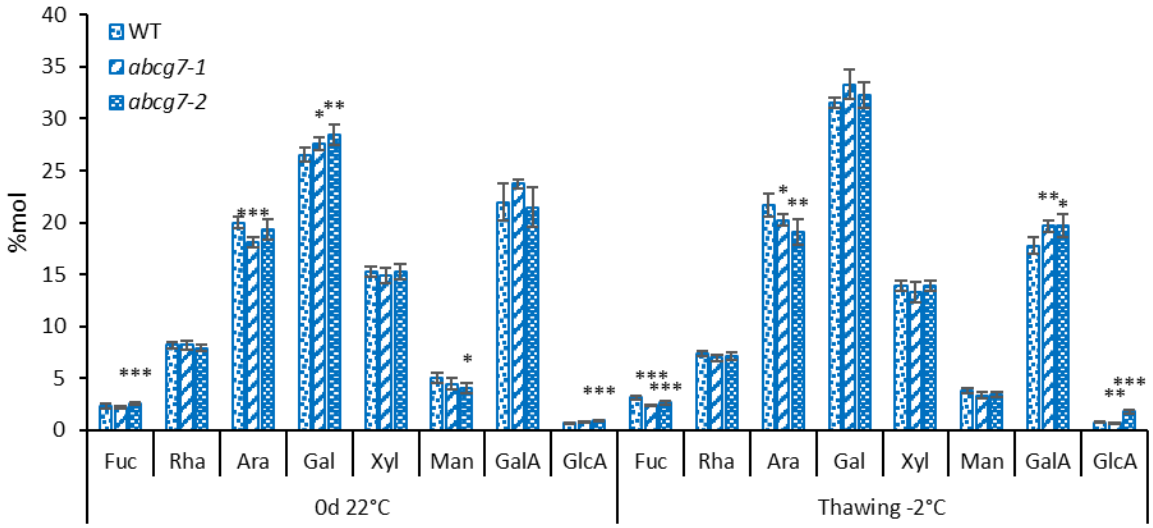

Figure 20: Cell wall sugar composition in the *abcg7* mutants before freezing stress and during the thawing process. Cell wall sugars were extracted from rosettes before the start (0d at 22°C) of the freezing experiment and during the thawing phase, when temperature reached -2°C. Asterisks indicate significant differences relative to wild types (n≥4; *P<0.05; **P<0.01; ***P<0.005). The Student's t-test was calculated in Microsoft Excel. Cell wall sugars were measured in collaboration with Prof. Dr. Raimund Tenhaken (Paris Lodron University in Salzburg).

3.5.3. Alterations in the lipid composition of the *abcg7* mutants

During cold acclimation, an accumulation of galactose was observed in the *abcg7* lines (Figure 10D), as well as a reduced transcription of cell wall-related genes (Figure 15). As changes in certain cell wall-related genes and cell wall sugars were observed in the freezing experiment (Figure 19), it could be assumed that the cold-specific galactose accumulation in the *abcg7* mutants is derived from the cell wall, as the cell wall contains a high amount of galactose (Höftberger *et al.,* 2022; Takahashi *et al.,* 2019, 2021, 2024).

However, the investigation of the cell wall composition during under control conditions at 22°revealed significantly elevated level of galactose in the mutants in comparison to wild types (Figure 20). Moreover, during the thawing phase at -2°C, an increase in the galactose contents in cell walls of both, wild types and *abcg7* loss-of-function lines, was observed (Figure 20). Thus, the cell wall does not appear to be the source of the observed galactose accumulation during cold acclimation in the *abcg7* mutants (Figure 10D).

Since the membranes also contain high levels of galactose (Cook *et al.,* 2021; Jouhet *et al.,* 2004; Maréchal & Bastien, 2014; Nilsson *et al.,* 2015), the membrane lipid composition of the *abcg7* mutants under control and thawing conditions was examined to determine the origin of the galactose accumulation during cold acclimation in *abcg7* mutants (Figure 21).

The main classes of phospholipids, i.e. phosphatidylethanolamine (PE) and phosphatidylcholine (PC), the main galactolipids, i.e. monogalactosyl diacylglycerol (MGDG) and digalactosyl diacylglycerol (DGDG), and the storage lipid triacylglycerol (TAG) were studied under control conditions (0d at 22°C; Supplementary Figure 10) and during the thawing phase at -2°C. The lipid measurements were performed in collaboration with Dr. Saleh Alseekh at the Max Planck Institute of Molecular Plant Physiology in Potsdam (Figure 21).

Under control conditions (0d at 22°C) no significant differences were observed in the lipid composition of wild types and *abcg7* lines (Supplementary Figure 10). However, during the thawing phase at -2°C, mutants showed lower levels of the phospholipids PE and PC, the galactolipid content of MGDG and DGDG, and the storage lipid TAG compared to wild types (Figure 21A).

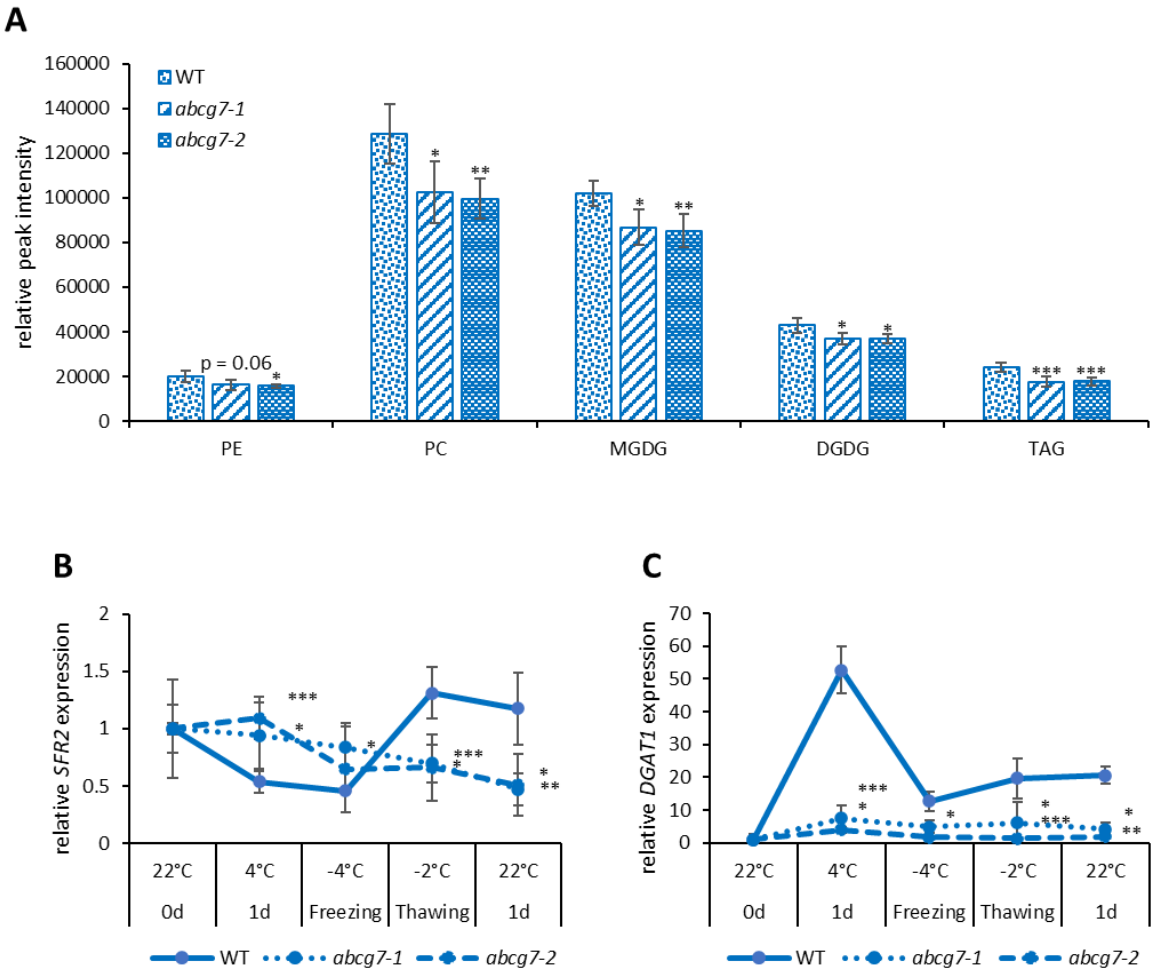

Figure 21: Lipid contents as well as *SFR2* and *DGAT1* expression in the *abcg7* loss-of-function mutants during freezing stress. The 4-week-old wild type, *abcg7-1* and *abcg7-2* plants were transferred to 4°C for 4 days, followed by freezing at -10°C for 15h before returning to 22°C. The lipid contents were measured before and during the thawing phase, when temperature was recovered to -2°C. Lipid measurements were performed in collaboration with Dr. Saleh Alseekh (Max Planck Institute of Molecular Plant Physiology, Potsdam). The expression of *SFR2* (A) and *DGAT1* (B) was analysed during cold acclimation, freezing, thawing and initial recovery by qPCR relative to the housekeeping gene *SAND*. The relative expression pattern was normalised to 0d at 22°C. Asterisks indicate significant difference relative to wild types (n≥3; *P<0.05; **P<0.01; ***P<0.005). The Student's t-test was calculated in Microsoft Excel.

Due to the reduced lipid contents observed in *abcg7* mutants during the thawing phase, the expression of key enzymes involved in membrane remodelling and triacylglycerol synthesis was investigated. Since the galactosyltransferase SFR2 uses MGDG to produce DGDG and other oligo-galactolipids (Moellering *et al.,* 2010; Moellering & Benning, 2011), and by-products of this process are used by the diacylglycerol acyltransferase DGAT1 to produce TAG (Arisz *et al.,* 2018; Tan *et al.,* 2018), the expression of corresponding genes was investigated. *SFR2* and *DGAT1* transcription was examined at the control temperature of 22°C, after 1 day at 4°C, at -4°C during freezing, at -2°C during thawing and 1 day after recovery back to 22°C to obtain a detailed overview of respective expression patterns in wild types, *abcg7-1* and *abcg7-2* (Figure 21B-C).

During the cold and freezing process, *SFR2* transcripts decreased in wild types, but increased again during the thawing phase, thus resembling the observed transcription pattern of *ABCG7* (Figure 18C). In contrast, both *abcg7* lines consistently maintained higher levels of *SFR2* transcripts during cold acclimation and freezing temperatures in comparison to wild types. However, during thawing and initial recovery, when the *SFR2* expression of the wild type increased, the transcript level did not rise in *abcg7-1* or *abcg7-2* and thus was lower than in wild types (Figure 21A).

Throughout the first day of cold exposure, *DGAT1* transcript levels increased by 52-fold in wild types and remained elevated between 12 to 20-fold during freezing, thawing, and the first day of recovery in wild types plants in comparison to the control temperature of 22°C (Figure 21B). However, the *DGAT1* expression in *abcg7-1* and *abcg7-2* peaked only about 3 to 6-fold after one day one at 4°C compared to 22°C and remained at a much lower transcription level than in the corresponding wild types all through the freezing experiment (Figure 21B).

The increased expression of *SFR2* in cold-acclimating *abcg7* mutants, together with the decreased levels of MGDG and DGDG during the thawing phase, suggests that the galactose accumulation observed after 4 days at 4°C in *abcg7* mutants may originate from the membranes. However, the overall lower levels of galactolipid, phospholipid and triacylglycerol observed in *abcg7* mutants suggest a widespread effect of the ABCG7 transporter on plant lipid metabolism.

3.6. Analysis of ABCG7 and SFR2 interaction

As the *abcg7* mutants exhibited a decreased frost tolerance and altered *SFR2* transcription during the freezing experiment (Figure 18C, Figure 21B), it seemed possible that ABCG7 might physically interact with SFR2 to ensure plant survival at sub-zero temperatures. As both proteins are located in the outer envelope of the chloroplast (Figure 7; Moellering, Muthan and Benning, 2010), a putative interaction between SFR2 and ABCG7 was investigated by BiFC analysis (Kerppola, 2008). Further, the outer envelope protein LACS9, which is also involved in the lipid metabolism, was utilised as a control to verify the specificity of a potential fluorescent signal (Schnurr *et al.,* 2002; Kitajima-Koga *et al.,* 2020). Fusion constructs were transiently expressed in *N. benthamiana* leaves and protoplasts were enriched from transfected tissue (Figure 22; Supplementary Figure 11).

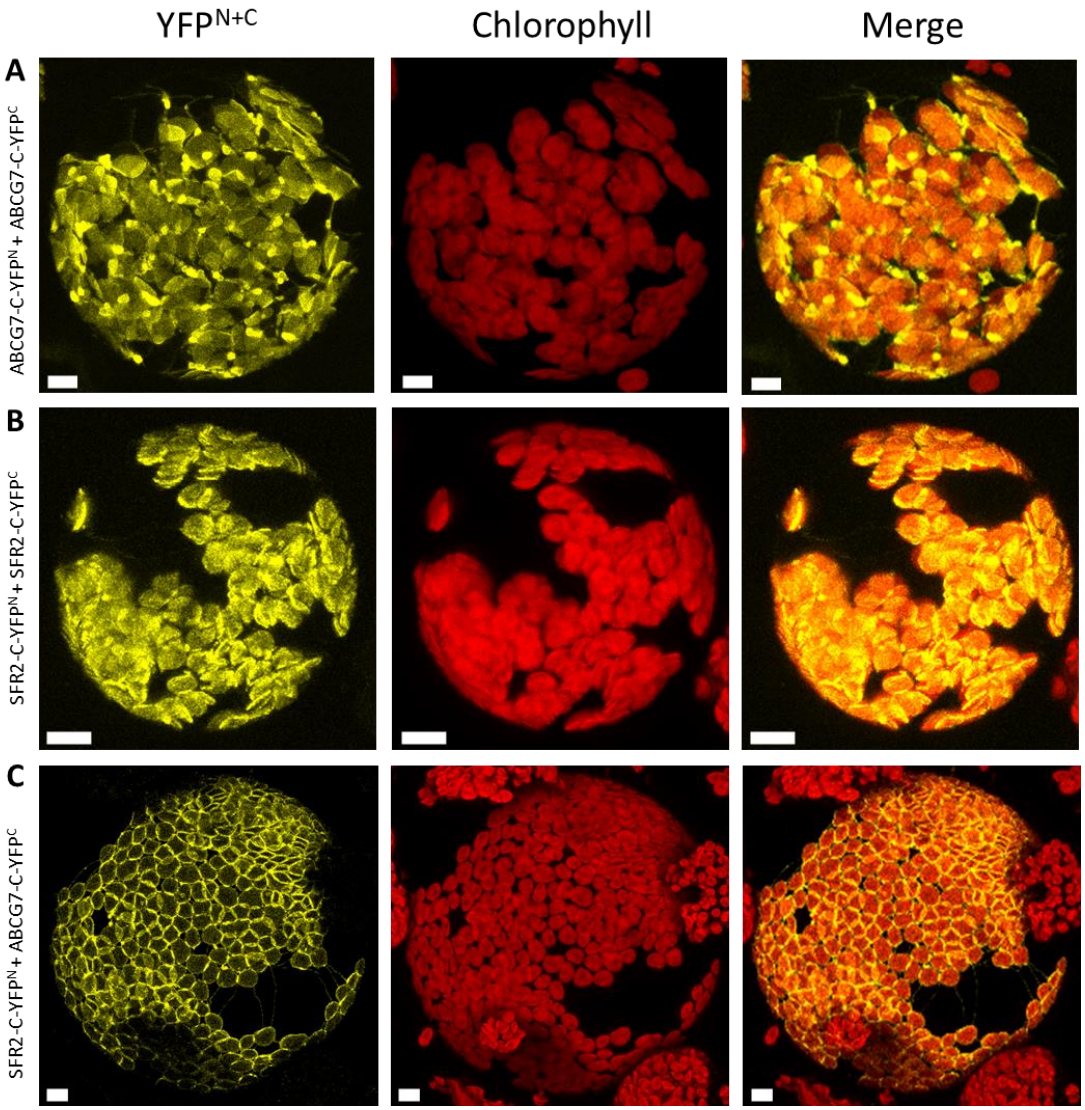

Figure 22: Interaction of ABCG7 and SFR2 revealed by BiFC analysis in protoplasts. Functionality of the cloned BiFC-constructs was verified by the interaction of ABCG7-C-YFP^N with ABCG7-C-YFP^C (A) as well as SFR2-C-YFP^N with SFR2-C-YFP^C. Specific interaction between SFR2-C-YFP^N and ABCG7-C-YFP^C was confirmed (C). *In planta* expression was driven by a *UBQ10* promoter. Images were taken 3 to 4 days after infiltration by a Leica Stellaris 5 Confocal Scanning Microscope at the Ludwig-Maximilians-University in Munich. The white bars indicate the scale: 7.5 µm (A) and 10 µm (B-C).

The functionality of the BiFC assay was proven by examining the interaction of split ABCG7-, SFR2- and LACS9-YFP constructs with themselves, resulting in a yellow signal due to reconstitution of the fluorophore (Figure 22A-B; Supplementary Figure 11A-C). Further, the fluorescent signals following the co-expression of ABCG7 with SFR2 or LACS9 were analysed. A yellow signal was observed in transfected tissue and enriched protoplasts synthesising both proteins, SFR2-C-YFP^N and ABCG7-C-YFP^C, indicating a close spatial interaction of the 2 partner molecules. However, no signal was observed between LACS9-C-YFP^N and ABCG7-C-YFP^C when co-expressed (Supplementary Figure 11E), verifying that ABCG7 in combination with SFR2 yields a specific fluorescent signal.

4. Discussion

4.2. Outer envelope localisation of the chloroplast transporter ABCG7

Chloroplasts have been identified as the key actors in acclimation, harbouring proteins and transporters that enable a dynamic response to stress, thus facilitating acclimation, adaptation and the acquisition of stress tolerance (Trentmann *et al.,* 2020; Kleine *et al.,* 2021). Although recent advances in proteomics allowed high throughput experiments on plastids, the overall number of transport proteins in chloroplasts is surprisingly limited (Ferro *et al.,* 2003, 2010).

About 100 proteins have been identified in the envelope fractions of chloroplasts, which are part of the protein import machinery or are involved in the transport of ions and metabolites or in the lipid metabolism of chloroplasts (Ferro *et al.,* 2003, 2010; Kleine *et al.,* 2021). Additionally, soluble proteins can interact with the envelope membranes, such as proteins associated with the carbon metabolism or proteins that are involved in stress responses (Ferro *et al.,* 2003). However, the exact localisation of most chloroplast proteins remains elusive, especially in the case of the envelope proteins (Ferro *et al.,* 2010).

The ABCG7 transporter has been detected in several chloroplast envelope proteome studies, but its localisation was not confirmed (Schleiff *et al.,* 2003; Zybailov *et al.,* 2008; Trentmann *et al.,* 2020). The transient expression of ABCG7-GFP in protoplasts derived from tobacco mesophyll cells revealed GFP signals, which are localised around the autofluorescence of the chloroplasts (Figure 6, Supplementary Figure 2). The fluorescence pattern is similar to that of other transport proteins fused to GFP and located in the envelope (Patzke *et al.,* 2019; Valifard *et al.,* 2023; Witz *et al.,* 2012). The microscopic study on the location of the ABCG7-GFP fusion protein, therefore, confirms that ABCG7 is located in the chloroplast (Figure 6).

Analysis of the ABCG7 amino acid sequence showed that this ABC-type transporter lacks a transit peptide at the N-terminus, which is a common feature for proteins imported into chloroplasts after translation (Supplementary Figure 1; Von Heijne, 1990). Nevertheless, several outer envelope proteins, such as OEP7, OEP16, OEP21, OPE21-like, OEP24, OEP37, some TOC components or SFR2, also lack N-terminal transit peptides, but have a highly hydrophobic domain within the first 30 to 65 amino acid residues, which is apparently also present in ABCG7 (Supplementary Figure 1; Li and Chen, 1996; Fourrier *et al.,* 2008; Ferro *et al.,* 2010; Kim *et al.,* 2015). Therefore, it might be speculated, that this hydrophobic N-terminus might guide the ABCG7 protein to the outer envelope of the chloroplast.

Since, the chloroplast is distinguished by the presence of an inner and outer envelope (K. Cline *et al.,* 1981; Kenneth Cline *et al.,* 1984), a protease assay was performed on tobacco chloroplasts to determine the exact localisation of the ABCG7 transporter (Figure 7). This assay, using trypsin and thermolysin, provided evidence that ABCG7 is sensitive to both proteases. The increased sensitivity to thermolysin suggests that ABCG7 is predominantly located in the outer envelope membrane of the chloroplast, as thermolysin cannot enter into intermembrane space (Figure 7; Cline, Andrews and Mersey, 1981; Cline *et al.,* 1984; Fourrier *et al.,* 2008; Bölter *et al.,* 2020).

Although the ATP-binding cassette superfamily is of particular interest, as it is one of the largest and most diverse transport families in plants (Higgins, 1992), little is known about ABCG7. A total of eight subfamilies of ABC transporters are present within the plant kingdom, including the ABCG subfamily, also known as the white brown complex (WBC) family (Verrier *et al.,* 2008). ABCG transporters have been demonstrated to play a crucial role in responding to biotic and abiotic stress, as well as during plant development (Ashraf *et al.,* 2021; Buda *et al.,* 2013; Leslie *et al.,* 2005; Matsuda *et al.,* 2012). To execute their function, ABC transporters require the presence of transmembrane domains and nucleotide-binding domains (Biemans-Oldehinkel, Doeven and Poolman, 2006; Roston, Hurlock and Benning, 2014).

To identify the potential transmembrane and nucleotide binding domains in ABCG7 of *Arabidopsis thaliana*, an amino acid sequence alignment was employed with the corresponding homolog of *Pisum sativum,* which was previously found and identified as an outer envelope protein in chloroplasts (Gutierrez-Carbonell *et al.,* 2014). By this alignment TMDs and NBDs were identified in the ABCG7 protein sequence (Supplementary Figure 1), including the Walker A, Walker B, and ABC signature motifs, which exhibit a high degree of conservation (Sánchez-Fernández *et al.,* 2001; Rea, 2007).

4.3. Improved cold tolerance in *abcg7* loss-of-function lines

Chloroplasts are responsible for photosynthesis and carbon assimilation, providing energy and reduction power to various metabolic pathways, including the synthesis of fatty acids, isoprenoids, tetrapyrroles, or the assimilation of nitrogen and sulphate for the production of amino acids (Finkemeier & Leister, 2010; Kleine *et al.,* 2021). Cold temperatures impact the central metabolic role of the chloroplast, thus affecting the entire plant metabolism, leading to a diminished plant performance and growth. Therefore, the chloroplast itself becomes involved and subjected to an acclimation process, which involves the dynamic adjustment of protein abundances in the envelopes (Trentmann *et al.,* 2020; Kleine *et al.,* 2021).

For instance, the protein abundance of the ATP importer NTT2 increases, whereas the maltose exporter MEX1 or the fatty acid exporter FAX1 decrease upon cold acclimation (Trentmann *et al.,* 2020). Evidence from both, overexpression and knock out lines, has demonstrated that the changes in NTT2, MEX1 or FAX1 levels contribute to the increased tolerance of Arabidopsis to cold (Trentmann *et al.,* 2020; John *et al.,* 2024). Since ABCG7 also responds dynamically to low temperature in Arabidopsis (Trentmann *et al.,* 2020), the function of the ABCG7 protein was investigated in the context of cold stress by exposing the *abcg7* loss-of-function lines to 4°C for up to 10 days (Figure 8).

The preceding study by Trentmann *et al.,* 2020 demonstrated that the abundance of the ABCG7 protein is downregulated following the onset of cold stress. This observation is consistent with the decrease in *ABCG7* transcript levels following transfer of wild types from 22°C to 4°C. The ABCG7 mRNA level decreased by more than 70% within the 1st day (Figure 8A). Consequently, the downregulation of *ABCG7* transcription can be interpreted as part of a molecular programme aimed to decrease the presence of the ABCG7 protein.

When wild types and *abcg7* loss-of-function lines were subjected to cold conditions an increased rosette size and dry weight was observed in *abcg7* plants, which can be attributed to the absence of the ABCG7 protein in the respective mutants (Figure 8B-C). Further, lower glucose and starch levels were detected in *abcg7-1* and *abcg7-2* during the exposure to a cold temperature of 4°C (Figure 10A, Supplementary Figure 5A, C), which were consistent with increased levels of the Krebs cycle intermediates fumarate, malate, and succinate (Figure 11). Thus, the higher biomass of the *abcg7* mutants can be apparently linked to an elevated utilisation of carbon for growth processes under cold conditions (Figure 23).

To elucidate the underlying differences between *abcg7* mutants and wild types during cold acclimation, an expression analysis of the cold-responsive gene *COR15A* was initiated by qPCR (Figure 8D). A lower *COR15A* transcription pattern was observed in *abcg7* mutants during the time course of the cold experiment in comparison to corresponding wild types (Figure 8D). Therefore, RNA sequencing was performed after 4 days at 4°C to further elucidate potential differences in the cold acclimation programme between wild types and abcg7 mutants. The RNA sequencing data revealed an overall reduced cold response at the gene expression level, as evidenced by reduced transcript levels such as *CBF1/DREB1b*, *CBF2/DREB1c* and *CBF3/DREB1a* in *abcg7* loss-of-function lines compared to wild types (Figure 9).

Further, a lower *ZAT10* and *ZAT12* transcription was observed in the RNA sequencing data of cold-acclimating *abcg7* lines relative to corresponding wild types (Figure 9). The expression of *ZAT10* and *ZAT12* in the *abcg7* mutants fits to the transcription pattern of the *DREB1a* to *b* factors, as *ZAT10* is assumed to be a sub-regulon of the CBF transcription factors, and *ZAT12* acts upstream of *ZAT10* (Mittler, 2002; Suzuki & Mittler, 2006; Vogel *et al.,* 2005; Xie *et al.,* 2019). As both are known to contribute to the antioxidant defence (Liu *et al.,* 2014; Qureshi *et al.,* 2013; Xie *et al.,* 2019), a lower ROS accumulation in the *abcg7* mutants during cold acclimation might be assumed. Either *abcg7* mutants experience less intracellular stress induced by chilling temperatures or have a higher cold tolerance due to the absence of ABCG7, which might reduce the need to undergo cold acclimation, thereby allowing improved plant growth (Figure 23).

Plant growth is regulated by the coordinated deposition, composition and modification of cell wall polysaccharides (Cavalier *et al.,* 2008; Fagerstedt & Karkonen, 2015; Zabotina *et al.,* 2008, 2012). During plant growth, the cell wall structure undergoes adjustments that enable a specific degree of flexibility, allowing turgor-supported cell expansion (Thompson, 2005; Tucker *et al.,* 2018). Given the established presence of galactose in the hemicellulose xyloglucan and the role of galactose in maintaining the cell wall strength during growth (Peña *et al.,* 2004), the higher galactose levels observed in cold-acclimating *abcg7* mutants might originate from the cell wall, either due to reduced incorporation or increased degradation (Figure 10D).

Under cold conditions, plants normally undergo cell wall modifications that slow growth rate but allow the development of freezing tolerance (Hannah *et al.,* 2005). An increase in pectin and xyloglucan content reduces the cell wall porosity and increases cell adhesion to achieve freezing tolerance (Kutsuno *et al.,* 2023; Qu *et al.,* 2011). For example, pectin methyl esterases are required to demethylate pectin, allowing the negatively charged pectin backbones to cross-link with calcium ions

under cold conditions, forming gel-like pectin structures to increase cell wall stiffness and frost hardiness (Le Gall *et al.,* 2015; Wormit & Usadel, 2018).

Further, xyloglucan endotransglucosylases and hydrolases are up regulated during the plant cell wall adaptation to maintain a certain degree of cell wall plasticity (Figure 23). Control of cell wall flexibility is crucial to resist potential cell collapse, which can occur during cell dehydration caused by extracellular ice formation under frost stress (Le Gall *et al.,* 2015; Pearce, 1999, 2001). Interestingly, several transcripts of cell wall synthesis (e.g. *CLSC4, FUT13, XXT1*) and remodelling genes (e.g. *PME2, PME41, XTH19, XTH22*) were lower in the *abcg7* lines than in wild types during the exposure to cold temperatures (Figure 15).

The enzyme CLSC4 is a cellulose synthase like C protein, that synthesises the glucan backbone of xyloglucan from glucose units (Cavalier *et al.,* 2008; Julian & Zabotina, 2022; Zabotina *et al.,* 2012), while XXT1 is involved in xylose decoration of the glucan backbone (Julian & Zabotina, 2022; Zabotina *et al.,* 2008, 2012). Xylose residues can be galactosylated and finally the attached galactose residues can be fucosylated by FUT enzymes (Hoffmann *et al.,* 2021; Julian & Zabotina, 2022). Thus, the lower transcription rate of *CLSC4*, *XXT1* and *FUT13* allows the assumption of an overall lower content of the polysaccharide xyloglucan within the cell walls of the *abcg7* mutants.

Further, an overall lower xyloglucan content within the cell wall could also affect the transcription of cell the xyloglucan endotransglucosylases and hydrolases, since the level of galactosylation can regulate the activity of this enzymes (Le Gall *et al.,* 2015; Pearce, 1999, 2001; Peña *et al.,* 2004; Rösti *et al.,* 2007). Moreover, changes in the xyloglucan content of the *abcg7* mutants could also impact the composition or ratio of cellulose, hemicellulose and pectin within the cell wall. This in turn could affect the galactose turnover during cell wall synthesis, modification or degradation during cold acclimation in the *abcg7* mutants.

However, it is unusual that after 4 days at 4°C, the overall transcription of cell wall-related genes was lower in the *abcg7* mutants than in wild types, since the up-regulation of cell wall remodelling genes is required to adjust the cell wall plasticity to withstand potential freezing stress, rather than to support growth. However, the reduced transcription pattern of cell wall-related genes in the *abcg7* lines appears to allow the maintenance of a cell wall structure that supports growth at 4°C, allowing the *abcg7* mutants to grow faster and accumulate more biomass than the wild types.

4.4. Effects of cold stress on the amino acid pools in *abcg7* mutants

When amino acids were analysed before and during the cold acclimation of wild types and *abcg7* lines, except for threonine, a number of amino acids were already lower in the mutants than in the wild types at 22°C (Supplementary Figure 6). However, following 4 days at 4°C, higher contents of the aromatic amino acids tyrosine and tryptophan were observed in *abcg7* mutants, whereas levels of phenylalanine remained comparable to those in wild types (Figure 12). Moreover, when the RNA sequencing data of the *abcg7* mutants was analysed to investigate expression changes affecting the biosynthesis of the abovementioned amino acids, major transcriptional changes were exclusively observed in biosynthetic pathways of tryptophan or phenylalanine (Figure 14).

Transcripts of tryptophan biosynthetic enzymes such as the phosphoribosyl anthranilate transferase 1 (*PAT1*), were elevated in *abcg7* lines at 22°C and after 4 days at 4°C, indicating the need for the mutants to synthesise tryptophan (Figure 14). Further, at 22°C lower transcript levels for *PAL1* were detected in the *abcg7* mutants compared to wild types. Since phenylalanine is the substrate of the phenylalanine ammonia lyase 1 (PAL1), this observation is also consistent with the lower phenylalanine contents in the mutants under control conditions (Figure 14).

However, after 4 days at 4°C, increased expression of phenylalanine biosynthesis genes was observed in *abcg7* mutants compared to wild types. For example, the *ADT* genes, which encode enzymes known as arogenate dehydratases, that catalyse the rate-limiting step of phenylalanine biosynthesis, were affected (El-Azaz *et al.,* 2022; Figure 14). Consequently, after 4 days at 4°C higher phenylalanine contents might have been expected in the *abcg7* lines than in wild types. However, no changes in phenylalanine levels were detected, instead a significant elevation in anthocyanin contents was remarked in the mutants (Figure 13).

Since PAL1 and PAL2 are the most relevant phenylalanine ammonia lyases for the generation of phenylpropanoids (Li *et al.,* 2017; Rohde *et al.,* 2004), the elevated expression of the *PAL* genes might indicate an up-regulation of the phenylpropanoid pathway in *Arabidopsis thaliana* (Howles *et al.,* 1996; Yokoyama, 2024). Further, heterologous overexpression of *PAL* genes from *Anoectochilus roxburghii* and *Anoectochilus formosanus* in Arabidopsis also showed increased production of anthocyanins in transgenic plants (Yang *et al.,* 2022). Thus, the increased expression of *PAL1* and *PAL2* in cold-acclimating mutants may indicate that phenylalanine is channelled towards anthocyanin synthesis in the *abcg7* loss-of-function lines (Figure 23).

The biosynthesis of the aromatic amino starts with the oxidative pentose-phosphate pathway, followed by the shikimate pathway and branched-chain amino acid biosynthesis, with chorismate being the major common intermediate from which tryptophan or tyrosine and phenylalanine are synthesised. Thus, perturbations of tryptophan or phenylalanine pools might also affect the synthesis of other amino acids and respective downstream pathways, such as the phenylpropanoid metabolism (Borevitz *et al.,* 2000; Dixon & Paiva, 1995; Li *et al.,* 2017).

For example, proline and histidine are well known to accumulate during long term cold adaptation, as low temperatures lower plant performance and growth by limiting photosynthesis, leading to ROS accumulation and limited energy supply. The accumulation of proline and histidine usually starts after 7 days of cold exposure (Asada, 2006; Kaplan *et al.,* 2007; Mittler, 2002; van Buer *et al.,* 2019). After 10 days at 4°C, higher contents of the amino acids proline and histidine were observed in the *abcg7* loss-of-function lines compared to wild types (Supplementary Figure 6). Since these amino acids act as compatible solutes and ROS scavengers, the accumulation of proline and histidine provide stress tolerance (Khan *et al.,* 2020; Singh *et al.,* 2024; Smirnoff & Cumbes, 1989).

Anthocyanins have also been shown to have protective antioxidant properties and can also scavenge reactive oxygen species due to their numerous hydroxyl groups (Hannah *et al.,* 2005, 2006; Kitashova *et al.,* 2023; Schulz *et al.,* 2015, 2016). In addition to their ROS-scavenging activity, anthocyanins play a photoprotective role at cold temperatures and can even influence the osmotic potential when accumulated in the vacuole (Chalker-Scott, 1999; Havaux & Kloppstech, 2001; Kitashova *et al.,* 2023).

In the *abcg7* loss-of-function lines seemingly, perturbations in amino acid synthesis and channelling of phenylalanine towards the phenylpropanoid metabolism, as well as increased proline, histidine and anthocyanin levels, may be beneficial during cold exposure. The apparent ROS scavenging and photoprotective properties, as well as the osmotic stabilisation at low temperatures, help the *abcg7* mutants to combat potential cold-induced stress and contribute to their improved cold tolerance (Figure 23).

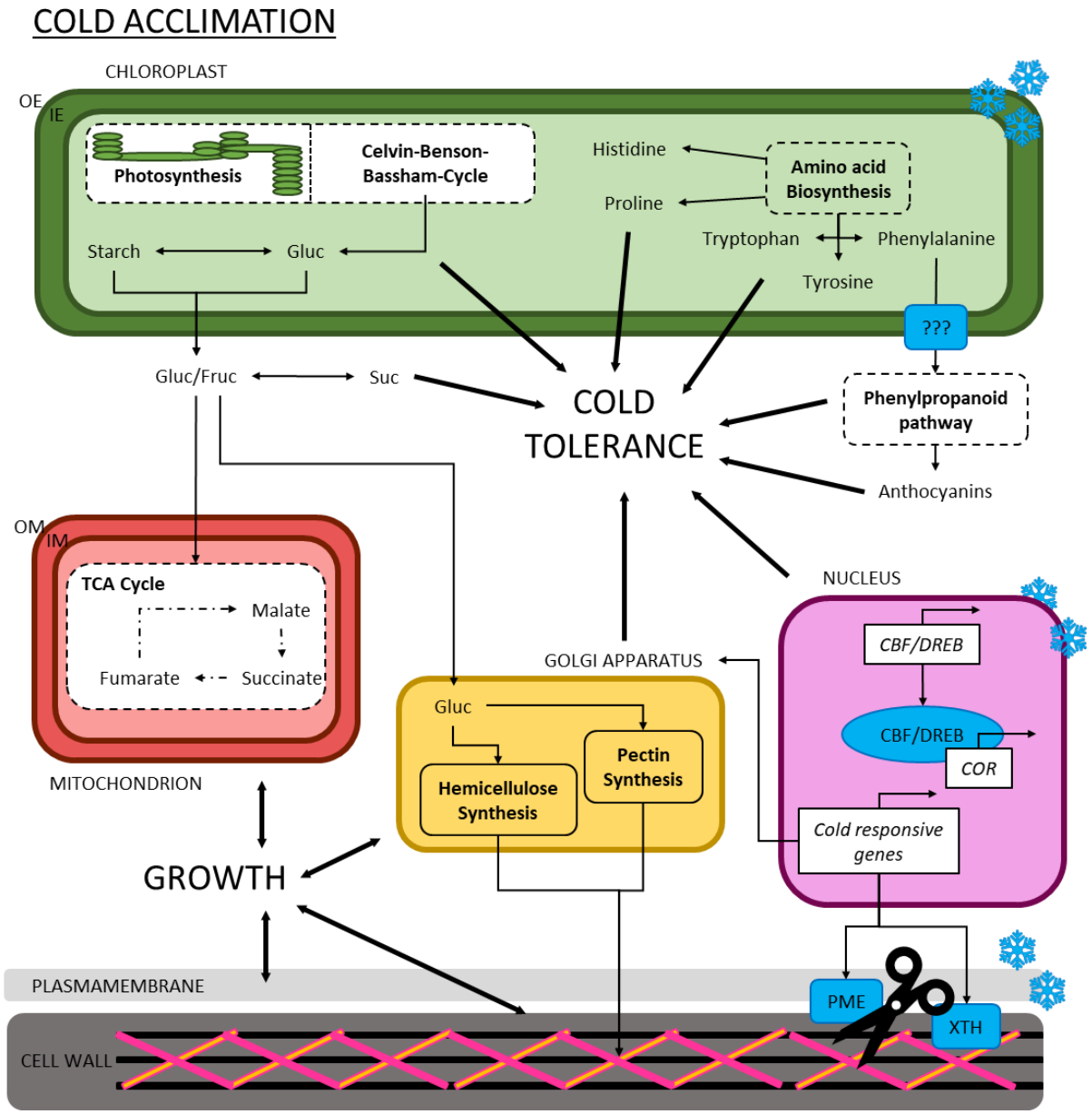

Figure 23: The role of the chloroplast in cold acclimation of Arabidopsis. Low temperatures have a deleterious effect on photosynthesis rates and carbon fixation in the chloroplast. In response several cold-responsive genes, including *CBF/DREB* transcription factors and cell wall remodelling genes such as *PMEs* and *XTHs,* are activated. Chloroplasts contribute to an increase in osmolytes, such as sugars or amino acid contents. Glucose, for example, is either stored in the form of starch or utilised by the tricarboxylic acid (TCA) cycle to generate energy and reductant equivalents required for the cold acclimation process and growth under cold conditions. In addition, chloroplast-derived glucose is subsequently converted to sucrose, and both sugars serve as starting points for the generation of cell wall components. These sugars are provided to the Golgi for cell wall polymer synthesis, such as hemicellulose or pectin.

4.5. Galactose induces anthocyanin production in *abcg7* mutants

The characterisation of the *abcg7* loss-of-function lines under cold conditions revealed a diminished need of this mutants to acclimate to low temperature stress, as reflected by their lower transcription pattern of cold-responsive genes (Figure 9). Further, various metabolic rearrangements were observed after 4 days at 4°C, such as the accumulation of galactose (Figure 10D). To investigate the influence of high galactose concentrations on wild types and the *abcg7* loss-of-function lines, seeds were plated on galactose containing plates (Figure 16). After a growth period of 2 weeks under standard conditions, an inhibitory growth effect of galactose on both, wild types and *abcg7* seedlings was observed. However, *abcg7* seedlings were larger compared to wild types, meaning that mutants may tolerate exogenous galactose better than wild types (Figure 16A-B).

Studies have shown that exogenous galactose is toxic in wild types due to the limited activity of uridine 5'-diphospho-glucose-4-epimerase (UDP-Glc epimerase). UDP-Glc epimerase converts UDP-galactose (UDP-Gal) to UDP-glucose (UDP-Glc) and controls galactose pools in Arabidopsis (Althammer *et al.,* 2020, 2022; Dörmann & Benning, 1998; Höftberger *et al.,* 2022; Pereyra *et al.,* 2023). The UDP-Glc epimerase activity is sufficient to prevent the toxic effects of intrinsic galactose production in Arabidopsis plants when grown under optimal soil conditions. However, when grown on galactose-containing plates, UDP-Glc epimerase activity is no longer sufficient, resulting in alterations of the carbohydrate metabolism, such as the accumulation of starch, sugars and anthocyanins. These variations are speculated to result from either an altered starch synthesis or degradation. Since starch is converted into triose-phosphate and exported to the cytosol, effects on starch pools in turn affect carbon export from the chloroplast (Althammer *et al.,* 2020, 2022; Dörmann & Benning, 1998; Höftberger *et al.,* 2022; Pereyra *et al.,* 2023).

Although sugar measurements of wild types and *abcg7* mutants grown in the presence of galactose showed no significant differences between the three lines (Supplementary Figure 8-9), *abcg7* lines still exhibited an increased anthocyanin production in comparison to corresponding wild types. Since the transcriptional and metabolic production of anthocyanins depends on the export of carbon from the chloroplast and the cellular sugar content, a sugar-specific induction of anthocyanin production in the *abcg7* mutants can be excluded (Figure 16C). Hence, phenylalanine contents were measured, revealing significantly lower levels in the *abcg7* mutants in comparison to wild types (Figure 16D). Apparently, galactose increases the utilisation of phenylalanine for anthocyanin synthesis in *abcg7* loss-of-function lines.

Since, it has been previously observed that galactose, similar to mannitol, causes osmotic stress in Arabidopsis (Höftberger *et al.,* 2022; Pritchard *et al.,* 2004), reduced transcription of *ABCG7* in the leaf discs of wild types, incubated in the presence mannitol or galactose, appears to be a response to osmotic stress rather than a galactose-specific response. Osmotic stress causes a wide range of responses on the molecular, cellular and morphological level, including the growth retardation of shoot tissue and metabolic adjustments in the carbon metabolism. In response, compatible solutes and anthocyanins are synthesised, acting as antioxidants and increasing the tolerance to osmotic stress (Ahmed *et al.,* 2014; Dixon & Paiva, 1995; Li *et al.,* 2017; Nakabayashi *et al.,* 2005; Xiong & Zhu, 2002).

Loss of ABCG7 appears to promote the channelling of phenylalanine towards anthocyanin production and accumulation in the *abcg7* loss-of-function lines. Higher levels of anthocyanins in turn may alleviate galactose-induced osmotic stress in the mutants, as anthocyanins have been shown to be water-soluble glycosides that can accumulate in the vacuole and affect the osmotic potential, thus providing an advantage compared to wild types (Chalker-Scott, 1999; Kitashova *et al.,* 2023).

4.6. The importance of the ABCG7 protein during frost

Although cold and freezing tolerance are acquired through distinct physiological processes, cold acclimation is widely recognised as a preparatory phase that enhances plant resilience to subsequent frost stress (Takahashi *et al.,* 2019, 2024; Xu *et al.,* 2023). Especially, cell wall and membrane modifications are thought to support the balance between cold acclimation, freezing tolerance, and post-stress recovery. However, the interplay between chilling- and freezing-induced metabolic changes, particularly during the recovery phase, remains poorly understood (Li *et al.,* 2008; Takahashi *et al.,* 2019, 2021). The present study therefore investigates the role of the ABCG7 transporter during cold exposure, subsequent freezing stress, and recovery (Figure 18).

The observed decline in *ABCG7* transcript and protein levels in response to low temperatures of 4°C may contribute to the enhanced cold tolerance in *abcg7* loss-of-function lines (Figure 8; Trentmann *et al.,* 2020). However, when exposed to sub-zero temperatures, the *abcg7* mutants exhibited a significantly impaired freezing recovery (Figure 18A-B). This contrast between improved performance under cold conditions and sensitivity to freezing suggests the importance of ABCG7 for frost stress tolerance. Examination of *ABCG7* expression in wild type plants during the freezing experiment, revealed an increase during the thawing phase at -2 °C (Figure 18C), indicating a possible role in recovery.

Since changes in the expression of cell wall-related genes were identified in the cold-acclimating *abcg7* mutants (Figure 15), genes with known function in the xyloglucan metabolism were selected from RNA sequencing data (Figure 19-20). The expression of xyloglucan biosynthesis genes, *XXT1* and *MUR3*, increased in wild type plants at -2°C, while this induction was markedly reduced in *abcg7-2* (Figure 19A, B), suggesting that the *abcg7* lines may have alterations in characteristics of xyloglucan. Altered xyloglucan content, composition, structure or deposition has previously been linked to cold sensitivity in knock out mutants, such as *xxt1* or*mur3* (Cavalier *et al.,* 2008; Peña *et al.,* 2004; Takahashi *et al.,* 2019, 2021, 2024; Xu *et al.,* 2023). Thus, the observed transcriptional changes in *XXT1* and *MUR3* hint toward a specific defect in the up-regulation of xyloglucan-related genes during recovery from freezing, which could be linked to the observed freezing sensitivity in the *abcg7* loss-of-function mutants.

Additionally, *XTH22*, a gene involved in xyloglucan remodelling, showed a strong increase in expression in wild type plants during thawing (Figure 19E), which is in line with previous studies by Takahashi *et al.,* 2019. In contrast, *abcg7-2* mutants showed only a weak induction of *XTH22* (Figure 19E), suggesting an impaired ability to initiate appropriate cell wall restructuring during recovery from freezing stress.

In contrast to *XTH22*, the expression of *XTH19* and *XTH21* remained largely unchanged in wild type plants during the thawing phase at -2°C. Interestingly, *abcg7-2* mutants showed a trend towards elevated transcript levels of both genes under the same conditions (Figure 19C-D). Given that *XTH19* and *XTH21* have been implicated in enhancing freezing tolerance through cold- and sub-zero-specific induction (Kutsuno *et al.,* 2023; Le Gall *et al.,* 2015; Shi & Chan, 2014; Takahashi *et al.,* 2021; Xu *et al.,* 2023), this up-regulation may represent a compensatory response to the reduced *XTH22* expression in *abcg7-2* (Figure 19E). As both enzymes, XTH21 and XTH19, affect cellulose and xyloglucan deposition and interconnection (Liu *et al.,* 2007), their altered expression might reflect attempts to restore cell wall function in the *abcg7* mutants.

These findings further raise the question of how ABCG7, a plastid-localised transporter, might influence the expression of genes involved in the synthesis or remodelling of apoplastic cell wall components, as a direct regulatory link seems unlikely due to the different subcellular localisations. However, a possibly increased channelling of phenylalanine towards the phenylpropanoid pathway in *abcg7* mutants (see chapters 4.4 and 4.5) suggests a metabolic shift that could indirectly affect the cell wall composition.

Phenylpropanoid-derived compounds not only serve as precursors for lignin and suberin but are also esterified to cell wall polysaccharides. For instance, in *Spinacia oleracea*, ferulic and coumaric acid residues are esterified to arabinose and galactose moieties in pectin (Fry, 1982, 1983; Rodney Croteau, Kutchan and Lewis, 2000; Herrmann and Entus, 2001; Maeda and Dudareva, 2012; Lynch and Dudareva, 2020). In *Arabidopsis*, ferulate and coumarate esters contribute to the cutin matrix, which is closely linked to the outer cell wall (Rautengarten *et al.,* 2012). Thus, an altered aromatic amino acid metabolism, could change the availability or incorporation of phenolic esters into the cell wall in *abcg7* mutants. This in turn, could influence the physical properties of the wall and thereby affect xyloglucan synthesis, deposition, or remodelling. Interestingly transcriptional alterations in *abcg7-2* during not limited to xyloglucan-related genes. For instance, the expression of *PME41*, a gene involved in pectin demethylesterification, was also differentially regulated compared to wild types (Figure 19F), pointing to ABCG7-dependent impacts on cell wall restructuring during recovery from freezing stress.

Differences in the expression of cell wall remodelling enzymes between wild types and *abcg7* mutants were confirmed by measuring cell wall sugars (Figure 20). For instance, galactose, galacturonic (GalA) and glucuronic acid (GlcA) levels were higher in *abcg7* mutants at 22°C (Figure 20). While galactose is present in both xyloglucan and pectin side chains, GalA and GlcA are key structural components of pectin (Bethke *et al.,* 2015). These sugar residues have been associated with cell wall rigidity and stress resilience (Fry, 1982; Peña *et al.,* 2004; Seguela-Arnaud *et al.,* 2015). Therefore, the increased abundance of these sugars in *abcg7* mutants may contribute to the enhanced low-temperature tolerance observed during cold acclimation (Figure 8).

However, sugar measurements at -2°C revealed changes in cell wall architecture, that potentially affect relevant mechanical properties during freezing stress (Figure 20). Cell wall sugar analyses showed lower levels of fucose and increased GalA and GlcA contents in *abcg7* mutants compared to wild types (Figure 20). Reduced fucose levels have been linked to increased cell wall fragility and freezing sensitivity in *mur1* and *mur3* mutants (Kong *et al.,* 2015; Liepman *et al.,* 2010; Panter *et al.,* 2019; Reiter *et al.,* 1993, 1997). On the other hand, elevated levels of acidic pectin components such as GalA and GlcA may reflect a shift in the mechanical balance of the cell wall. This shift could favour increased stiffness mediated by pectin, while compromising the flexibility associated with xyloglucan content and remodelling. This in turn might interfere with proper expansion or contraction of the cell wall during freeze–thaw cycles (Seguela-Arnaud *et al.,* 2015; Takahashi *et al.,* 2019, 2021, 2024). Thus, the loss of ABCG7 affects the dynamic regulation of cell wall architecture, particularly under sub-zero conditions, and may thereby compromise the mechanical adaptations required for successful post-freezing recovery.

Nevertheless, one discrepancy concerning the galactose content in the cell wall remains to be clarified. In *abcg7* mutants, galactose levels were already elevated under control conditions (22 °C) and further increased during the thawing phase at –2 °C. However, at this sub-zero temperature, no significant differences in cell wall-bound galactose were detected between *abcg7* mutants and wild types (Figure 20). This finding, together with the pronounced galactose accumulation observed in cold-acclimating *abcg7* mutants at 4 °C (Figure 10D), points towards additional, non-cell wall sources of galactose that may be particularly affected in the *abcg7* lines during low temperatures.

Given that plastidial membranes, especially chloroplast envelopes, contain large amounts of galactose-rich galactolipids, and are particularly prone to cold-induced remodelling (Moellering, Muthan and Benning, 2010; Moellering and Benning, 2011; Qu *et al.,* 2011; Kutsuno *et al.,* 2023), an altered membrane lipid turnover may contribute to the cold-induced galactose accumulation in the *abcg7* mutants. To investigate this, the lipid composition and expression of membrane remodelling genes were analysed in *abcg7* and wild type plants during the thawing phase (Figure 21).

4.7. The chloroplast outer envelope proteins ABCG7 and SFR2

The present study has demonstrated significant variations in the frost sensitivity exhibited by the *abcg7* loss-of-function lines (Figure 18). In addition to the restructuring of cell walls, which was evidently affected in the mutants (Figure 19-20), the remodelling of lipids is also a key factor in the development of frost tolerance (Moellering *et al.,* 2010; Moellering & Benning, 2011; Thorlby *et al.,* 2004). Overall lower levels of phospholipids PE and PC, the galactolipid contents of MGDG and DGDG, as well as TAG contents were observed in the *abcg7* mutants during thawing at -2°C compared to wild types (Figure 21A).

Although phospholipid classes can decline during the freezing stress in plants (Li *et al.,* 2008), diminished levels of PC and DGDG might be particularly problematic, as the respective lipid head groups have bilayer stabilising properties and thus contribute to freezing tolerance (Degenkolbe *et al.,* 2012; Li *et al.,* 2008; Steponkus *et al.,* 1988; Uemura & Steponkus, 1997; Welti *et al.,* 2002). Further, MDGD-dependent synthesis of DGDG, mediated by the glycosyl hydrolase SFR2, offers protection to membranes. Besides the MDGD-dependent membrane remodelling, SFR2 also utilises DGDG to produce oligo-galactolipids, which has been demonstrated to stabilise membranes, prevent freezing injury and maintain organelle integrity (Moellering *et al.,* 2010; Moellering & Benning, 2011; Thorlby *et al.,* 2004). To prevent the accumulation of membrane remodelling intermediates, TAG synthesis via DGAT1 is activated under cold stress (Tan *et al.,* 2018).

Further, in the preceding study by Barnes, Benning and Roston (2016), ABCG7 was identified as potential interaction partner of the SFR2 protein. Moreover, it was hypothesised that transient protein interactions with SFR2 might be necessary to regulate glycosyl hydrolase activity, since SFR2 appears to be constitutively active when heterologously expressed in yeast (Barnes *et al.,* 2016; Roston, Wang, *et al.,* 2014). Since SFR2 and ABCG7 localise to the outer chloroplast envelope (Figure 7; Fourrier *et al.,* 2008; Roston *et al.,* 2014), a physical interaction was tested via BiFC analysis, and confirmed that ABCG7 and SFR2 are interaction partners (Figure 22, Figure 24, Supplementary Figure 11).

When, the *SFR2* transcription was investigated in the *abcg7* mutants during the freezing experiment, significantly higher expression during the cold acclimation phase, but lower mRNA level during the thawing process was observed in comparison to wild types (Figure 21B). Consequently, the abnormal *SFR2* expression pattern of the *abcg7* mutants could be attributed to the absence of the ABCG7 protein (Figure 21B).

Together, these findings suggest that the loss of ABCG7 impairs the dynamic regulation of SFR2 during cold acclimation, freezing stress and recovery (Figure 21B). An impacted SFR2 functionality could lead to degradation of MGDG and DGDG lipids in the in the mutants (Figure 21A). Further, the production of protective oligo-galactolipids would also be compromised. This may destabilise chloroplast membranes, contributing to the observed freezing sensitivity and impaired recovery in the *abcg7* lines (Figure 18). Disturbed membrane remodelling would also provide fewer lipid intermediates for TAG synthesis, providing a plausible explanation for the observed missing and overall, significantly lower *DGAT1* expression in the *abcg7* mutants compared wild types (Figure 21C).

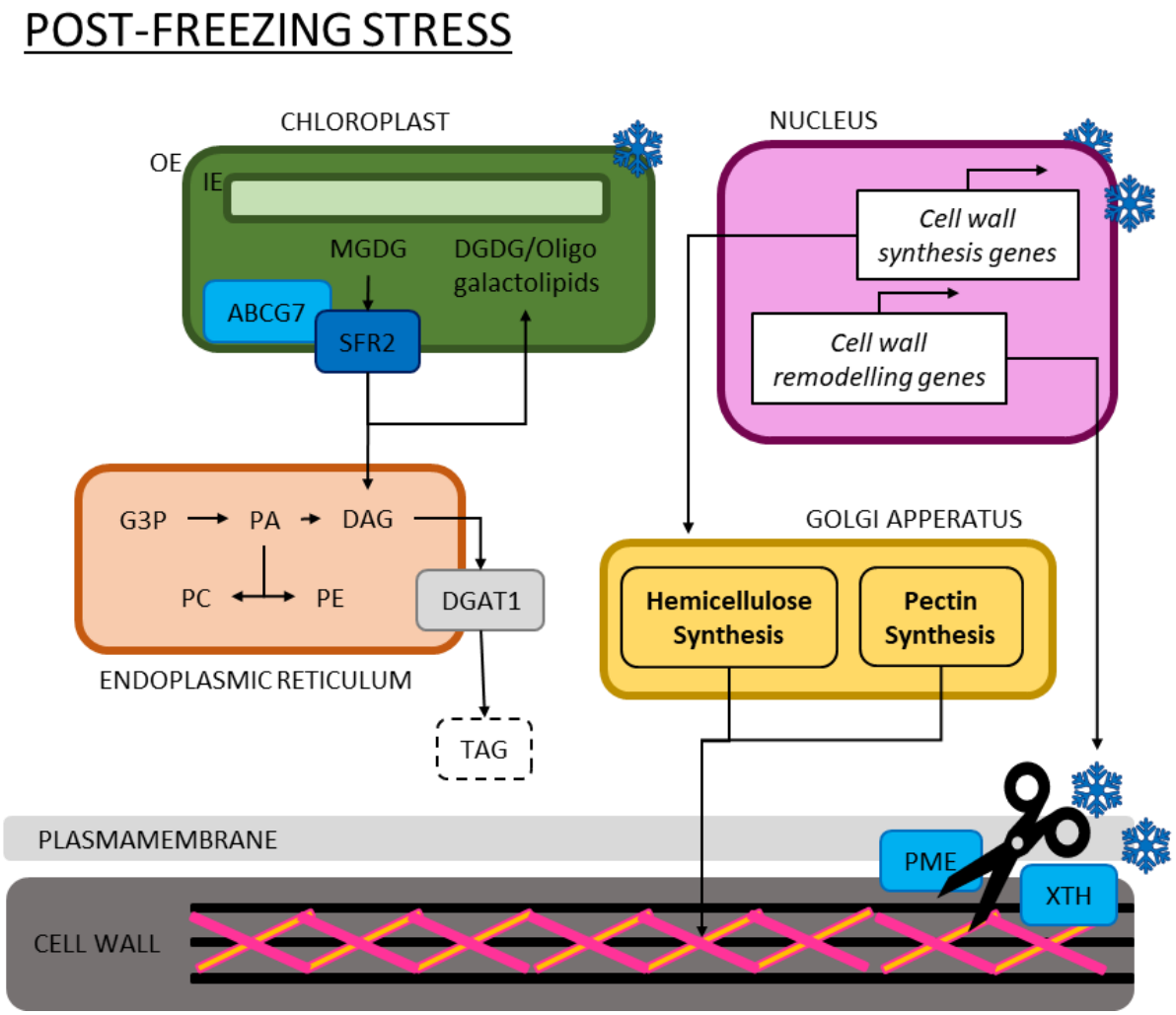

Figure 24: Role of ABCG7 in the freezing tolerance of Arabidopsis plants. Frost temperatures damage chloroplast membranes. The interaction of ABCG7 with SFR2 is presumably required to allow the conversion of MGDG into DGDG or oligo-galactolipids, which possess cryoprotective properties. By-products such as DAG can be converted into TAGs by the diacylglycerol acyltransferase (DGAT1). Further, sub-zero temperatures activate a set of frost-responsive genes responsible for cell wall synthesis and remodelling, to adjust the cell wall organisation.

4.8. Conclusion

In summary, it was shown that the ABCG7 protein is an outer envelope protein of the chloroplast (Figure 6-7). Further, ABCG7 appears to play a crucial role in the regulation of membrane remodelling during freezing stress, likely through its interaction with the outer envelope protein SFR2 (Figure 22; Supplementary Figure 11). In *abcg7* loss-of-function mutants, the absence of the ABCG7 protein leads to a dysregulated membrane remodelling process, as indicated by altered SFR2 expression during cold acclimation and reduced levels of key lipid species such as DGDG, MGDG, and TAG during the thawing phase (Figure 21). This impairment is further supported by the accumulation of galactose under cold conditions (Figure 10D), which may result from defective lipid turnover.

Further, it appears that the increased levels of galactose in the *abcg7* mutants can promote biosynthesis of anthocyanins (see chapter 3.4), which may in turn enhance the cold tolerance in the *abcg7* mutants (Figure 8). However, the impaired regulation of SFR2-mediated membrane remodelling, together with secondary effects on the cell wall composition, likely caused by altered phenylalanine flux through the phenylpropanoid pathway, suggests broader disruptions to the cellular metabolic activity. Overall, these findings point to a multifaceted role of ABCG7 at the interface of membrane and cell wall metabolism. The absence of a functional ABCG7 protein leads to imbalances in both structures, which ultimately compromised the ability of the *abcg7* mutants to withstand freezing stress (Figure 18).

4.9. Outlook

Although ABCG7 interacts with SFR2, the absence of the ABCG7 protein does not indicate the transport activity of a specific lipid class such as for example MGDG or DGDG. In contrast, lipid phenotypes in *abcg7* mutants subjected to sub-zero temperatures showed a broad impact on the lipid metabolism rather than a specific effect on the galactolipid contents (Figure 21A).

Corresponding ABCG7 protein homologs in *Drosophila melanogaster* are involved in the transport of eye pigment precursors with highly hydrophobic ring structures, such as kynurenine, guanine or tryptophan (Gräfe & Schmitt, 2021; Mackenzie *et al.,* 2000). Thus, it can be speculated that the ABCG7 transporter in Arabidopsis may also translocate metabolites with aromatic ring structures, such as chorismate or aromatic amino acid. Particularly, since there is no known transport system that can export aromatic metabolites from the chloroplast to the cytosol (Lynch and Dudareva, 2020)

When the *ABCG7* expression was tested in wild type leaf discs incubated in the presence of chorismate, the precursor of aromatic amino acids (Rohde *et al.,* 2004), the transcription levels of *ABCG7* declined (Supplementary Figure 12). Further, when leaf discs of wild types were incubated in the presence of phenylalanine or tryptophane, *ABCG7* expression also declined in the presence of both aromatic amino acids (Supplementary Figure 13).

This prompts the following questions:

(I) Might the ABCG7 transporter mediate the export of chorismate or aromatic amino acids across the outer envelope membrane of the chloroplast?

(II) If so, how would such a transport activity influence the phenylpropanoid pathway?

(III) Could ABCG7 thus represent a regulatory hub that connects the phenylpropanoid metabolism with both, cell wall and lipid metabolism?

5. Summaries in English and German

5.2. Summary

Although ABCG7 protein levels decrease in the plastid proteome under cold conditions (Trentmann *et al.,* 2020), the physiological role of the plastid ABC-type transporter ABCG7 during cold acclimation and freezing stress remains poorly understood and its localisation had not been experimentally confirmed. Employing transient expression of ABCG7-GFP in *Nicotiana benthamiana* and proteolytic assays in isolated chloroplasts, ABCG7 was shown to localise to the outer chloroplast envelope (Figure 6-7).

Characterisation of *abcg7* loss-of-function mutants under cold stress revealed increased biomass accumulation (Figure 8B-C), decreased glucose and starch levels (Supplementary Figure 5), and elevated Krebs cycle intermediates (Figure 11). Metabolic changes were accompanied by increased anthocyanin synthesis (Figure 13) and decreased phenylalanine levels (Figure 12C), suggesting a shift of phenylalanine flux towards secondary metabolism, potentially contributing to enhanced cold tolerance. Further, a striking galactose accumulation was observed in *abcg7* mutants during cold acclimation (Figure 10D). When seedlings were grown on galactose supplemented plates, anthocyanin synthesis in *abcg7* mutants was observed, and may explain the observed phenylalanine depletion (Figure 16).

Despite the cold tolerance, *abcg7* mutants exhibited increased sensitivity to freezing. Expression and cell wall sugar analyses during post-freezing stress revealed altered cell wall composition, indicating cell wall fragility under sub-zero conditions (Figure 19-20). Freezing stress also triggered increased ABCG7 expression in wild types, suggesting a specific role in post-freezing recovery Figure 18C.

Given that plastid membranes are rich in galactolipids and highly vulnerable to freezing injury, the lipid composition and expression of membrane remodelling genes were analysed. In *abcg7* mutants, lower levels of phosphor-, galacto- and storage lipids were detected during thawing, alongside with an altered expression pattern of the membrane remodelling enzyme SFR2 (Figure 21). BiFC analysis confirmed a physical interaction between ABCG7 and SFR2 (Figure 22), indicating a possible role for ABCG7 in the regulation of SFR2 activity and plastid membrane remodelling during freezing stress.

5.3. Zusammenfassung

Obwohl die ABCG7-Proteinmenge im plastidären Proteom unter Kältebedingungen abnimmt (Trentmann *et al.,* 2020), ist die physiologische Rolle dieses plastidären ABC-Transporters während der Kälteakklimatisierung und des Froststresses bislang kaum verstanden und seine subzelluläre Lokalisation war experimentell noch nicht bestätigt. Durch transiente Expression eines ABCG7-GFP-Fusionsproteins in *Nicotiana benthamiana* sowie proteolytische Verdauung isolierter Chloroplasten konnte ABCG7 in der äußeren Hüllmembran des Chloroplasten lokalisiert werden (Abbildung 6–7).

Die Charakterisierung von *abcg7* loss-of-function Mutanten unter Kältestress zeigte eine erhöhte Biomasseakkumulation (Abbildung 8B–C), verringerte Glukose- und Stärkegehalte (Ergänzende Abbildung 5) sowie erhöhte Konzentrationen von Metaboliten des Citratzyklus (Abbildung 11). Diese metabolischen Veränderungen gingen mit einer verstärkten Anthocyaninbiosynthese (Abbildung 13) und einer Reduktion des Phenylalaninspiegels (Abbildung 12C) einher, was auf eine Umleitung von Phenylalanin in den sekundären Metabolismus hindeutet und möglicherweise zur verbesserten Kältetoleranz der Mutanten beiträgt. Darüber hinaus wurde eine auffällige Anreicherung von Galactose in *abcg7*-Pflanzen während der Kälteakklimatisierung beobachtet (Abbildung 10D). Bei Anzucht auf galaktosehaltigen Agarplatten wurde eine verstärkte Anthocyaninsynthese in den *abcg7*-Mutanten festgestellt (Abbildung 16), was die reduzierte Phenylalaninkonzentration erklären könnte.

Trotz dieser kälterelevanten Anpassungen zeigten die *abcg7*-Mutanten eine erhöhte Frostempfindlichkeit. Genexpressions- und Zuckeranalysen der Zellwand nach Frostexposition offenbarten eine veränderte Zellwandzusammensetzung, was auf eine erhöhte Zellwandfragilität unter Frostbedingungen hinweist (Abbildung 19–20). Zudem wurde im Wildtyp eine erhöhte *ABCG7*-Expression nach Froststress beobachtet, was auf eine spezifische Funktion des Transporters bei der Regeneration nach Frost hinweist (Abbildung 18C).

Da Plastidmembranen reich an Galaktolipiden sind und besonders anfällig für Frostschäden, wurden die Lipidzusammensetzung sowie die Expression von Genen des Membranumbaus untersucht. In *abcg7*-Mutanten konnten während der Auftauphase verringerte Mengen an Phospho-, Galakto- und Speicherlipiden festgestellt werden, begleitet von einer veränderten Expressions des Membranumbau-Enzyms SFR2 (Abbildung 21). Eine BiFC-Analyse bestätigte zudem eine physikalische Interaktion zwischen ABCG7 und SFR2 (Abbildung 22), was auf eine mögliche Rolle von ABCG7 in der Regulation der SFR2-Aktivität und der plastidären Membranremodellierung während Froststress hindeutet.

6. References

Ahmed, N. U., Park, J. I., Jung, H. J., Hur, Y., & Nou, I. S. (2014). Characterization of dihydroflavonol 4-reductase (DFR) genes and their association with cold and freezing stress in *Brassica rapa*. *Gene, 550*(1), 46–55.

Althammer, M., Blöchl, C., Reischl, R., Huber, C. G., & Tenhaken, R. (2020). Phosphoglucomutase is not the target for galactose toxicity in plants. *Frontiers in Plant Science, 11*(167), 1-9.

Althammer, M., Regl, C., Herburger, K., Blöchl, C., Voglas, E., Huber, C. G., & Tenhaken, R. (2022). Overexpression of UDP-sugar pyrophosphorylase leads to higher sensitivity towards galactose, providing new insights into the mechanisms of galactose toxicity in plants. *The Plant Journal, 109*(6), 1416–1426.

Andersson, M. X., & Dörmann, P. (2008). The chloroplast: Interactions with the environment. In *The Chloroplast: Interactions with the Environment*, 125–158, Springer

Araguirang, G. E., Venn, B., Kelber, N. M., Feil, R., Lunn, J., Kleine, T., Leister, D., Mühlhaus, T., & Richter, A. S. (2024). Spliceosomal complex components are critical for adjusting the C:N balance during high-light acclimation. *Plant Journal, 119*(1), 153–175.

Aranda, P. S., LaJoie, D. M., & Jorcyk, C. L. (2012). Bleach gel: A simple agarose gel for analyzing RNA integrity. *Electrophoresis, 33*(2), 366–369.

Arisz, S. A., Heo, J. Y., Koevoets, I. T., Zhao, T., van Egmond, P., Meyer, A. J., Zeng, W., Niu, X., Wang, B., Mitchell-Olds, T., Schranz, M. E., & Testerink, C. (2018). Diacylglycerol acyltransferase1 contributes to freezing tolerance. *Plant Physiology, 177*(4), 1410–1424.

Armenteros, J. J. A., Salvatore, M., Emanuelsson, O., Winther, O., von Heijne, G., Elofsson, A., & Nielsen, H. (2019). Detecting sequence signals in targeting peptides using deep learning. *Life Science Alliance, 2*(5), e201900429.

Arnon, D. I. (1949). Copper enzymes in isolated chloroplasts. Polyphenoloxidase in *Beta vulgaris*. *Plant Physiology, 24*(1), 1–15.

Asada, K. (2006). Production and scavenging of reactive oxygen species in chloroplasts and their functions. *Plant Physiology, 141*(2), 391–396.

Ashraf, M. A., Akihiro, T., Ito, K., Kumagai, S., Sugita, R., Tanoi, K., & Rahman, A. (2021). ATP binding cassette proteins ABCG37 and ABCG33 function as potassium-independent cesium uptake carriers in Arabidopsis roots. *Molecular Plant, 14*(4), 664–678.

Baker, A., Graham, I. A., Holdsworth, M., Smith, S. M., & Theodoulou, F. L. (2006). Chewing the fat: β-oxidation in signalling and development. *Trends in Plant Science, 11*(3), 124–132.

Barnes, A. C., Benning, C., & Roston, R. L. (2016). Chloroplast membrane remodeling during freezing stress is accompanied by cytoplasmic acidification activating SENSITIVE TO FREEZING2. *Plant Physiology, 171*(3), 2140–2149.

Bertani, G. (1951): Studies on lysogenesis. I. The mode of phage liberation by lysogenic Escherichia coli. *Journal of Bacteriology, 62*(3), 293–300.

Bethke, G., Thao, A., Xiong, G., Li, B., Soltis, N. E., Hatsugai, N., Hillmer, R. A., Katagiri, F., Kliebenstein, D. J., Pauly, M., & Glazebrook, J. (2015). Pectin biosynthesis is critical for cell wall integrity and immunity in *Arabidopsis thaliana. Plant Cell, 28*(2), 537–556.

Biemans-Oldehinkel, E., Doeven, M. K., Poolman, B. (2006). ABC transporter architecture and regulatory roles of accessory domains. *FEBS Letters, 580*(4), 1023–1035.

Birnboim, H. C., Doly, J. (1979). A rapid alkaline extraction procedure for screening recombinant plasmid DNA. *Nucleic Acids Research, 7*(6), 1513–1524.

Bölter, B., Mitterreiter, M. J., Schwenkert, S., Finkemeier, I., & Kunz, H. H. (2020). The topology of plastid inner envelope potassium cation efflux antiporter KEA1 provides new insights into its regulatory features. *Photosynthesis Research, 145*(1), 43–54.

Bonawitz, N. D., Chapple, C. (2010). The genetics of lignin biosynthesis: Connecting genotype to phenotype. *Annual Review of Genetics, 44*, 337–363.

Borevitz, J. O., Xia, Y., Blount, J., Dixon, R. A., Lamb, C. (2000). Activation tagging identifies a conserved MYB regulator of phenylpropanoid biosynthesis. *Plant Cell, 12*(12), 2383–2393.

Boyer, J. S. (1982). Plant productivity and environment. *Science, 218*(4571), 443–448.

Bradford, M. M. (1976). A rapid and sensitive method for the quantification of microgram quantities of protein utilizing the principle of protein-dye binding. *Analytical Biochemistry, 72*, 248–254.

Breuers, F. K. H., Bräutigam, A., Weber, A. P. M. (2011). The plastid outer envelope – A highly dynamic interface between plastid and cytoplasm. *Frontiers in Plant Science, 2*(97), 1-20.

Broglie, R. M., Hunter, C. N., Delepelaire, P., Niederman, R. A., Chua, N. H., & Clayton, R. K. (1980). Isolation and characterization of the pigment-protein complexes *of Rhodopseudomonas sphaeroides* by lithium dodecyl sulphate/polyacrylamide gel electrophoresis. *Proceedings of the National Academy of Sciences USA, 77*(1), 87–91.

Buda, G. J., Barnes, W. J., Fich, E. A., Park, S., Yeats, T. H., Zhao, L., Domozych, D. S., Rose, J. K. C. (2013). An ATP binding cassette transporter is required for cuticular wax deposition and desiccation tolerance in the moss Physcomitrella patens. *Plant Cell, 25*(10), 4000–4013.

Bullock, W. O. (1987). XL1-Blue: A high-efficiency plasmid transforming recA *Escherichia coli* strain with beta-galactosidase selection. *BioTechniques, 5*, 376–379.

Cavalier, D. M., Lerouxel, O., Neumetzler, L., Yamauchi, K., Reinecke, A., Freshour, G., Zabotina, O. A., Hahn, M. G., Burgert, I., Pauly, M., Raikhel, N. V., & Keegstra, K. (2008). Disrupting two *Arabidopsis thaliana* xylosyltransferase genes results in plants deficient in xyloglucan, a major primary cell wall component. *Plant Cell, 20*(6), 1519–1537.

Chalker-Scott, L. (1999). Environmental significance of anthocyanins in plant stress responses. *Photochemistry and Photobiology, 70*(1), 1–9.

Chou, M. L., Fitzpatrick, L. M., Tu, S. L., Budziszewski, G., Potter-Lewis, S., Akita, M., Levin, J. Z., Keegstra, K., Li, H. M. (2003). Tic40, a membrane-anchored co-chaperone homolog in the chloroplast protein translocon. *EMBO Journal, 22*(12), 2970–2980.

Choudhury, F. K., Rivero, R. M., Blumwald, E., Mittler, R. (2017). Reactive oxygen species, abiotic stress and stress combination. *Plant Journal, 90*(5), 856–867.

Cline, K., Andrews, J., Mersey, B. (1981). Separation and characterization of inner and outer envelope membranes of pea chloroplasts. *Proceedings of the National Academy of Sciences USA, 78*(6), 3595–3599.

Cline, Kenneth, Werner-washburne, M., Andrews, J., & Keegstra, K. (1984). Thermolysin is a suitable protease for probing the surface of intact pea chloroplasts*. Plant Physiology, 75*, 675-678.

Cook, D., Fowler, S., Fiehn, O., Thomashow, M. F. (2004). A prominent role for the CBF cold response pathway in configuring the low-temperature metabolome of Arabidopsis. *Proceedings of the National Academy of Sciences USA, 101*(42), 15243–15248.

Cook, R., Lupette, J., Benning, C. (2021). The role of chloroplast membrane lipid metabolism in plant environmental responses. *Cells, 10*(3), 1–20.

Coruzzi, G. M. (2003). Primary N-assimilation into amino acids in Arabidopsis. *The Arabidopsis Book (e0010).* American Society of Plant Biologists.

Crosatti, C., Rizza, F., Badeck, F. W., Mazzucotelli, E., Cattivelli, L. (2013). Harden the chloroplast to protect the plant. *Physiologia Plantarum, 147*(1), 55–63.

Cypionka, H. (2010). Grundlagen der Mikrobiologie. Berlin, Heidelberg: Springer.

Degenkolbe, T., Giavalisco, P., Zuther, E., Seiwert, B., Hincha, D. K., & Willmitzer, L. (2012). Differential remodeling of the lipidome during cold acclimation in natural accessions of *Arabidopsis thaliana. Plant Journal, 72*(6), 972–982.

Desjardins, P., Conklin, D. (2010). NanoDrop microvolume quantitation of nucleic acids. *Journal of Visualized Experiments, (45),* 1–4.

Dixon, R. A., Paiva, N. L. (1995). Stress-induced phenylpropanoid metabolism. *Plant Cell, 7*(7), 1085–1097.

Doherty, C. J., Van Buskirk, H. A., Myers, S. J., Thomashow, M. F. (2009). Roles for Arabidopsis CAMTA transcription factors in cold-regulated gene expression and freezing tolerance. *Plant Cell, 21*(3), 972–984.

Dörmann, P., Benning, C. (1998). The role of UDP-glucose epimerase in carbohydrate metabolism of Arabidopsis. *Plant Journal, 13*(5), 641–652.

Eckart, K., Eichacker, L. A., Sohrt, K., Schleiff, E., Heins, L., Soll, J. (2002). A Toc75-like protein import channel is abundant in chloroplasts. *EMBO Reports, 3*(6), 557–562.

Eklöf, J. M., Brumer, H. (2010). The XTH gene family: An update on enzyme structure, function, and phylogeny in xyloglucan remodeling. *Plant Physiology, 153*(2), 456–466.

El-Azaz, J., Cánovas, F. M., Barcelona, B., Ávila, C., & de la Torre, F. (2022). Deregulation of phenylalanine biosynthesis evolved with the emergence of vascular plants. *Plant Physiology, 188*(1), 134–150.

Fagerstedt, K., Karkonen, A. (2015). The plant cell wall. *Journal of Integrative Plant Biology, 57*(11), 861–862.

Fan, J., Yan, C., Xu, C. (2013). Phospholipid:diacylglycerol acyltransferase-mediated triacylglycerol biosynthesis is crucial for protection against fatty acid-induced cell death in growing tissues of Arabidopsis. *Plant Journal, 76*(6), 930–942.

Ferro, M., Brugière, S., Salvi, D., Seigneurin-Berny, D., Moyet, L., Ramus, C., Miras, S., Mellal, M., Le Gall, S., Kieffer-Jacquinod, S., Bruley, C., Garin, J., Joyard, J., Rolland, N. (2010). AT-CHLORO, a comprehensive chloroplast proteome database with subplastidial localization and curated information on envelope proteins. *Molecular and Cellular Proteomics, 9*(6), 1063–1084.

Ferro, M., Salvi, D., Riviere-Rolland, H., Vermat, T., Seigneurin-Berny, D., Grunwald, D., Garin, J., Joyard, J., Rolland, N. (2003). Proteomics of the chloroplast envelope membranes from Arabidopsis thaliana. *Molecular and Cellular Proteomics, 2*(5), 325–345.

Finkemeier, I., Leister, D. (2010). Plant chloroplasts and other plastids. *Encyclopedia of Life Sciences, (ELS)*. John Wiley & Sons, Ltd.

Fourrier, N., Bédard, J., Lopez-Juez, E., Barbrook, A., Bowyer, J., Jarvis, P., Warren, G., & Thorlby, G. (2008). A role for SENSITIVE TO FREEZING2 in protecting chloroplasts against freeze-induced damage in Arabidopsis. *Plant Journal, 55*(5), 734–745.

Fowler, S., Thomashow, M. F. (2002). Arabidopsis transcriptome profiling indicates that multiple regulatory pathways are activated during cold acclimation in addition to the CBF cold response pathway. *Plant Cell, 14*(8), 1675–1690.

Fry, S. C. (1982). Phenolic components of the plant cell wall. *Biochemical Journal, 203*, 493–504.

Fry, S. C. (1983). Feruloylated pectins from the primary cell wall: Their structure and possible functions. *Planta, 157*(2), 111–123.

Garcia-Molina, A., Kleine, T., Schneider, K., Mühlhaus, T., Lehmann, M., & Leister, D. (2020). Translational components contribute to acclimation responses to high light, heat, and cold in Arabidopsis. iScience, 23(7), 1-21.

Giavalisco, P., Li, Y., Matthes, A., Eckhardt, A., Hubberten, H. M., Hesse, H., Segu, S., Hummel, J., Köhl, K., Willmitzer, L. (2011). Elemental formula annotation of polar and lipophilic metabolites using 13C, 15N and 34S isotope labelling, in combination with high-resolution mass spectrometry. *Plant Journal, 68*(2), 364–376.

Gilmour, S. J., Sebolt, A. M., Salazar, M. P., Everard, J. D., Thomashow, M. F. (2000). Overexpression of the Arabidopsis CBF3 transcriptional activator mimics multiple biochemical changes associated with cold acclimation. *Plant Physiology, 124*(4), 1854–1865.

Gordon-Kamm, W. J., Steponkus, P. L. (1984). The influence of cold acclimation on the behavior of the plasma membrane following osmotic contraction of isolated protoplasts. *Protoplasma, 123*(3), 161–173.

Gräfe, K., Schmitt, L. (2021). The ABC transporter G subfamily in *Arabidopsis thaliana. Journal of Experimental Botany, 72*(1), 92–106.

Grefen, C., Donald, N., Hashimoto, K., Kudla, J., Schumacher, K., Blatt, M. R. (2010). A *ubiquitin-10* promoter-based vector set for fluorescent protein tagging facilitates temporal stability and native protein distribution in transient and stable expression studies. *Plant Journal, 64*(2), 355–365.

Gutierrez-Carbonell, E., Takahashi, D., Lattanzio, G., Rodríguez-Celma, J., Kehr, J., Soll, J., Philippar, K., Uemura, M., Abadía, J., & López-Millán, A. F. (2014). The distinct functional roles of the inner and outer chloroplast envelope of pea (*Pisum sativum*) as revealed by proteomic approaches. *Journal of Proteome Research, 13*(6), 2941–2953.

Guy, C. L. (1990). Cold acclimation and freezing stress tolerance: Role of protein metabolism. *Annual Review of Plant Physiology and Plant Molecular Biology, 41*(1), 187–223.

Haake, V., Cook, D., Riechmann, J. L., Pineda, O., Thomashow, M. F., Zhang, J. Z. (2002). Transcription factor CBF4 is a regulator of drought adaptation in Arabidopsis. *Plant Physiology, 130*(2), 639–648.

Hannah, M. A., Heyer, A. G., Hincha, D. K. (2005). A global survey of gene regulation during cold acclimation in *Arabidopsis thaliana. PLoS Genetics, 1*(2), 179–196.

Hannah, M. A., Wiese, D., Freund, S., Fiehn, O., Heyer, A. G., & Hincha, D. K. (2006). Natural genetic variation of freezing tolerance in Arabidopsis. *Plant Physiology, 142*(1), 98–112

Harholt, J., Suttangkakul, A., Scheller, H. V. (2010). Biosynthesis of pectin. P*lant Physiology, 153*(2), 384–395.

Havaux, M., Kloppstech, K. (2001). The protective functions of carotenoid and flavonoid pigments against excess visible radiation at chilling temperature investigated in Arabidopsis *npq* and *tt* mutants. *Planta, 213*(6), 953–966.

Herrmann, K., Entus, R. (2001). Shikimate pathway: Aromatic amino acids and beyond. *Encyclopedia of Life Sciences*, 1–6.

Higgins, C. F. (1992). ABC transporters: From microorganisms to man. *Annual Review of Cell Biology, 8,* 67–113.

Higgins, C. F., Linton, K. J. (2004). The ATP switch model for ABC transporters. *Nature Structural and Molecular Biology, 11*(10), 918–926.

Hoermiller, I. I., Naegele, T., Augustin, H., Kempa, S., Heyer, A. G. (2017). Subcellular reprogramming of metabolism during cold acclimation in *Arabidopsis thaliana*. *Plant Cell and Environment, 40*(5), 602–610.

Hoffmann, N., King, S., Samuels, A. L., & McFarlane, H. E. (2021). Subcellular coordination of plant cell wall synthesis. *Developmental Cell, 56*(7), 933–948.

Höfgen, R., Willmitzer, L. (1988). Competent agrobacteria. *Nucleic Acids Research, 16*(20), 9877.

Höftberger, M., Glössl, J., Bohdanowicz, J., Altmann, F., Tenhaken, R. (2022). Galactose induces formation of cell wall stubs and cell death in Arabidopsis roots. *Planta, 256*(2), 1–13.

Howles, P. A., Sewalt, V. J. H., Paiva, N. L., Elkind, Y., Bate, N. J., Lamb, C., Dixon, R. A. (1996). Overexpression of L-phenylalanine ammonia-lyase in transgenic tobacco plants reveals control points for flux into phenylpropanoid biosynthesis. *Plant Physiology, 112*(4), 1617–1624.

Hu, Y., Jiang, L., Wang, F., Yu, D. (2017). Jasmonate regulates leaf senescence and tolerance to cold stress: Crosstalk with other phytohormones. *Journal of Experimental Botany, 68*(6), 1361-1369.

Ishida, K., & Yokoyama, R. (2022). Reconsidering the function of the xyloglucan endotransglucosylase/hydrolase family. *Journal of Plant Research*, *135*(2), 145–156.

Jackson, D. T., Froehlich, J. E., Keegstra, K. (1998). The hydrophilic domain of tic110, an inner envelope membrane component of the chloroplastic protein translocation apparatus, faces stromal compartment. *Journal of Biological Chemistry, 273*(26), 16583–16588.

Jaglo-Ottosen, K. R., Gilmour, S. J., Zarka, D. G., Schabenberger, O., Thomashow, M. F. (1998). Arabidopsis *CBF1* overexpression induces *COR* genes and enhances freezing tolerance. *Science, 280*(5360), 104–106.

Jarvis, M. C., McCann, M. C. (2000). Macromolecular biophysics of the plant cell wall: Concepts and methodology. *Plant Physiology and Biochemistry, 38*(1–2), 1–13.

John, A., Krämer, M., Lehmann, M., Kunz, H. H., Aarabi, F., Alseekh, S., Fernie, A., Sommer, F., Schroda, M., Zimmer, D., Mühlhaus, T., Peisker, H., Gutbrod, K., Dörmann, P., Neunzig, J., Philippar, K., & Neuhaus, H. E. (2024). Degradation of FATTY ACID EXPORT PROTEIN1 by RHOMBOID-LIKE PROTEASE11 contributes to cold tolerance in Arabidopsis. *Plant Cell, 36*(5), 1937–1962.

Johnston, M. L., Luethy, M. H., Miernyk, J. A., & Randall, D. D. (1997). Cloning and molecular analyses of the *Arabidopsis thaliana* plastid pyruvate dehydrogenase subunits*. Biochimica et Biophysica Acta - Bioenergetics, 1321*(3), 200–206.

Jouhet, J., Maréchal, E., Baldan, B., Bligny, R., Joyard, J., & Block, M. A. (2004). Phosphate deprivation induces transfer of DGDG galactolipid from chloroplast to mitochondria. *Journal of Cell Biology, 167*(5), 863–874.

Julian, J. D., Zabotina, O. A. (2022). Xyloglucan biosynthesis: From genes to proteins and their functions. *Frontiers in Plant Science, 13*(920494), 1-14.

Kaplan, F., Kopka, J., Haskell, D. W., Schiller, C. K., Gatzke, N., Sung, D. Y., Zhao, W., Guy, C. L. (2004). Exploring the temperature-stress metabolome. *Plant Physiology, 136,* 4159–4168

Kaplan, F., Kopka, J., Haskell, D. W., Zhao, W., Schiller, K. C., Gatzke, N., Sung, D. Y., Guy, C. L. (2007). Transcript and metabolite profiling during cold acclimation of Arabidopsis reveals an intricate relationship of cold-regulated gene expression with modifications in metabolite content. *Plant Journal, 50*(6), 967–981

Karimi, M., Inzé, D., Depicker, A. (2002). GATEWAY vectors for Agrobacterium-mediated transformation. *Trends in Plant Science, 7*(5), 193–195.

Keller, I., Müdsam, C., Rodrigues, C. M., Kischka, D., Zierer, W., Sonnewald, U., Harms, K., Czarnecki, O., Fiedler-Wiechers, K., Koch, W., Neuhaus, H. E., Ludewig, F., & Pommerrenig, B. (2021). Cold-triggered induction of ROS- and raffinose metabolism in freezing-sensitive taproot tissue of sugar beet. *Frontiers in Plant Science, 12*(715767), 1-19.

Kerppola, T. K. (2008). Bimolecular fluorescence complementation (BiFC) analysis as a probe of protein interactions in living cells. *Annual Review of Biophysics, 37*, 465–487.

Khan, N., Bano, A., Rahman, M. A., Rathinasabapathi, B., Babar, M. A. (2020). Role of sugars, amino acids and organic acids in improving plant abiotic stress tolerance. *Pakistan Journal of Botany, 52*(2), 355–363.

Kim, D. H., Lee, J. E., Xu, Z. Y., Geem, K. R., Kwon, Y., Park, J. W., & Hwang, I. (2015). Cytosolic targeting factor AKR2A captures chloroplast outer membrane-localized client proteins at the ribosome during translation. *Nature Communications, 6*(6843), 1–13.

Kitajima-Koga, A., Baslam, M., Hamada, Y., Ito, N., Taniuchi, T., Takamatsu, T., Oikawa, K., Kaneko, K., & Mitsui, T. (2020). Functional analysis of rice long-chain acyl-CoA synthetase 9 (OsLACS9) in the chloroplast envelope membrane*. International Journal of Molecular Sciences, 21*(2223), 1–16.

Kitashova, A., Adler, S. O., Richter, A. S., Eberlein, S., Dziubek, D., Klipp, E., & Nägele, T. (2023). Limitation of sucrose biosynthesis shapes carbon partitioning during plant cold acclimation. *Plant Cell and Environment, 46*(2), 464–478

Kleine, T., Leister, D. (2013). Retrograde signals galore. *Frontiers in Plant Science, 4*(45), 1–3.

Kleine, T., Nägele, T., Neuhaus, H. E., Schmitz-Linneweber, C., Fernie, A. R., Geigenberger, P., Grimm, B., Kaufmann, K., Klipp, E., Meurer, J., Möhlmann, T., Mühlhaus, T., Naranjo, B., Nickelsen, J., Richter, A., Ruwe, H., Schroda, M., Schwenkert, S., Trentmann, O., Willmund, F., Zoschke, R., Leister, D. (2021). Acclimation in plants – the Green Hub consortium. *Plant Journal, 106*(1), 23–40.

Klotke, J., Kopka, J., Gatzke, N., & Heyer, A. G. (2004). Impact of soluble sugar concentrations on the acquisition of freezing tolerance in accessions of *Arabidopsis thaliana* with contrasting cold adaptation – Evidence for a role of raffinose in cold acclimation. *Plant, Cell and Environment,* 27(11), 1395–1404.

Kodama, Y., Hu, C. D. (2012). Bimolecular fluorescence complementation (BiFC): A 5-year update and future perspectives. *BioTechniques, 53*(5), 285–298.

Koncz, C., Schell, J. (1986). The promoter of TL-DNA gene 5 controls the tissue-specific expression of chimaeric genes carried by a novel type of Agrobacterium binary vector. *Molecular & General Genetics, 204*(3), 383–396

Kong, Y., Peña, M. J., Renna, L., Avci, U., Pattathil, S., Tuomivaara, S. T., Li, X., Reiter, W. D., Brandizzi, F., Hahn, M. G., Darvill, A. G., York, W. S., & O'neill, M. A. (2015). Galactose-depleted xyloglucan is dysfunctional and leads to dwarfism in Arabidopsis. *Plant Physiology, 167*(4), 1296-1306

Konishi, T., Shinohara, K., Yamada, K., & Sasaki, Y. (1996). Acetyl-CoA carboxylase in higher plants: Most plants other than Gramineae have both the prokaryotic and the eukaryotic forms of this enzyme. *Plant and Cell Physiology, 37*(2), 117–122.

Korn, M., Peterek, S., Mock, H. P., Heyer, A. G., & Hincha, D. K. (2008). Heterosis in the freezing tolerance, and sugar and flavonoid contents of crosses between *Arabidopsis thaliana* accessions of widely varying freezing tolerance. *Plant, Cell and Environment, 31*(6), 813–827.

Kutsuno, T., Chowhan, S., Kotake, T., & Takahashi, D. (2023). Temporal cell wall changes during cold acclimation and deacclimation and their potential involvement in freezing tolerance and growth. *Physiologia Plantarum, 175*(1), 1–11.

Le Gall, H., Philippe, F., Domon, J.-M., Gillet, F., Pelloux, J., Rayon, C. (2015). Cell wall metabolism in response to abiotic stress. *Plants, 4(*1), 112–166.

Le, M. Q., Engelsberger, W. R., Hincha, D. K. (2008). Natural genetic variation in acclimation capacity at sub-zero temperatures after cold acclimation at 4°C in different *Arabidopsis thaliana* accessions. *Cryobiology, 57*(2), 104–112.

Leslie, E. M., Deeley, R. G., Cole, S. P. C. (2005). Multidrug resistance proteins: Role of P-glycoprotein, MRP1, MRP2, and BCRP (ABCG2) in tissue defense. *Toxicology and Applied Pharmacology, 204*(3), 216-237.

Levesque-Tremblay, G., Pelloux, J., Braybrook, S. A., & Müller, K. (2015). Tuning of pectin methylesterification: Consequences for cell wall biomechanics and development. *Planta, 242*(4), 791-811.

Leyva, A., Jarillo, J. A., Salinas, J., & Martinez-Zapater, J. M. (1995). Low temperature induces the accumulation of phenylalanine ammonia-lyase and chalcone synthase mRNAs of *Arabidopsis thaliana* in a light-dependent manner. *Plant Physiology, 108*(1), 39–46.

Li, H. M., Chen, L. J. (1996). Protein targeting and integration signal for the chloroplastic outer envelope membrane. *Plant Cell, 8*(11), 2117–2126.

Li, J., Zhao, J., Rose, A. B., Schmidt, R., & Last, R. L. (1995). Arabidopsis phosphoribosylanthranilate isomerase: Molecular genetic analysis of triplicate tryptophan pathway genes. *Plant Cell, 7*(4), 447-461.

Li, P., Li, Y. J., Zhang, F. J., Zhang, G. Z., Jiang, X. Y., Yu, H. M., & Hou, B. K. (2017). The Arabidopsis UDP-glycosyltransferases UGT79B2 and UGT79B3 contribute to cold, salt and drought stress tolerance via modulating anthocyanin accumulation. *Plant Journal, 89*(1), 85-103.

Li, W., Li, M., Zhang, W., Welti, R., & Wang, X. (2004). The plasma membrane-bound phospholipase Dδ enhances freezing tolerance in *Arabidopsis thaliana*. *Nature Biotechnology, 22*(4), 427–433.

Li, W., Wang, R., Li, M., Li, X., Wang, C., Welti, R., & Wang, X. (2008). Differential degradation of extraplastidic and plastidic lipids during freezing and post-freezing recovery in *Arabidopsis thaliana. Journal of Biological Chemistry, 283*(1), 461–468.

Li-Beisson, Y., Shorrosh, B., Beisson, F., Andersson, M. X., Arondel, V., Bates, P. D., Baud, S., Bird, D., DeBono, A., Durrett, T. P., Franke, R. B., Graham, I. A., Katayama, K., Kelly, A. A., Larson, T., Markham, J. E., Miquel, M., Molina, I., Nishida, I., Rowland, O., Samuels, L.,Schmid, K. M., Wada, H., Welti, R.,

Xu, C., Zallot, R., Ohlrogge, J. (2013). Acyl-lipid metabolism. *The Arabidopsis Book (e00161).* American Society of Plant Biologists.

Liepman, A. H., Wightman, R., Geshi, N., Turner, S. R., & Scheller, H. V. (2010). Arabidopsis – A powerful model system for plant cell wall research. *Plant Journal, 61*(6), 1107–1121.

Liu, J., Gilmour, S. J., Thomashow, M. F., & Van Nocker, S. (2002). Cold signalling associated with vernalization in *Arabidopsis thaliana* does not involve CBF1 or abscisic acid. *Physiologia Plantarum, 114*(1), 125–134.

Liu, X. M., An, J., Han, H. J., Kim, S. H., Lim, C. O., Yun, D. J., & Chung, W. S. (2014). ZAT11, a zinc finger transcription factor, is a negative regulator of nickel ion tolerance in Arabidopsis. *Plant Cell Reports, 33*(12), 2015–2021.

Liu, Y. B., Lu, S. M., Zhang, J. F., Liu, S., & Lu, Y. T. (2007). A xyloglucan endotransglucosylase/hydrolase involves in growth of primary root and alters the deposition of cellulose in Arabidopsis. Planta, 226(6), 1547–1560.

Livak, K. J., Schmittgen, T. D. (2001). Analysis of relative gene expression data using real-time quantitative PCR and the 2–ΔΔCT method. *Methods, 25*(4), 402–408.

Lu, J., Xu, Y., Wang, J., Singer, S. D., & Chen, G. (2020). The role of triacylglycerol in plant stress response. *Plants, 9*(472), 1–13.

Lynch, J. H., Dudareva, N. (2020). Aromatic amino acids: A complex network ripe for future exploration. *Trends in Plant Science, 25*(7), 670–681.

Mackenzie, S. M., Howells, A. J., Cox, G. B., & Ewart, G. D. (2000). Sub-cellular localisation of the White/Scarlet ABC transporter to pigment granule membranes within the compound eye of *Drosophila melanogaster. Genetica, 108*(3), 239–252.

Maeda, H., Dudareva, N. (2012). The shikimate pathway and aromatic amino acid biosynthesis in plants. *Annual Review of Plant Biology, 63*, 73–105.

Mahajan, S., Tuteja, N. (2005). Cold, salinity and drought stresses: An overview. *Archives of Biochemistry and Biophysics, 444*(2), 139–158.

Mancinelli, A. L. (1984). Photoregulation of anthocyanin synthesis. *Plant Physiology, 75*(2), 447-453.

Mandel, M., Higa, A. (1970). Calcium-dependent bacteriophage DNA infection. *Journal of Molecular Biology, 53*(1), 159–162.

Maréchal, E., Bastien, O. (2014). Modeling of regulatory loops controlling galactolipid biosynthesis in the inner envelope membrane of chloroplasts. *Journal of Theoretical Biology*, 361, 1–13.

Martinoia, E., Klein, M., Geisler, M., Bovet, L., Forestier, C., Kolukisaoglu, Ü., Müller-Röber, B., & Schulz, B. (2002). Multifunctionality of plant ABC transporters – More than just detoxifiers. *Planta, 214*(3), 345–355.

Matsuda, S., Funabiki, A., Furukawa, K., Komori, N., Koike, M., Tokuji, Y., Takamure, I., & Kato, K. (2012). Genome-wide analysis and expression profiling of half-size ABC protein subgroup G in rice in response to abiotic stress and phytohormone treatments. *Molecular Genetics and Genomics, 287*(10), 819–835.

McFadden, G. I. (1999). Endosymbiosis and evolution of the plant cell. *Current Opinion in Plant Biology, 2*(6), 513–519.

McFadden, G. I. (2001). Primary and secondary endosymbiosis and the origin of plastids. *Journal of Phycology, 37*(6), 951–959.

McKown, R., Kuroki, G., Warren, G. (1996). Cold responses of Arabidopsis mutants impaired in freezing tolerance. *Journal of Experimental Botany, 47*(305), 1919–1925.

McNeil, M., Darvill, A. G., Fry, S. C., & Albersheim, P. (1984). Structure and function of the primary cell walls of plants. *Annual Review of Biochemistry, 53,* 625–663.

Medina, J., Bargues, M., Terol, J., Pérez-Alonso, M., & Salinas, J. (1999). The Arabidopsis *CBF* gene family is composed of three genes encoding AP2 domain-containing proteins whose expression is regulated by low temperature but not by abscisic acid or dehydration. *Plant Physiology, 119*(2), 463–469.

Mittler, R. (2002). Oxidative stress, antioxidants and stress tolerance. *Trends in Plant Science, 7*(9), 405–410.

Moellering, E. R., Benning, C. (2011). Galactoglycerolipid metabolism under stress: A time for remodeling. *Trends in Plant Science, 16*(2), 98–107.

Moellering, E. R., Muthan, B., Benning, C. (2010). Freezing tolerance in plants requires lipid remodeling at the outer chloroplast membrane. *Science, 330*(6001), 226–228.

Mueller, S. P., Unger, M., Guender, L., Fekete, A., & Mueller, M. J. (2017). Phospholipid:Diacylglycerol acyltransferase-mediated triacylglycerol synthesis augments basal thermotolerance. *Plant Physiology, 175*(1), 486–497.

Mülhardt, C. (2009). Der Experimentator: Molekularbiologie/Genomics. Heidelberg: Springer.

Murina, V., Kasari, M., Takada, H., Hinnu, M., Saha, C. K., Grimshaw, J. W., Seki, T., Reith, M., Putrinš, M., Tenson, T., Strahl, H., Hauryliuk, V., & Atkinson, G. C. (2019). ABCF ATPases involved in protein synthesis, ribosome assembly and antibiotic resistance: Structural and functional diversification across the tree of life. *Journal of Molecular Biology, 431*(18), 3568-3590.

Nägele, T., Stutz, S., Hörmiller, I. I., & Heyer, A. G. (2012). Identification of a metabolic bottleneck for cold acclimation in *Arabidopsis thaliana. Plant Journal, 72*(1), 102–114.

Nakabayashi, K., Okamoto, M., Koshiba, T., Kamiya, Y., & Nambara, E. (2005). Genome-wide profiling of stored mRNA in *Arabidopsis thaliana* seed germination: Epigenetic and genetic regulation of transcription in seed. *Plant Journal, 41*(5), 697–709.

Nilsson, A. K., Johansson, O. N., Fahlberg, P., Kommuri, M., Töpel, M., Bodin, L. J., Sikora, P., Modarres, M., Ekengren, S., Nguyen, C. T., Farmer, E. E., Olsson, O., Ellerström, M., & Andersson, M. X. (2015). Acylated monogalactosyl diacylglycerol: Prevalence in the plant kingdom and identification of an enzyme catalyzing galactolipid head group acylation in *Arabidopsis thaliana. Plant Journal, 84*(6), 1152–1166.

Panter, P. E., Kent, O., Dale, M., Smith, S. J., Skipsey, M., Thorlby, G., Cummins, I., Ramsay, N., Begum, R. A., Sanhueza, D., Fry, S. C., Knight, M. R., & Knight, H. (2019). MUR1-mediated cell-wall fucosylation is required for freezing tolerance in *Arabidopsis thaliana. New Phytologist, 224*(4), 1518–1531.

Park, Y. B., & Cosgrove, D. J. (2012). Changes in cell wall biomechanical properties in the xyloglucan-deficient *xxt1/xxt2* mutant of Arabidopsis. *Plant Physiology, 158*(1), 465–475.

Patzke, K., Prananingrum, P., Klemens, P. A. W., Trentmann, O., Rodrigues, C. M., Keller, I., Fernie, A. R., Geigenberger, P., Bölter, B., Lehmann, M., Schmitz-Esser, S., Pommerrenig, B., Haferkamp, I., & Ekkehard Neuhaus, H. (2019). The plastidic sugar transporter pSuT influences flowering and affects cold responses 1. *Plant Physiology, 179*(2), 569–587.

Pearce, R. S. (1999). Molecular analysis of acclimation to cold. *Plant Growth Regulation, 29*(1-2), 47–76.

Pearce, R. S. (2001). Plant freezing and damage. *Annals of Botany, 87*(4), 417–424.

Peña, M. J., Ryden, P., Madson, M., Smith, A. C., & Carpita, N. C. (2004). The galactose residues of xyloglucan are essential to maintain mechanical strength of the primary cell walls in Arabidopsis during growth. *Plant Physiology, 134*(1), 443–451.

Pereyra, C., Parola, R., Lando, A. P., Rodriguez, M., & Martínez-Noël, G. M. A. (2023). High sugar concentration inhibits TOR signaling pathway in *Arabidopsis thaliana. Journal of Plant Growth Regulation, 42*(7), 4309–4323.

Pritchard, J., Tomos, A. D., Farrar, J. F., Minchin, P. E. H., Gould, N., Paul, M. J., MacRae, E. A., Ferrieri, R. A., Gray, D. W., & Thorpe, M. R. (2004). Turgor, solute import and growth in maize roots treated with galactose. *Functional Plant Biology, 31*(11), 1095–1103.

Qu, T., Liu, R., Wang, W., An, L., Chen, T., Liu, G., & Zhao, Z. (2011). Brassinosteroids regulate pectin methylesterase activity and *At*PME41 expression in Arabidopsis under chilling stress. *Cryobiology, 63*(2), 111–117.

Qureshi, M. K., Sujeeth, N., Gechev, T. S., & Hille, J. (2013). The zinc finger protein ZAT11 modulates paraquat-induced programmed cell death in *Arabidopsis thaliana. Acta Physiologiae Plantarum, 35*(6), 1863–1871.

Rajashekar, C. B., Lafta, A. (1996). Cell-wall changes and cell tension in response to cold acclimation and exogenous abscisic acid in leaves and cell cultures. *Plant Physiology, 111*(2), 605–612.

Ramon, R., Ellis, S., Singh, S., Norman G. Lewis, & Towers, N. (1998). Nitrogen recycling during phenylpropanoid metabolism in sweet potato tubers. *Journal of Plant Physiology, 153*(3–4), 316–323.

Rautengarten, C., Ebert, B., Ouellet, M., Nafisi, M., Baidoo, E. E. K., Benke, P., Stranne, M., Mukhopadhyay, A., Keasling, J. D., Sakuragi, Y., & Scheller, H. V. (2012). Arabidopsis Deficient in Cutin Ferulate encodes a transferase required for feruloylation of ω-hydroxy fatty acids in cutin polyester. *Plant Physiology, 158*(2), 654–665.

Rea, P. A. (2007). Plant ATP-binding cassette transporters. *Annual Review of Plant Biology, 58,* 347–375.

Reinhold, T., Alawady, A., Grimm, B., Beran, K. C., Jahns, P., Conrath, U., Bauer, J., Reiser, J., Melzer, M., Jeblick, W., & Neuhaus, H. E. (2007). Limitation of nocturnal import of ATP into Arabidopsis chloroplasts leads to photooxidative damage. *Plant Journal, 50*(2), 293–304.

Reiter, W. D., Chapple, C. C. S., Somerville, C. R. (1993). Altered growth and cell walls in a fucose-deficient mutant of Arabidopsis. *Science, 261*(5124), 1032–1035.

Reiter, W. D., Chapple, C., Somerville, C. R. (1997). Mutants *of Arabidopsis thaliana* with altered cell wall polysaccharide composition. *Plant Journal, 12*(2), 335–345.

Reyes-Díaz, M., Ulloa, N., Zúñiga-Feest, A., Gutiérrez, A., Gidekel, M., Alberdi, M., Corcuera, L. J., & Bravo, L. A. (2006). *Arabidopsis thaliana* avoids freezing by supercooling. *Journal of Experimental Botany, 57*(14), 3687–3696.

Reyes-Prieto, A., Moustafa, A. (2012). Plastid-localized amino acid biosynthetic pathways of Plantae are predominantly composed of non-cyanobacterial enzymes. Scientific Reports, 2, 1–12

Rice-Evans, C. A., Miller, N. J., Paganga, G. (1996). Structure-antioxidant activity relationships of flavonoids and phenolic acids. *Free Radical Biology and Medicine, 20*(7), 933–956.

Rodney Croteau, Kutchan, T. M., Lewis, N. G. (2000). Chapter 24: Natural Products (Secondary Metabolites). *Biochemistry and Molecular Biology of Plants*, 1250–1318.

Rohde, A., Morreel, K., Ralph, J., Goeminne, G., Hostyn, V., De Rycke, R., Kushnir, S., Van Doorsselaere, J., Joseleau, J. P., Vuylsteke, M., Van Driessche, G., Van Beeumen, J., Messens, E., & Boerjan, W. (2004). Molecular phenotyping of the *pal1* and *pal2* mutants of *Arabidopsis thaliana* reveals far-reaching consequences on phenylpropanoid, amino acid, and carbohydrate metabolism. *Plant Cell, 16*(10), 2749–2771.

Rose, A. B., Last, R. L. (1997). Introns act post-transcriptionally to increase expression of the *Arabidopsis thaliana* tryptophan pathway gene *PAT1. Plant Journal, 11*(3), 455–464.

Rose, J. K. C., Braam, J., Fry, S. C., & Nishitani, K. (2002). The XTH family of enzymes involved in xyloglucan endotransglucosylation and endohydrolysis: Current perspectives and a new unifying nomenclature. *Plant and Cell Physiology, 43*(12), 1421–1435.

Rösti, J., Barton, C. J., Albrecht, S., Dupree, P., Pauly, M., Findlay, K., Roberts, K., & Seifert, G. J. (2007). UDP-glucose 4-epimerase isoforms UGE2 and UGE4 cooperate in providing UDP-galactose for cell wall biosynthesis and growth of *Arabidopsis thaliana. Plant Cell, 19*(5), 1565–1579.

Roston, R. L., Hurlock, A. K., Benning, C. (2014a): Plastidic ABC Proteins. *Plastid Biology*, Springer, Kapitel 7.

Roston, R. L., Wang, K., Kuhn, L. A., & Benning, C. (2014b). Structural determinants allowing transferase activity in sensitive to freezing 2, classified as a family I glycosyl hydrolase. *Journal of Biological Chemistry, 289*(38), 26089–26106.

Ruelland, E., Vaultier, M. N., Zachowski, A., & Hurry, V. (2009). Chapter 2: Cold signalling and cold acclimation in plants. Advances in Botanical Research, (1st ed., Vol. 49, Issue C). Elesvier Ltd.

Saiki, R. K., Gelfand, D. H., Stoffel, S., Scharf, S. J., Higuchi, R., Horn, G. T., Mullis, K. B., & Erlich, H. A. (1988). Primer-directed enzymatic amplification of DNA with a thermostable DNA polymerase. *Science, 239*(4839), 487–491.

Salem, M. A., Yoshida, T., Perez de Souza, L., Alseekh, S., Bajdzienko, K., Fernie, A. R., & Giavalisco, P. (2020). An improved extraction method enables the comprehensive analysis of lipids, proteins, metabolites and phytohormones from a single sample of leaf tissue under water-deficit stress. *Plant Journal, 103*(4), 1614–1632.

Salem, M., Bernach, M., Bajdzienko, K., & Giavalisco, P. (2017). A simple fractionated extraction method for the comprehensive analysis of metabolites, lipids, and proteins from a single sample. *Journal of Visualized Experiments*, 2017(124), 1–10.

Sambrook, J., Russell, D. W. (2001). Molecular Cloning: A Laboratory Manual. 3rd ed. Cold Spring Harbor, NY: Cold Spring Harbor Laboratory Press.

Sambrook, J., Russell, D. W. (2006). Detection of DNA in Agarose Gels. Cold Spring Harbor Protocols, 2006(1), pdb.prot4022.

Sánchez-Fernández, R., Davies, T. G. E., Coleman, J. O. D., & Rea, P. A. (2001). The *Arabidopsis thaliana* ABC protein superfamily, a complete inventory. *Journal of Biological Chemistry, 276*(32), 30231–30244.

Scheler, C., Weitbrecht, K., Pearce, S. P., Hampstead, A., Büttner-Mainik, A., Lee, K. J. D., Voegele, A., Oracz, K., Dekkers, B. J. W., Wang, X., Wood, A. T. A., Bentsink, L., King, J. R., Knox, J. P., Holdsworth, M. J., Müller, K., & Leubner-Metzger, G. (2015). Promotion of testa rupture during garden cress germination involves seed compartment-specific expression and activity of pectin methylesterases. *Plant Physiology, 167*(1), 200–215.

Schleiff, E., Eichacker, L., Eckart, K., Becker, T., Mirus, O., Stahl, T., Soll, J. (2003). Prediction of the plant beta-barrel proteome: A case study of the chloroplast outer envelope. *Protein Science, 12*(4), 748–759.

Schnurr, J. A., Shockey, J. M., De Boer, G. J., & Browse, J. A. (2002). Fatty acid export from the chloroplast. Molecular characterization of a major plastidial acyl-coenzyme A synthetase from Arabidopsis. *Plant Physiology, 129*(4), 1700–1709.

Schulz, E., Tohge, T., Zuther, E., Fernie, A. R., & Hincha, D. K. (2015). Natural variation in flavonol and anthocyanin metabolism during cold acclimation in *Arabidopsis thaliana* accessions. *Plant Cell and Environment, 38*(8), 1658–1672.

Schulz, E., Tohge, T., Zuther, E., Fernie, A. R., & Hincha, D. K. (2016). Flavonoids are determinants of freezing tolerance and cold acclimation in *Arabidopsis thaliana*. *Scientific Reports, 6*(34027), 1–10.

Seguela-Arnaud, M., Smith, C., Uribe, M. C., May, S., Fischl, H., McKenzie, N., & Bevan, M. W. (2015). The Mediator complex subunits MED25/PFT1 and MED8 are required for transcriptional responses to changes in cell wall arabinose composition and glucose treatment in *Arabidopsis thaliana*. *BMC Plant Biology, 15*(1), 1–13.

Shi, H., Chan, Z. (2014). *At*HAP5A modulates freezing stress resistance in Arabidopsis independent of the CBF pathway. *New Phytologist*, *203*, 554–567.

Singh, K., Gulyás, Z., Athmer, B., Kovács, B., Mednyánszky, Z., Galiba, G., Stein, N., Simon-Sarkadi, L., & Kocsy, G. (2024). Comparative study of free amino acids at metabolite and gene expression levels in *Triticeae* during cold acclimation. *Journal of Plant Biochemistry and Biotechnology, 33*(4), 558–569.

Smallwood, M., Bowles, D. J., Gerday, C., Marahiel, M. A., Davies, P. L., Bradbeer, W., & Warren, G. (2002). Plants in a cold climate. *Philosophical Transactions of the Royal Society B: Biological Sciences, 357*(1423), 831–847.

Smirnoff, N., Cumbes, Q. J. (1989). Hydroxyl radical scavenging activity of compatible solutes. *Phytochemistry, 28*(4), 1057–1060.

Solecka, D., Zebrowski, J., Kacperska, A. (2008). Are pectins involved in cold acclimation and de-acclimation of winter oil-seed rape plants? *Annals of Botany, 101*(4), 521–530.

Song, Y., Zoong Lwe, Z. S., Wickramasinghe, P. A. D. B. V., & Welti, R. (2021). Head-group acylation of chloroplast membrane lipids. *Molecules*, *26*(1273), 1–10.

Stahl, T., Glockmann, C., Soll, J., & Heins, L. (1999). Tic40, a new "old" subunit of the chloroplast protein import translocon. *Journal of Biological Chemistry, 274*(52), 37467–37472.

Steponkus, P. L. (1984). Injury and cold acclimation. *Annual Review of Plant Physiology, 35*(221), 543–584.

Steponkus, P. L., Uemura, M., Balsamo, R. A., Arvinte, T., & Lynch, D. V. (1988). Transformation of the cryobehavior of rye protoplasts by modification of the plasma membrane lipid composition. *Proceedings of the National Academy of Sciences, 85*(23), 9026–9030.

Steponkus, P. L., Uemura, M., Joseph, R. A., Gilmour, S. J., & Thomashow, M. F. (1998). Mode of action of the *COR15a* gene on the freezing tolerance of *Arabidopsis thaliana. Proceedings of the National Academy of Sciences of the United States of America, 95*(24), 14570–14575.

Stitt, M., Lilley, R. M. C., Heldt, H. W. (1989). [32] Metabolite levels in specific cells and subcellular compartments of plant leaves. *Methods in Enzymology, 174*(1984), 518–552.

Suzuki, N., Mittler, R. (2006). Reactive oxygen species and temperature stresses: A delicate balance between signaling and destruction. *Physiologia Plantarum, 126*(1), 45–51.

Taji, T., Ohsumi, C., Iuchi, S., Seki, M., Kasuga, M., Kobayashi, M., Yamaguchi-Shinozaki, K., & Shinozaki, K. (2002). Important roles of drought- and cold-inducible genes for galactinol synthase in stress tolerance in *Arabidopsis thaliana. Plant Journal, 29*(4), 417–426.

Takahashi, D., Gorka, M., Erban, A., Graf, A., Kopka, J., Zuther, E., & Hincha, D. K. (2019). Both cold and sub-zero acclimation induce cell wall modification and changes in the extracellular proteome in *Arabidopsis thaliana. Scientific Reports, 9*(1), 1–15.

Takahashi, D., Johnson, K. L., Hao, P., Tuong, T., Erban, A., Sampathkumar, A., Bacic, A., Livingston, D. P., Kopka, J., Kuroha, T., Yokoyama, R., Nishitani, K., Zuther, E., & Hincha, D. K. (2021). Cell wall modification by the xyloglucan endotransglucosylase/hydrolase XTH19 influences freezing tolerance after cold and sub-zero acclimation. *Plant Cell and Environment, 44*(3), 915–930.

Takahashi, D., Soga, K., Kikuchi, T., Kutsuno, T., Hao, P., Sasaki, K., Nishiyama, Y., Kidokoro, S., Sampathkumar, A., Bacic, A., Johnson, K. L., & Kotake, T. (2024). Structural changes in cell wall pectic polymers contribute to freezing tolerance induced by cold acclimation in plants*. Current Biology, 34*(5), 958–968.e5.

Tan, W. J., Yang, Y. C., Zhou, Y., Huang, L. P., Xu, L., Chen, Q. F., Yu, L. J., & Xiao, S. (2018). DIACYLGLYCEROL ACYLTRANSFERASE and DIACYLGLYCEROL KINASE modulate triacylglycerol and phosphatidic acid production in the plant response to freezing stress. *Plant Physiology, 177*(3), 1303–1318.

Taylor, R. G., Walker, D. C., McInnes, R. R. (1993). *E. coli* host strains. *Nucleic Acids Research, 21*(7), 1677–1678.

Thalhammer, A., Hundertmark, M., Popova, A. V., Seckler, R., & Hincha, D. K. (2010). Interaction of two intrinsically disordered plant stress proteins (COR15A and COR15B) with lipid membranes in the dry state. *Biochimica et Biophysica Acta - Biomembranes, 1798*(9), 1812-1820.

T**heodoulou, F. L. (2000).** Plant ABC transporters. *Biochimica et Biophysica Acta - Biomembranes, 1465*(1–2), 79–103.

Thomashow, M. F. (1998). Role of cold-responsive genes in plant freezing tolerance. *Plant Physiology, 118*(1), 1–7.

Thomashow, M. F. (1999). Plant cold acclimation: Freezing tolerance genes and regulatory mechanisms. *Annual Review of Plant Biology*, 50, 571–599.

Thompson, D. S. (2005). How do cell walls regulate plant growth? *Journal of Experimental Botany, 56*(419), 2275–2285.

Thorlby, G., Fourrier, N., Warren, G. (2004). The Sensitive to Freezing2 gene, required for freezing tolerance in *Arabidopsis thaliana*, encodes a β-glucosidase. *Plant Cell, 16(*8), 2192-2203.

Trentmann, O, Mühlhaus, T., Zimmer, D., Sommer, F., Schroda, M., Haferkamp, I., Keller, I., Pommerrenig, B., & Neuhaus, E. (2020). Identification of chloroplast envelope proteins with critical importance for cold acclimation. *Plant Physiology, 182*(3), 1239–1255.

Tucker, M. R., Lou, H., Aubert, M. K., Wilkinson, L. G., Little, A., Houston, K., Pinto, S. C., & Shirley, N. J. (2018). Exploring the role of cell wall-related genes and polysaccharides during plant development. *Plants, 7*(2), 1–17.

Uemura, M., Steponkus, P. L. (1997). Effect of cold acclimation on the lipid composition of the inner and outer membrane of the chloroplast envelope isolated from rye leaves. *Plant Physiology, 114*(4), 1493–1500.

Valifard, M., Fernie, A. R., Kitashova, A., Nägele, T., Schröder, R., Meinert, M., Pommerrenig, B., Mehner-Breitfeld, D., Witte, C. P., Brüser, T., Keller, I., & Neuhaus, H. E. (2023). The novel chloroplast glucose transporter pGlcT2 affects adaptation to extended light periods. *Journal of Biological Chemistry, 299*(6), 1–18.

van Buer, J., Prescher, A., & Baier, M. (2019). Cold-priming of chloroplast ROS signalling is developmentally regulated and is locally controlled at the thylakoid membrane. *Scientific Reports*, *9*(1), 1–14.

Verrier, P. J., Bird, D., Burla, B., Dassa, E., Forestier, C., Geisler, M., Klein, M., Kolukisaoglu, Ü., Lee, Y., Martinoia, E., Murphy, A., Rea, P. A., Samuels, L., Schulz, B., Spalding, E. J., Yazaki, K., & Theodoulou, F. L. (2008). Plant ABC proteins – a unified nomenclature and updated inventory. *Trends in Plant Science, 13*(4), 151–159.

Vogel, J. T., Zarka, D. G., Van Buskirk, H. A., Fowler, S. G., & Thomashow, M. F. (2005). Roles of the CBF2 and ZAT12 transcription factors in configuring the low temperature transcriptome of Arabidopsis. *Plant Journal, 41*(2), 195–211.

Voinnet, O., Vain, P., Angell, S., & Baulcombe, D. C. (1998). Systemic spread of sequence-specific transgene RNA degradation in plants is initiated by localized introduction of ectopic promoterless DNA. *Cell, 95*(2), 177–187.

Von Heijne, G. (1990). The Signal Peptide. *The Journal of Membrane Biology*, *115*, 195–201.

Walker, J. E., Saraste, M., Runswick, M. J., & Gay, N. J. (1982). Distantly related sequences in the alpha- and beta-subunits of ATP synthase, myosin, kinases and other ATP-requiring enzymes and a common nucleotide binding fold. *The EMBO Journal, 1*(8), 945–951.

Wanner, L. A., Junttila, O. (1999). Cold-induced freezing tolerance in Arabidopsis. *Plant Physiology, 120*(2), 391–399.

Weigel, D., & Glazebrook, J. (2002). Arabidopsis: A Laboratory Manual. Arabidopsis : A Laboratory Manual. *The University of Chicago Press Journals, 77*(3), 330–331.

Welti, R., Li, W., Li, M., Sang, Y., Biesiada, H., Zhou, H. E., Rajashekar, C. B., Williams, T. D., & Wang, X. (2002). Profiling membrane lipids in plant stress responses: Role of phospholipase Dα in freezing-induced lipid changes in Arabidopsis. *Journal of Biological Chemistry, 277*(35), 31994–32002.

Witz, S., Jung, B., Fürst, S., & Möhlmann, T. (2012). *De novo* pyrimidine nucleotide synthesis mainly occurs outside of plastids, but a previously undiscovered nucleobase importer provides substrates for the essential salvage pathway in Arabidopsis. *Plant Cell, 24*(4), 1549–1559.

Wormit, A., Usadel, B. (2018). The multifaceted role of pectin methylesterase inhibitors (PMEIs). *International Journal of Molecular Sciences, 19*(10), 1–19.

Xie, M., Sun, J., Gong, D., & Kong, Y. (2019). The roles of Arabidopsis C1-2i subclass of C2H2-type zinc-finger transcription factors. *Genes*, *10*(653), 1–15.

Xiong, L., Zhu, J. K. (2002). Molecular and genetic aspects of plant responses to osmotic stress. *Plant, Cell and Environment, 25*(2), 131–139.

Xu, C., Fan, J., Cornish, A. J., & Benning, C. (2008). Lipid trafficking between the endoplasmic reticulum and the plastid in Arabidopsis requires the extraplastidic TGD4 protein. *Plant Cell, 20*(8), 2190–2204.

Xu, Y., Kambhampati, S., Morley, S. A., Cook, R., Froehlich, J. E., Allen, D. K., & Benning, C. (2023). Arabidopsis ACYL CARRIER PROTEIN4 and RHOMBOID LIKE10 act independently in chloroplast phosphatidate synthesis. *Plant Physiology, 193*(4), 2661–2676.

Yang, L., Li, W. C., Fu, F. L., Qu, J., Sun, F., Yu, H., & Zhang, J. (2022). Characterization of phenylalanine ammonia-lyase genes facilitating flavonoid biosynthesis from two species of medicinal plant Anoectochilus. *PeerJ, 10*, 1–16.

Yokoyama, R. (2024). Evolution of aromatic amino acid metabolism in plants: a key driving force behind plant chemical diversity in aromatic natural products. *Philosophical Transactions of the Royal Society of London. Series B, Biological Sciences, 379*(1914), 20230352.

Yu, L., Zhou, C., Fan, J., Shanklin, J., & Xu, C. (2021). Mechanisms and functions of membrane lipid remodeling in plants. *Plant Journal, 107*(1), 37–53.

Zabotina, O. A., Avci, U., Cavalier, D., Pattathil, S., Chou, Y. H., Eberhard, S., Danhof, L., Keegstra, K., & Hahn, M. G. (2012). Mutations in multiple *XXT* genes of Arabidopsis reveal the complexity of xyloglucan biosynthesis. *Plant Physiology, 159*(4), 1367–1384.

Zabotina, O. A., Van De Ven, W. T. G., Freshour, G., Drakakaki, G., Cavalier, D., Mouille, G., Hahn, M. G., Keegstra, K., & Raikhel, N. V. (2008). Arabidopsis *XXT5* gene encodes a putative α-1,6-xylosyltransferase that is involved in xyloglucan biosynthesis. *Plant Journal, 56*(1), 101-115.

Zheng, G., Li, L., Li, W. (2016). Glycerolipidome responses to freezing- and chilling-induced injuries: Examples in Arabidopsis and rice. *BMC Plant Biology, 16*(1), 1–15.

Zipper, H., Brunner, H., Bernhagen, J., & Vitzthum, F. (2004). Investigations on DNA intercalation and surface binding by SYBR Green I, its structure determination and methodological implications. *Nucleic Acids Research, 32*(12), 1–10.

Zybailov, B., Rutschow, H., Friso, G., Rudella, A., Emanuelsson, O., Sun, Q., & van Wijk, K. J. (2008). Sorting signals, N-terminal modifications and abundance of the chloroplast proteome. PLoS ONE, 3(4), 1–19.

7. Supplements

7.1. Abbreviations

ABC	ATP binding cassette
ADP	adenosine diphosphate
ASA1	α-subunit of the anthranilate synthase complex
ATP	adenosine triphosphate
BIFC	Bimolecular Fluorescence Complementation
CBF	C-repeat (CRT)/dehydration responsive element (DRE)-binding factors
cDNA	complementary deoxyribonucleic acid
CHS	chalcone synthase
CRT	C-repeat
Ct value	cycle threshold value
DAG	diacyl glycerol
DGAT1	diacylglycerol acyltransferase 1
DGDG	digalactosyldiacylglycerol
dNTPs	deoxyribonucleoside triphosphates
DRE	dehydration responsive element
ER	endoplasmic reticulum
ethidium bromide	3,8-diamino-5-ethyl-6-phenylphenanthridinium bromide
EtOH	ethanol
FFS	free fatty acids
FID	flame ionisation detector
FUT13	α-1,4-fucosyltransferase 13
GalA	galacturonic acid
GC	gas chromatography

gDNA	genomic deoxyribonucleic acid
GFP	green fluorescent protein
GlcA	glucuronic acid
GO	Gene Ontology
HPLC	high performance liquid chromatography
HRP	horseradish peroxidase
LC-MS/MS	liquid chromatography coupled to tandem mass spectrometry
MGDG	monogalactosyldiacylglycerol
MUR3	xyloglucan galactosyltransferase MURUS3
NADH	nicotinamide adenine dinucleotide hydrogen
NaOAc	sodium acetate
NBD	nucleotide-binding domains
OD	optical density
PAI	phosphoribosyl anthranilate isomerases
PAL	phenylalanine ammonia lyase
PAT1	phosphoribosyl anthranilate transferase 1
PC	phosphatidylcholine
PCR	polymerase chain reaction
PE	phosphatidylethanolamine
PE150	paired-end 150bp
PG	phosphatidylglycerol
Pi	phosphate group
PME	pectin methyl esterase
PMEI	pectin methyl esterase inhibitor
qPCR	quantitative polymerase chain reaction
Rif	Rifampicin

ROS	reactive oxygen species
SBS	sequencing by synthesis
SDS	sodium dodecyl sulphate
SFR2	sensitive to freezing 2
Spec	Spectinomycin
SQDG	sulfoquinovosyldiacylglycerol
TAG	triacyl glycerol
TDT	dicarboxylic acid transporter
TFA	tri-fluor acetic acid
TMD	transmembrane domain
TMT	monosaccharide transporter
U	units
UPLC-FT-MS	ultra-performance liquid chromatography coupled with Fourier transform mass
WBC	white brown complex
WT	wild type
XTH	xyloglucan endotransglucosylases/hydrolases
XXT1	xyloglucan α-1,6-xylosyltransferase 1
YFP	yellow fluorescent protein

7.2. Supplementary figures

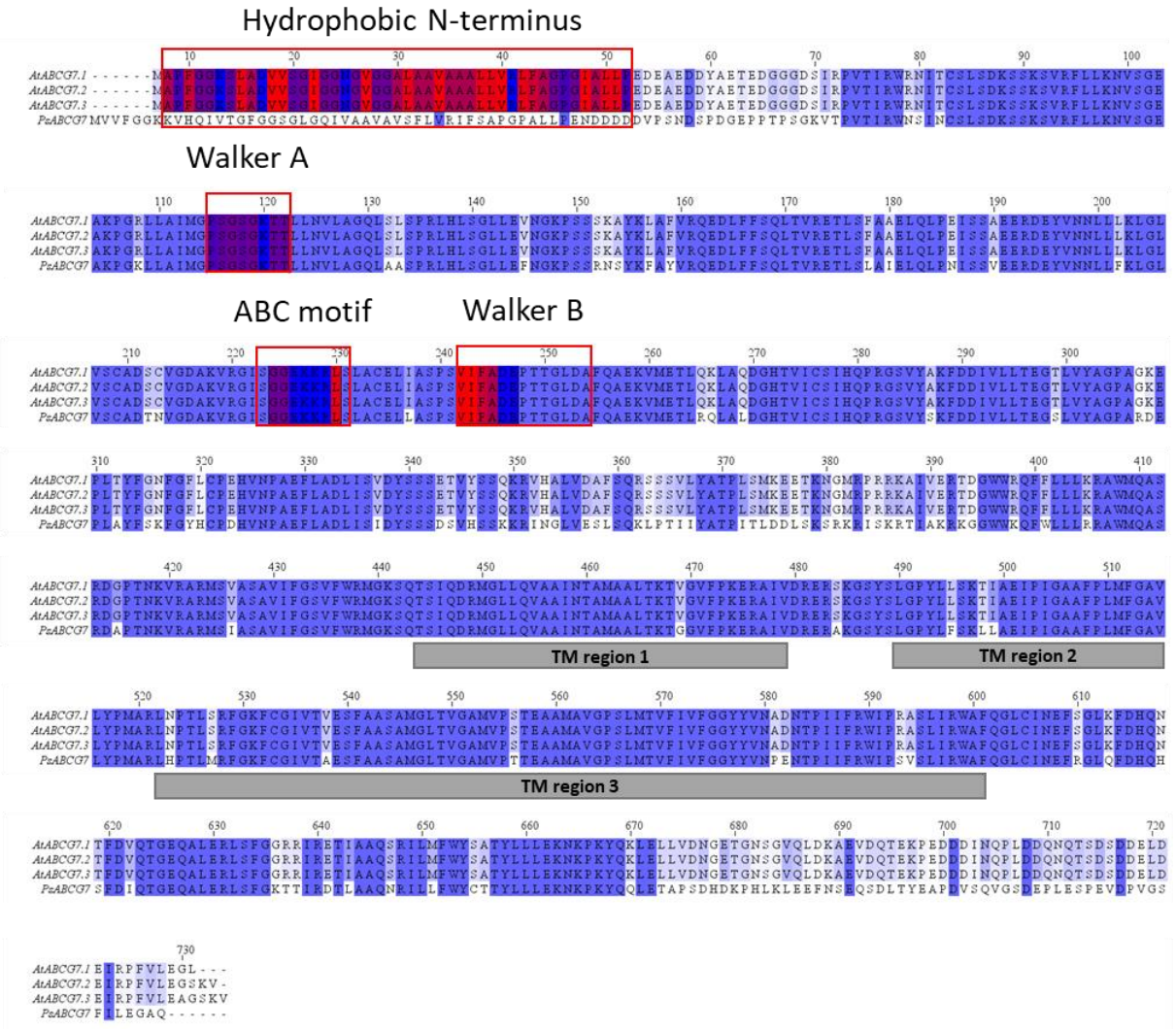

Supplementary Figure 1: Alignment of the *At*ABCG7 splice variants 1 to 3 from *Arabidopsis thaliana* and *Ps*ABCG7 from *Pisum sativum*. The hydrophobicity colouring in Jalview 2.11.2.6 suggests that the N-terminal region is highly hydrophobic. Conserved amino acids are shown in dark blue. Putative Walker A, B and ABC motifs were identified according to Sánchez-Fernández *et al.,* 2001 and are indicated by red boxes. Putative transmembrane regions are indicated by grey boxes (TM region 1 to 3, according to ARAMEMNON 8.1, FlüggeLab, 2002-2023, University of Cologne).

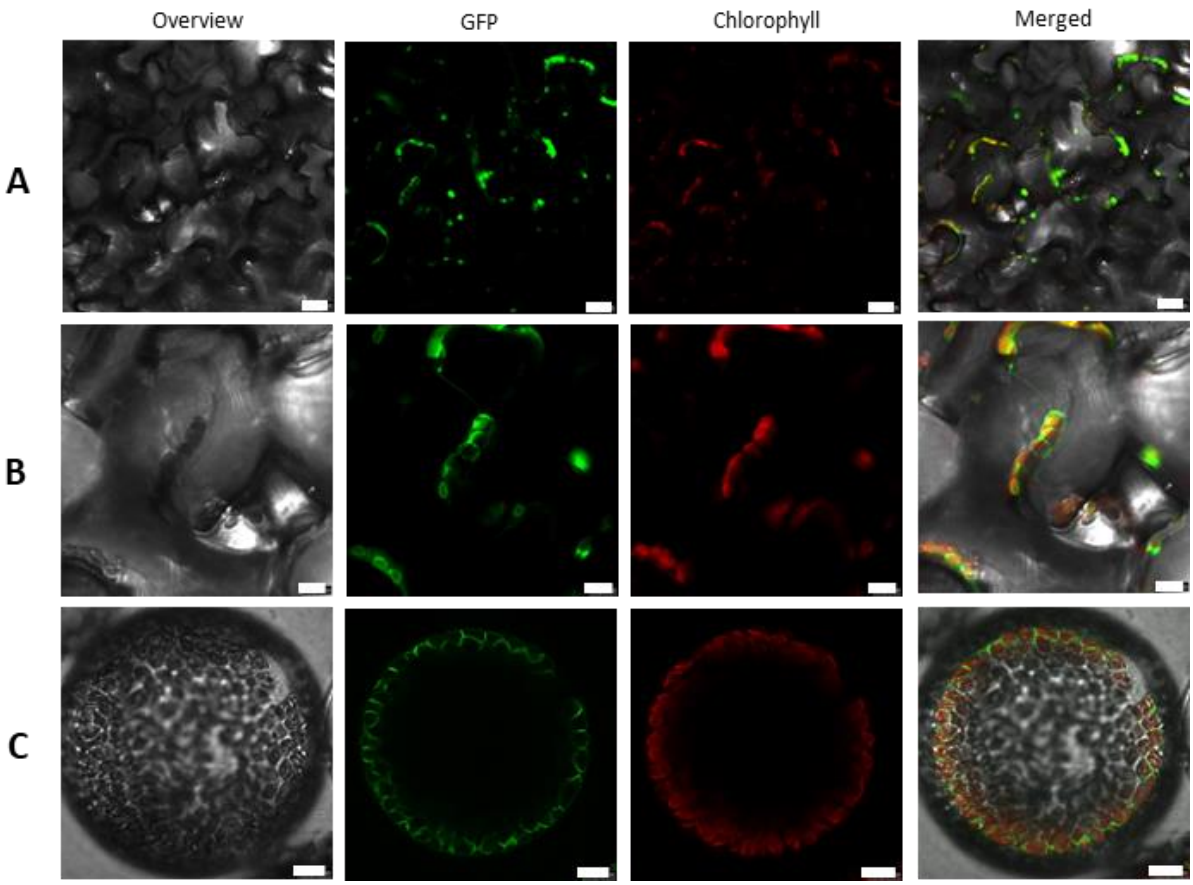

Supplementary Figure 2: ABCG7-GFP locates to the chloroplast envelope. Confocal laser microscopy of transfected tissue from *N. benthamiana* (A, B) and a protoplast (C) transiently expressing the ABCG7-C-GFP protein. *In planta* expression was driven by an *UBQ10* promotor. The images were taken 3 to 4 days after infiltration. The following microscope pictures were taken from left to right: bright field image, GFP signal, chlorophyll autofluorescence as well as the merged image. White bars indicate the scale: 25 µm for A and B, 10 µm for C. Pictures ware taken with a Leica TCS SP5II Microscope at the RPTU Kaiserslautern.

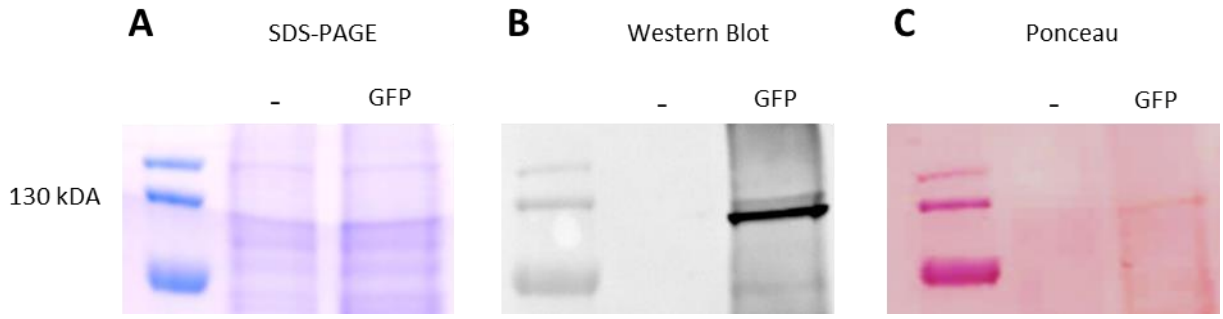

Supplementary Figure 3: Immunological analyses of total protein lysate extracted from ABCG7-GFP transfected *N. benthamiana* leaves. Total protein content was isolated from the transient overexpression of ABCG7-GFP in tobacco. An amount of 20 µg protein was loaded in each lane of the SDS-PAGE (A). The proteins were transferred via western blotting onto a nitrocellulose membrane and the ABCG7-GFP was detected with a GFP-specific antibody (B). Protein transfer from SDS-PAGE to nitrocellulose membrane was confirmed by Ponceau staining (C).

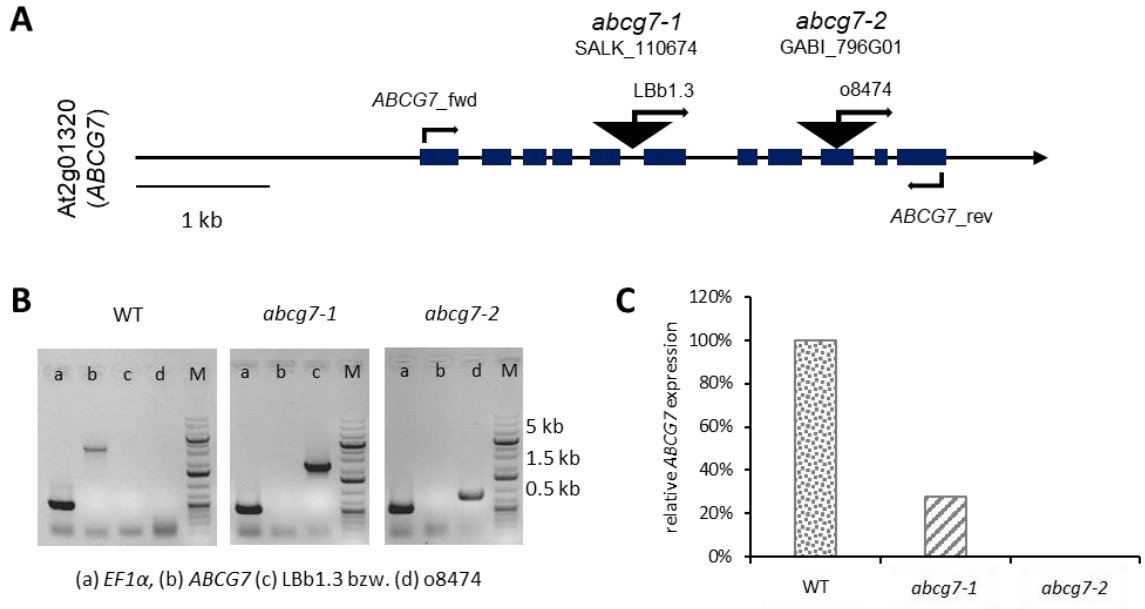

Supplementary Figure 4: Genotyping of two independent *abcg7* loss-of-function lines. The T-DNA insertions within the coding sequence of *ABCG7* in *abcg1-1* (SALK_110674) and *abcg7-2* (GABI_796G01) were identified by sequencing (A). Homozygosity was tested by extracting gDNA. The agarose gel was stained with ethidium bromide and showed approximately 500 bp fragments for EF1α as the intrinsic PCR control. The PCR with *ABCG7* specific primers (*ABCG7*_fwd and *ABCG7*_rev) showed fragments of 3392 bp for wild types (WT; B). PCR results showed no fragments in the *abcg7* lines when using *ABCG7* gene-specific primers. Amplification of T-DNA fragments of about 2000 bp in *abcg7-1* and about 700 bp in *abcg7-2* were observed when using corresponding primers (LBb1.3 or o8474; B). The gene expression of *ABCG7* in the mutants was tested relative to the housekeeping gene *SAND* via quantitative PCR (C).

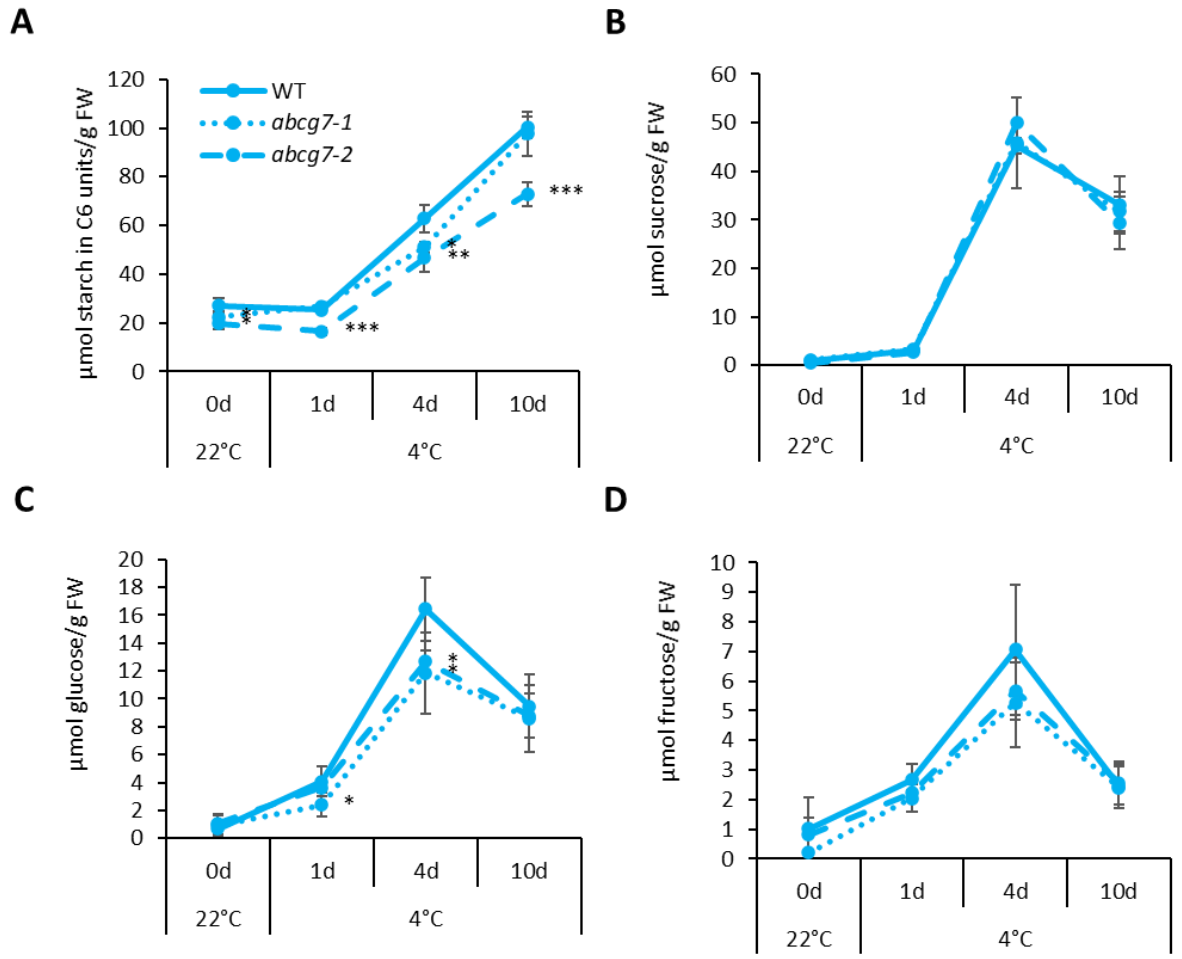

Supplementary Figure 5: Sugar contents of cold acclimated *abcg7* lines. The 4-week-old wild types and *abcg7* lines, grown on soil under short day conditions, were transferred from 22°C to 4°C for 10 days. The contents of starch (A), sucrose (B), glucose (C) and fructose (D) were measured. Asterisks indicate significant differences relative to wild types (n=5; *P<0.05; **P<0.01; ***P<0.005). The Student's T-test was calculated using Microsoft Excel.

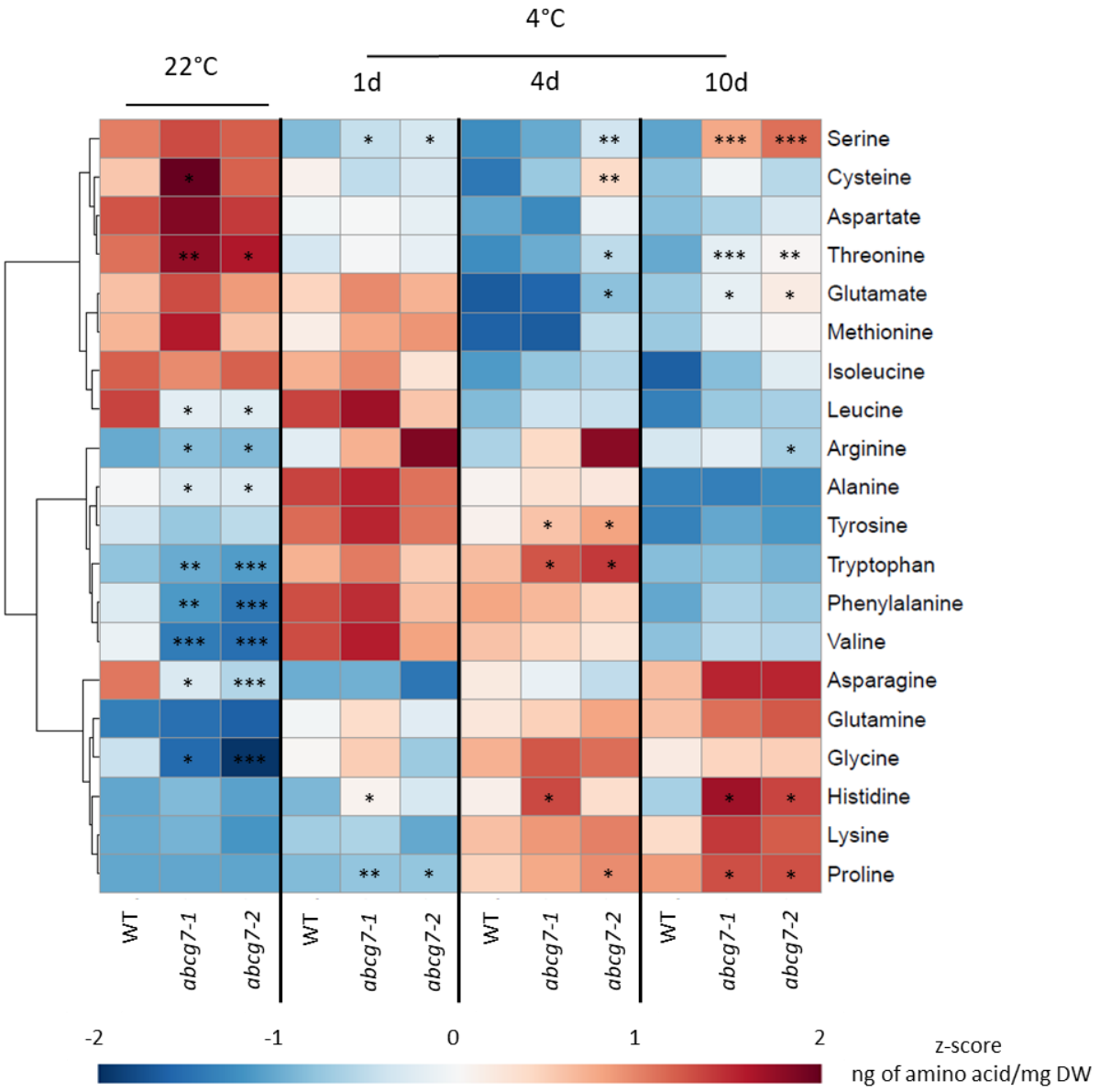

Supplementary Figure 6: Altered amino acid contents in *abcg7* mutants during cold acclimation. The 4-week-old Arabidopsis wild type and *abcg7* lines, grown on soil under standard conditions, were transferred for cold acclimation from 22°C to 4°C to measure changes in amino acids after 1, 4 and 10 days of cold. The z-score for the mean amino acids in ng/mg DW was visualised as a heat map using R studio version 2023.12.1 build 402. Asterisks indicate significant differences relative to wild types at the respective day (n≥3; *P<0.05; **P<0.01; ***P<0.005). The Student's T Test was calculated using Microsoft Excel.

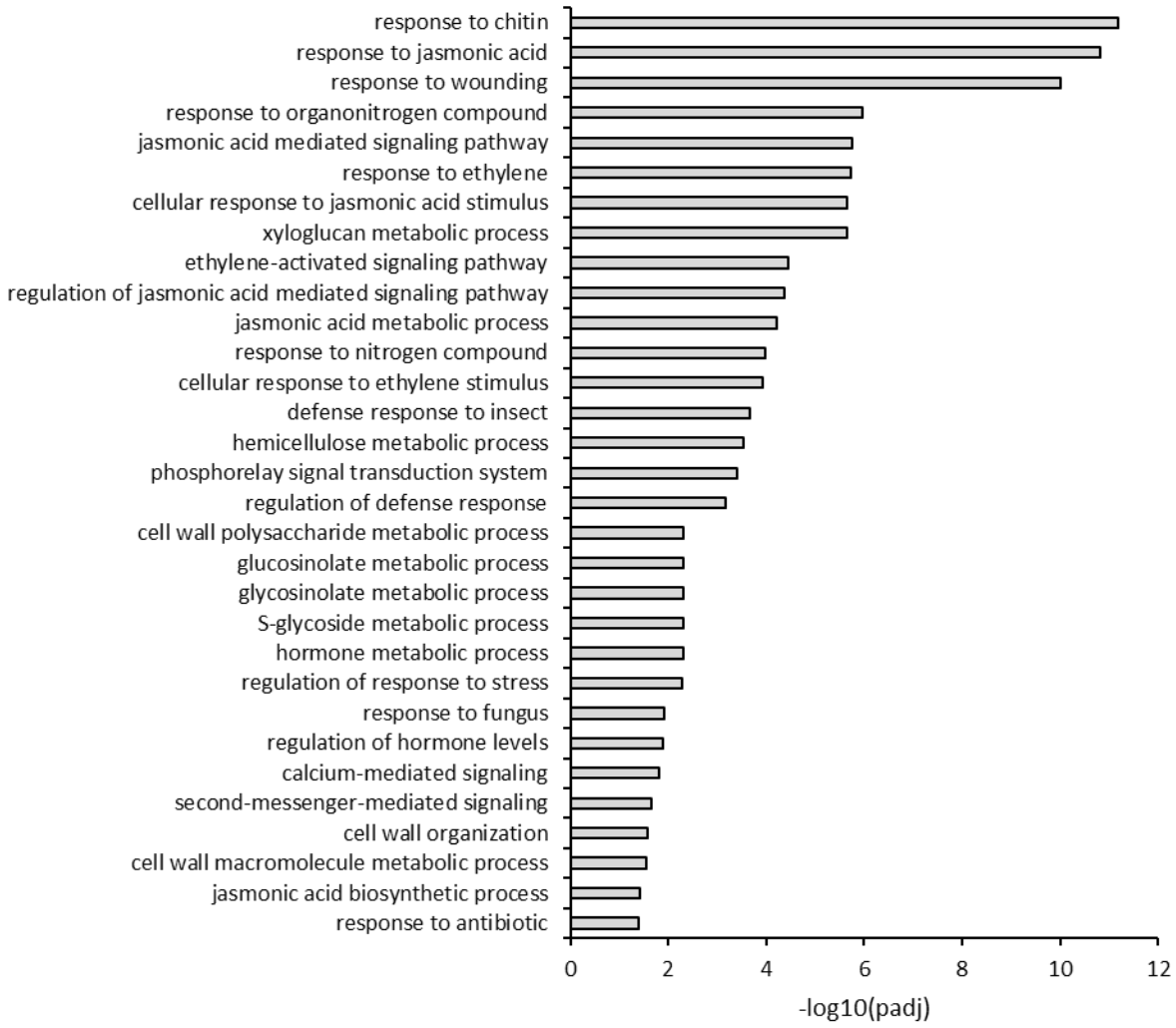

Supplementary Figure 7: Cold temperatures cause the down regulation of various GO term *abcg7-2*. Wild type and *abcg7-2* plants were grown at 22°C for 4 weeks under standard conditions. Subsequently the plants were transferred to 4°C. RNA sequencing samples were harvested on after 4 days at 4°C (n=3, 3 rosettes per n). The x-axis indicates the significant differences in *abcg7-2* relative to the wild type. Bioinformatic analysis and statistical analysis of the RNA sequencing results was performed by Novogene.

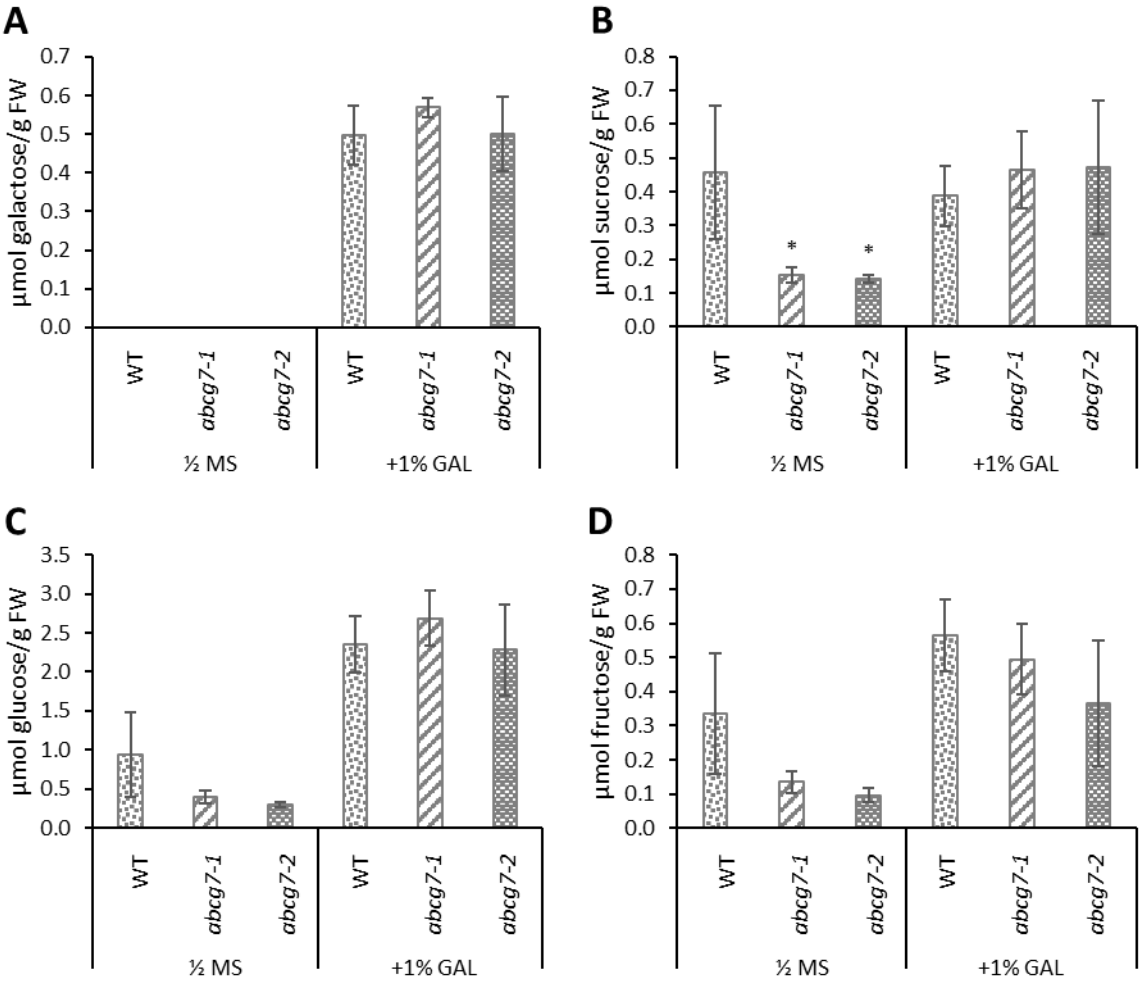

Supplementary Figure 8: Exogenous galactose supply causes sugar accumulation in wild types and *abcg7* lines grown on ½ MS plates with galactose. Sugar and contents of 14-day-old seedling of wild types and *abcg7* lines, grown on plates under short day conditions either without (½ MS) or with galactose (+1% GAL) were measured. The contents of galactose (A), sucrose (B), glucose (C) and fructose (D) were measured. Asterisks indicate significant differences relative to wild types (n≥3; *P<0.05; **P<0.01; ***P<0.005). The Student's T-test was calculated using Microsoft Excel.

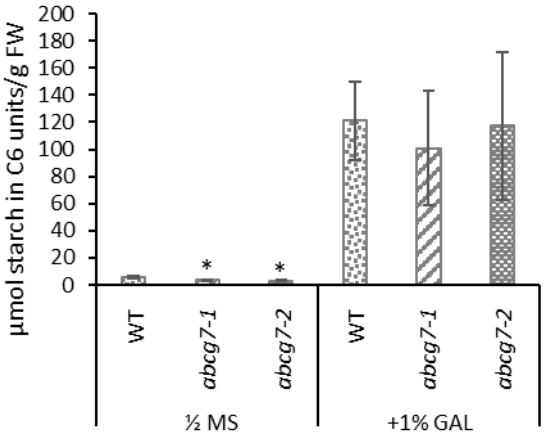

Supplementary Figure 9: Starch contents of wild types and *abcg7* lines grown on ½ MS plates with galactose. Starch contents of 14-day-old seedling of wild types and *abcg7* lines, grown on plates without (½ MS) or with galactose (+1% GAL) were measured. Asterisks indicate significant differences relative to wild types (n≥3; *P<0.05; **P<0.01; ***P<0.005). The Student's T-test was calculated using Microsoft Excel.

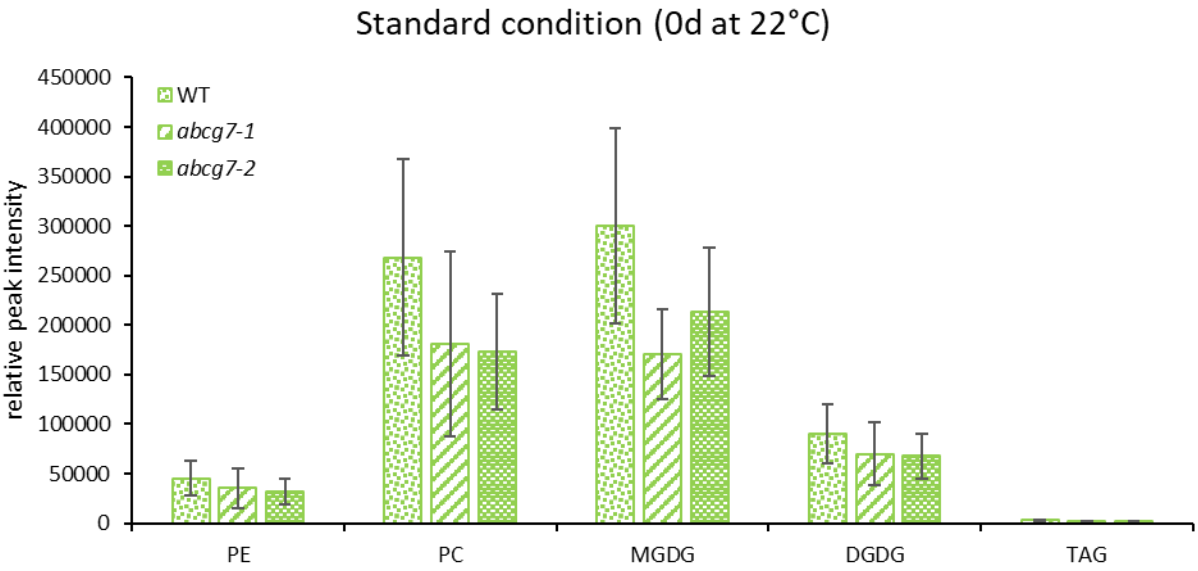

Supplementary Figure 10: Major lipid contents of wild types and *abcg7* loss-of-function lines at standard growth conditions. The lipid contents of 4-week-old wild types and *abcg7* plants grown on soil under control conditions were measured before the start of the freezing experiment (0d at 22°C; n≥3) in collaboration with Dr. Saleh Alseekh (Max Planck Institute of Molecular Plant Physiology, Potsdam).

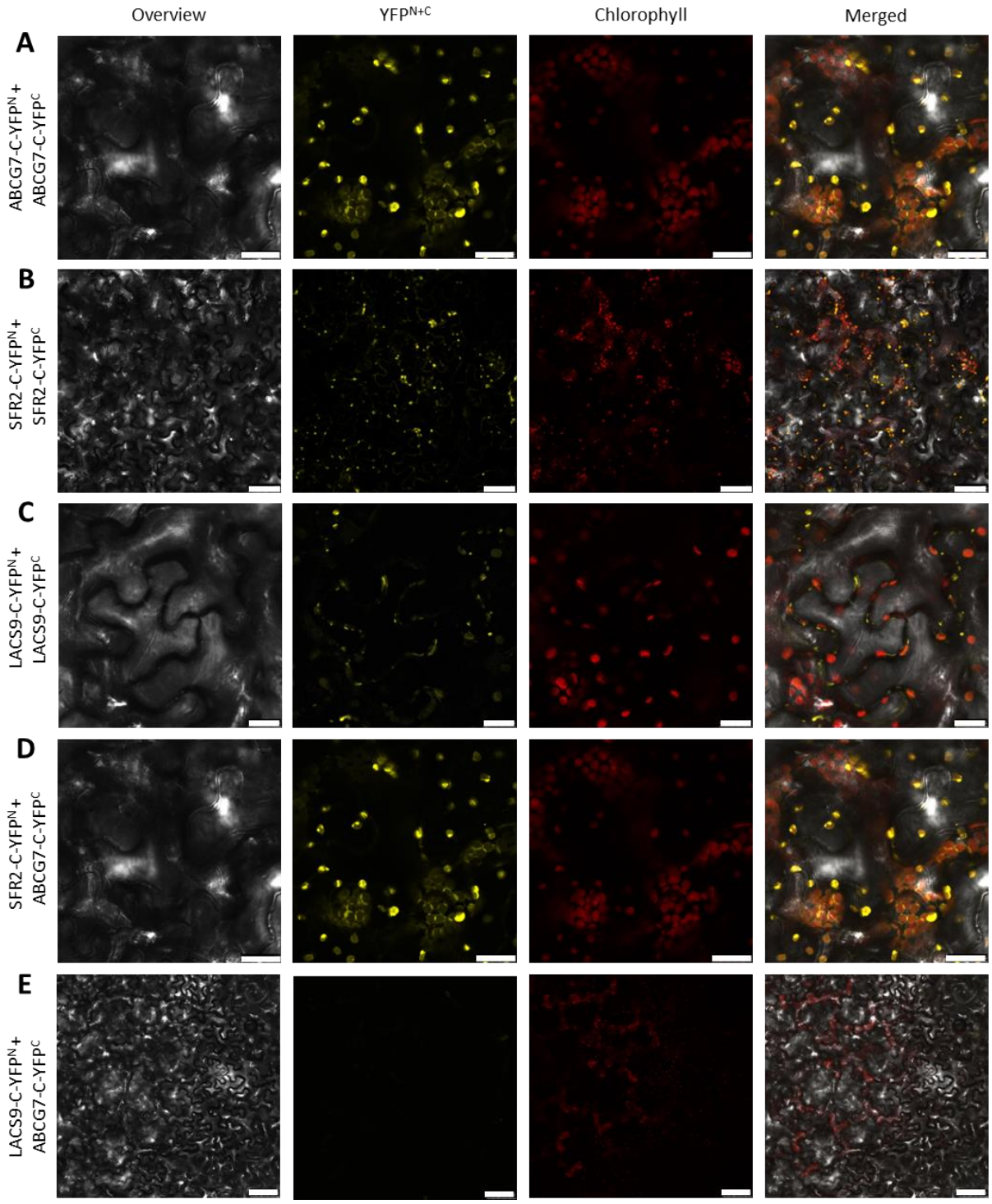

Supplementary Figure 11: Interaction of ABCG7 and SFR2. Fluorescence of BiFC constructs was analysed for ABCG7 (ABCG7-C-YFP^N + ABCG7-C-YFP^C; A), SFR2 (SFR2-C-YFP^N + SFR2-C-YFP^C; B), LACS9 (LACS9-C-YFP^N + LACS9-C-YFP^C; C). Interaction of ABCG7 and SFR2 was observed for the BiFC combination ABCG7-C-YFP^C + SFR2-C-YFP^N (D). As a negative control, ABCG7-C-YFP^C + LACS9-C-YFP^N were used (E). Transient *in planta* co-expression was driven by a *UBQ10* promoter and analysed in transfected *N. benthamiana* tissue by confocal laser microscopy. Images were taken 3 to 4 days after infiltration using a Leica Stellaris 5 Confocal Scanning Microscope at the Ludwig-Maximilians-University in Munich. The white bar indicates the scale: 25 µm in A, C and D; 75 µm in B and 100 µm in E.

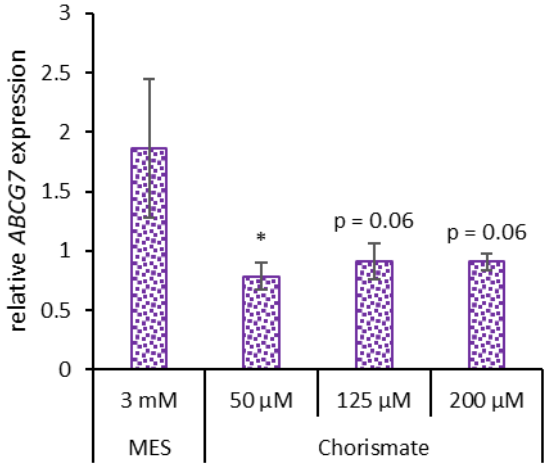

Supplementary Figure 12: Effect of chorismate on *ABCG7* expression in leaf discs of wild types. Approximately 4-week-old plants cultivated under standard conditions were utilised for the extraction of leaf discs (5 mm in diameter each). About 5 leaves per n were incubated in 5 mL of 3 mM MES (pH 5.6) and in respective MES buffer with 50 to 200 µM chorismate. The expression levels of *ABCG7* were evaluated via qPCR using *SAND* as the reference gene. Asterisks indicate significant differences within the lines relative to the MES buffer (n≥3; *P<0.05; **P<0.01; ***P<0.005). The Student's T-Test was calculated in Microsoft Excel.

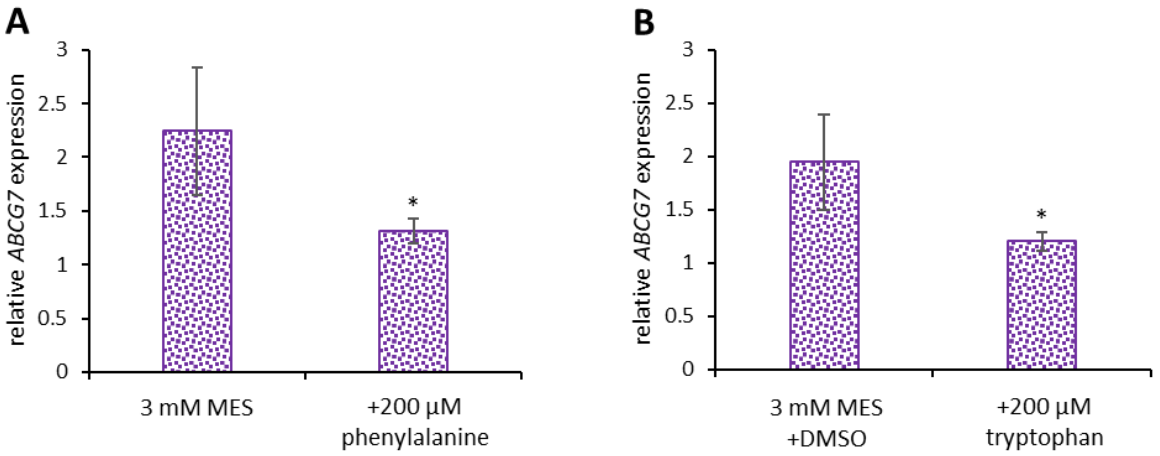

Supplementary Figure 13: Effect of phenylalanine and tryptophan on *ABCG7* expression in leaf discs of wild types. Approximately 4-week-old plants cultivated under standard conditions were utilised for the extraction of leaf discs (5 mm in diameter each). About 5 leaf per n were incubated in 5 mL of 3 mM MES (pH 5.6) and in respective MES buffer with 200 µM phenylalanine or 200 µM tryptophan. As tryptophan was dissolved in 30% (v/v) DMSO corresponding controls were prepared. The expression levels of *ABCG7* in the presence of phenylalanine (A) or tryptophan (B) were evaluated via qPCR using *SAND* as reference gene. Asterisks indicate significant differences within the lines relative to the MES buffer (n≥3; *P<0.05; **P<0.01; ***P<0.005). The Student's T Test was calculated in Microsoft Excel.

Acknowledgement

First and foremost, I would like to express my profound gratitude to Prof. Dr. H. Ekkehard Neuhaus for his provision of this challenging dissertation topic, guidance and commitment to scientific discussion during this dissertation project, as well as his valuable consistent support throughout the years.

I would also like to express my gratitude to Professor Dr. Matthias Hahn. I began my scientific career as an undergraduate student in his laboratory, where he diligently and compassionately taught me all the fundamental principles I required during my studies and provided me with invaluable guidance. In addition, he thoroughly reviewed this thesis.

Furthermore, I would like to express my deepest gratitude to Professor Dr. Nicole Frankenberg-Dinkel. It was due to her that I was granted the opportunity to study Geomicrobiology during my Master's degree, a privilege that I also had the chance to experience under the supervision of Dr. Michelle M. Gehringer. Throughout the entire process, Dr. Frankenberg-Dinkel and Dr. Michelle M. Gehringer fostered an environment characterised by inclusivity, support and understanding.

I would also like to thank Dr Bettina Bölter, Susanne Mühlbauer and Professor Dr Hans-Henning Kunz at the Ludwig-Maximilians-University in Munich for their support in clarifying the location of the ABCG7 transporter and for the warm welcome I received during my visit to their department. Further, I would like to express my sincere gratitude to Kathrin Jahnke, Christine Kühn, Dr Stefan Timm and Junior Professor Dr Andreas Richter from the University of Rostock. I am very grateful for the invaluable guidance I received during the metabolite measurements and for their kind hospitality during my visit to Rostock. In addition, I am thankful to Professor Dr Raimund Tenhaken from the Paris Lodron University in Salzburg for the valuable insights into the cell wall that he provided during the MBP conference in Hennef 2024 and for his invaluable help in measuring cell wall sugars. I would like to express my gratitude to Dr Saleh Alseekh at the Max Planck Institute of Molecular Plant Physiology in Potsdam for the rapid measurement of the lipids.

Further, I like to express my sincere gratitude to Dr Isabel Keller, who provided me with invaluable support from the outset of my position within the Department of Plant Physiology. She was always willing to discuss the results of my research with me, and I am also indebted to my students Michelle Fritzler, Mirko Kreuels, Antonia Katz, Carmen Altmeier, Maximilian Blug and Michelle Kölsch, who carried out numerous experiments with me and made an important contribution to this project.

In addition, I am indebted to Ruth Wartenberg, who generously shared her extensive expertise in cloning and microscopy, which proved invaluable to the success of this project. Finally, I would like to express my heartfelt gratitude to our dedicated technical assistants Verena Müller, Frank Reinhardt and Adrian Heide, whose tireless support throughout the project, especially in connection with numerous experiments and measurements, contributed significantly to the successful completion of this endeavour. Expressions of gratitude are also extended to the entire Plant Physiology department. The atmosphere was consistently pleasant, and the experience was thoroughly enjoyable.

It is important to acknowledge the contribution of Lukas, Sadia and Adriana, who have made a substantial impact on the coffee meetings and the scientific discourse. Additionally, Eva and Melike have demonstrated an unwavering commitment to maintaining morale. My closest friends Sinthusha and Li-Hsuan have shown an exceptional level of understanding and support over the years, enriching my life considerably.

Since the beginning of my studies in Kaiserslautern, I have been accompanied by a man and his dog. I am grateful for the familial support, affection and love I have received from them. This chapter of my life started with their presence, and the next one will now begin in their company. I love you, Sven and Sam.

Curriculum vitae

Katharina Waldemarowna Ebel | Kasachstan (Kustanai)

2021– Today

PhD | Plant physiology | Prof. Dr. Ekkehard Neuhaus | RPTU KL

„Role of the chloroplast transporter ABCG7 in the acclimation of Arabidopsis to cold and freezing conditions“

2018 – 2020

Master of Science in Biology | Microbiology | Prof. Dr. Nicole Frankenberg-Dinkel | TU KL

„Transcriptional and translational analysis of carbon and nitrogen fixation genes in *Nostoc sp. PCC7524* under elevated CO_2 concentration“

2015 – 2018

Bachelors of Science in Biology | Plant pathology | Prof. Dr. Matthias Hahn | TU KL

„Trials to establish CRISPR/Cas9 in *B. cinerea*“

_____

Datum, Unterschrift Doktorand

DARLEGUNG DES EIGENANTEIL

Katharina Waldemarowna Ebel

Role of the chloroplast transporter ABCG7 in the acclimation of Arabidopsis to cold and freezing conditions

Lokalisierung des ABCG7-Transporters: Ruth Wartenberg (RPTU Kaiserslautern), Dr. Bettina Bölter und Susanne Mühlbauer (LMU München) waren an der Aufklärung der ABCG7-Lokalisation beteiligt. Die Konzeption, Planung, Literaturrecherche sowie das Versuchsdesign zur Identifizierung der ABCG7-Lokalisation wurden von mir durchgeführt. Ruth Wartenberg unterstützte mich bei der Klonierung der Mikroskopiekonstrukte sowie bei der Aufnahme der Mikroskopiebilder. Susanne Mühlbauer war teilweise an der Mikroskopie beteiligt. Dr. Bettina Bölter führte den Proteaseverdau durch, stellte den zugehörigen Methodenteil bereit und erstellte die entsprechende Abbildung.

Die **Abbildungen 6 und 22** sowie die **Zusatzabbildungen 2 und 11** zeigen Mikroskopieaufnahmen, die in Zusammenarbeit mit Ruth Wartenberg (RPTU Kaiserslautern) und Susanne Mühlbauer (LMU München) entstanden sind. **Abbildung 7** zeigt den Proteaseverdau, der von Dr. Bettina Bölter (LMU München) durchgeführt wurde.

Metabolitmessungen: Die Konzeption, Planung, Literaturrecherche und das Versuchsdesign zu den Metabolitmessungen erfolgten durch mich. An den Metabolitmessungen waren Adrian Heide und Frank Reinhardt (RPTU Kaiserslautern), Kathrin Jahnke, Dr. Stefan Timm sowie Juniorprofessor Dr. Andreas Richter (Universität Rostock) beteiligt. Die Auswertung, Interpretation und Diskussion der Ergebnisse erfolgten eigenständig. Prof. Dr. Andreas Richter stellte den Methodenteil für die in Rostock durchgeführten Messungen zur Verfügung und sowie ein Template zur Erstellung der Heatmaps mit R Studio.

Die **Abbildungen 10–12** sowie die **Zusatzabbildung 6** zeigen Messungen, die in Zusammenarbeit mit Kathrin Jahnke, Dr. Stefan Timm und Prof. Dr. Andreas Richter (Universität Rostock) durchgeführt wurden. **Abbildung 16D** zeigt Aminosäureanalysen, die in Zusammenarbeit mit Adrian Heide (RPTU Kaiserslautern) entstanden sind. **Zusatzabbildung 8** zeigt eine Zuckermessung, die in Zusammenarbeit mit Frank Reinhardt (RPTU Kaiserslautern) durchgeführt wurde.

Zellwandzuckermessungen: Die Konzeption, Planung, Literaturrecherche und das Versuchsdesign wurden von mir durchgeführt. Die Messungen wurden von Prof. Dr. Raimund Tenhaken (Paris Lodron Universität Salzburg) durchgeführt, der zudem den Methodenteil zur Verfügung stellte. Die Auswertung, Interpretation und Diskussion der Ergebnisse erfolgten eigenständig.

Abbildung 20 zeigt Zellwandzuckerdaten, die von Prof. Dr. Raimund Tenhaken (Paris Lodron Universität Salzburg) gemessen wurden.

Lipidmessungen: Die Konzeption, Planung, Literaturrecherche und das Versuchsdesign erfolgten durch mich. Dr. Saleh Alseekh (Max-Planck-Institut für Molekulare Pflanzenphysiologie, Potsdam) führte die Lipidmessungen durch und stellte den Methodenteil zur Verfügung.

Abbildung 21A sowie **Zusatzabbildung 10** zeigen Lipidanalysen, die von Dr. Saleh Alseekh (MPI Potsdam) durchgeführt wurden.

Die vorliegende Einschätzung über die erbrachte Leistung Dritter wurde mit den genannten Personen einvernehmlich abgestimmt.

_____ _____

Datum, Unterschrift Doktorand/in Datum, Unterschrift Betreuer/in

DARLEGUNG DES EIGENANTEIL

Katharina Waldemarowna Ebel

Role of the chloroplast transporter ABCG7 in the acclimation of Arabidopsis to cold and freezing conditions

Analyse der Proteinsequenzen in **Zusatzabbildung 1** erfolgte mit dem Tool **Jalview (Version 2.11.2.6)**.

Für das Primerdesign wurde das Online-Tool **Primer3 (https://primer3.ut.ee/)** verwendet.

Die Berechnung der qPCR-Effizienzen erfolgte mit dem Online-Tool **Primer Efficiency Calculator** von Thermo Fisher Scientific **(https://www.thermofisher.com/).**

Die Erstellung von Heatmaps erfolgte mit **R Studio (Version 2023.12.1 Build 402)**. Die Erstellung wurde durch Prof. Dr. Andreas Richter (Universität Rostock) angeleitet.

Die Arbeit wurde von **Dr. Isabel Keller (RPTU Kaiserslautern)** inhaltlich und sprachlich Korrektur gelesen.

Zur Verbesserung der sprachlichen Qualität der Dissertation wurden **ChatGPT (OpenAI, GPT-4)** und **DeepL Write** eingesetzt.

_____

Datum, Unterschrift Doktorand/in